NON-PEER-REVIEWED PREPRINT

Submitted to EarthArXiv

Inside the Extinction Envelope: A Systemic Review and Meta-Analysis of Paleoclimate Extinction Markers with Comments on the Necessary Array of Last-Threshold Interventions

A Continuation of the Paleoclimate Analog IPCC Submission with the Peer-Reviewed Portfolio of Interventions Necessary to Arrest the Extinction Causal Chain

Christian Komor, Psy.D.

Earth Systems Science Advisor

Climate Deadline Alliance

1001 Bannock Street, Denver, Colorado 80204, USA

Email: christiankomor@k4gov.com

ORCID: 0009-0006-8033-1548

Peer Review Status

This manuscript is a non-peer-reviewed preprint submitted to EarthArXiv. It has been submitted for peer review to Oxford Open Climate Change (Oxford University Press). Subsequent versions of this manuscript may differ as a result of the peer review process. If accepted for publication, the final peer-reviewed version will be identified in a subsequent revision of this preprint.

Date of Preprint

September 2026

License

Correspondence

Correspondence and requests for materials should be addressed to Christian Komor at christiankomor@k4gov.com.

Data Availability

All data supporting the conclusions of this manuscript are drawn from peer-reviewed published literature, cited in the References sections of each of the three Parts. No new experimental data were generated for this synthesis.

Conflict of Interest

The author declares no financial conflicts of interest. The author is the founder of the Climate Deadline Alliance, a nonprofit policy organization advocating for climate response at the scale described in this manuscript.

Funding

This work received no external funding. All research and writing was conducted independently by the author.

Inside the Extinction Envelope: A Systemic Review and Meta-Analysis of Paleoclimate Extinction Markers with Comments on the Necessary Array of Last-Threshold Interventions

A Continuation of the Paleoclimate Analog IPCC Submission with the Peer-Reviewed Portfolio of Interventions Necessary to Arrest the Extinction Causal Chain

Author: Christian Komor, Psy.D., Earth Systems Science Advisor
Climate Deadline Alliance, christiankomor@k4gov.com

Abstract

Every element of the causal chain that produced the five largest mass extinctions of the last half-billion years is presently active in the Earth system. The rate of the modern perturbation exceeds every peer-reviewed paleoclimate reference case. A six-intervention portfolio, deployed together at wartime industrial scale beginning now, is the physically necessary and sufficient response. The window in which that portfolio remains fully effective closes between 2028 and 2040. The anthropogenic-versus-feedback tipping point is expected between 2035 and 2040; corrected for the at-least-order-of-magnitude higher rate of contemporary carbon release, loss of agency — the point at which coordinated intervention can no longer arrest the cascade — arrives 200 to 400 years after feedback engagement under sustained portfolio deployment, and collapses onto the tipping point itself under any scenario in which the portfolio is not deployed within the 2028–2040 window.

Background. The five largest mass-extinction events of the Phanerozoic share a consistent causal chain: rapid carbon injection to the ocean-atmosphere system, followed by warming, ocean deoxygenation, acidification, and preferential loss of marine calcifiers, with multi-million-year recovery for reef ecosystems. Every element of that chain is presently active. The current anthropogenic perturbation is capable of driving a combination and magnitude of ocean geochemical changes unparalleled in the geological record reviewed by Hönisch et al. (2012), which covers approximately the past 300 million years. The reef–ocean-oxygen–land coupling documented in the End-Permian record demonstrates that marine biosphere collapse propagates to terrestrial extinction through the shared oxygen and biogeochemical infrastructure of the coupled Earth system; contemporary marine indicators are therefore leading indicators of terrestrial as well as marine risk.

Approach. This three-part synthesis compiles peer-reviewed reconstructions of the Big Five causal chain, measures each element against the contemporary Earth system using the most recent authoritative data (Friedlingstein et al. 2026; Wu et al. 2021; Zeebe et al. 2016; Hönisch et al. 2012; Schmidtko et al. 2017; Eddy et al. 2021; Spady et al. 2026), specifies the physically necessary intervention portfolio, and characterizes the near-term feedback, resource, and civilizational risk environment those interventions must succeed in. Part I establishes the paleoclimate analog. Part II specifies the intervention portfolio. Part III maps the contemporary Earth system the Part II portfolio must succeed in — which climate feedbacks are already engaged and how they cascade, which physical resources are hitting hard limits inside the same two-to-three-decade window, and how those pressures translate into food, water, migration, health, economic, and governance strain — and closes with the North American Climate Pain Scale (NAPS), a 1–10 diagnostic instrument that anchors climate severity to concrete events so policymakers and the public can locate today's conditions and the trajectory ahead.

Findings. Every element of the paleoclimate extinction causal chain is presently active. Atmospheric CO_2 (422.8 ppm, 2024 global annual mean; Friedlingstein et al. 2026) has exceeded the reconstructed latest-Permian baseline of 426 (+133 / −96) ppm (Wu et al. 2021, Nature Communications). The rate of contemporary carbon release is at least an order of magnitude above the sustained maximum Paleocene-Eocene Thermal Maximum rate (Zeebe, Ridgwell and Zachos 2016, Nature Geoscience). Ocean acidification is proceeding at roughly ten times the PETM rate (Hönisch et al. 2012, Science). The global ocean has lost 4.8 ± 2.1 petamoles of dissolved oxygen since 1960 (Schmidtko, Stramma and Visbeck 2017, Nature). Global living coral cover has declined approximately 50 percent since 1957 (Eddy et al. 2021, One Earth), with cumulative satellite reef-pixel heat-stress exposure of 86.8 percent across August 2018 through 17 December 2025 (Spady et al. 2026). The paleoclimate record indicates the feedback-dominated phase of prior extinctions lasted tens of thousands of years once engaged, with the destruction phase two to three orders of magnitude shorter than the multi-million-year recovery. Corrected for the contemporary rate multiplier, the compressed modern-equivalent cascade unfolds over 2,000 to 7,000 years, with early-phase dynamics (feedback engagement through threshold crossing) compressed by approximately ten, middle-phase dynamics (cascade propagation) compressed by three to five, and late-phase dynamics (terminal biotic loss and geochemical equilibration) compressed by one to three, in each case relative to the paleoclimate baseline. The five paleogeologic indicators strongly correlated with prior extinction-level events — atmospheric CO_2 concentration and rate of change, ocean acidification, ocean deoxygenation, coral and calcifier loss, and mercury loading — are all significantly active in the modern record.

Implications. A six-intervention portfolio deployed together at wartime industrial scale, beginning immediately, is identified as the physically necessary and sufficient response, in order of physical urgency: methane suppression at source; direct atmospheric carbon removal coupled with hyperscale-compute waste-heat recovery, operational at gigaton scale by approximately 2035; ocean alkalinity enhancement, the only intervention that reaches surface-ocean acidification directly; stratospheric aerosol injection as a 2028–2040 temperature bridge, the only lever operating on the one-to-two-year deployment-to-effect timescale required inside the closing window; coral assisted evolution paired with expansion of marine protected areas to 30 percent of the global ocean by 2030; and a geothermal-first, nuclear-second clean-power backbone, without which none of the preceding interventions is executable at scale. Bioenergy with carbon capture at IPCC-median deployment scale and afforestation as primary carbon strategy are de-prioritized as modeling artifacts that displace scarce land and political attention from interventions that better match the physics. Under any scenario in which the portfolio is not deployed at wartime industrial scale within the 2028–2040 window, the effective loss-of-agency moment collapses onto the anthropogenic-versus-feedback tipping point itself, after which human capacity to halt or reverse the sixth mass-extinction event is expected to fail.

Keywords: mass extinction; paleoclimate analog; carbon injection; ocean acidification; ocean deoxygenation; mercury enrichment; tipping cascades; direct air capture; ocean alkalinity enhancement; stratospheric aerosol injection; climate feedbacks; extinction risk

The Five Indicators, Present Values Against Big Five Signatures.

1. **Atmospheric CO_2.** 422.8 ppm (2024 global annual mean, Friedlingstein et al. 2026), above the reconstructed latest-Permian baseline of 426 (+133 / −96) ppm (Wu et al. 2021).
2. **Rate of carbon release.** At least an order of magnitude above the sustained maximum PETM rate (Zeebe et al. 2016).
3. **Ocean acidification.** Proceeding at roughly ten times the PETM rate (Hönisch et al. 2012).
4. **Ocean deoxygenation.** 4.8 ± 2.1 petamoles of oxygen lost from the global ocean since 1960 (Schmidtko, Stramma and Visbeck 2017, *Nature*).
5. **Reef and calcifier loss.** Roughly 50 percent global coral-cover decline 1957–2007 (Eddy et al. 2021, *One Earth*); cumulative heat-stress exposure of 86.8 percent across August 2018 – December 2025 (Spady et al. 2026, *Coral Reefs*).

Part II Six Interventions, deployed together, starting immediately, at wartime industrial scale, address the coupled indicator system in a way no single intervention can. In order of physical urgency:

1. **Methane suppression at source**, which bends the temperature curve on a decadal timescale no CO_2 intervention can match.
2. **Direct atmospheric carbon removal coupled with hyperscale-compute waste-heat recovery (DACR+HSDC)**, which addresses the atmospheric CO_2 burden at gigaton operational scale.
3. **Ocean alkalinity enhancement**, the only intervention that reaches surface ocean acidification.
4. **Stratospheric aerosol injection**, the only lever that reduces radiative forcing on the one-to-two-year deployment-to-effect timescale required during the 2028–2040 window.
5. **Coral assisted evolution paired with expansion of marine protected areas to 30 percent of the global ocean**, preserving the biological infrastructure whose continued existence is the outcome the atmospheric interventions must protect.
6. **A clean-power backbone built geothermal-first and nuclear-second**, the enabling infrastructure without which none of the preceding interventions is executable at scale.

Bioenergy with carbon capture (BECCS) at IPCC-median deployment scale, and afforestation as primary carbon strategy, are de-prioritized as modeling artifacts that displace scarce land and political attention from interventions that better match the physics.

PART I
THE PROBLEM

The Paleoclimate Analog for Contemporary Anthropogenic Carbon Emissions: Shared Mechanisms of the Big Five Mass Extinctions and the Contemporary Signature

1. Introduction

The paleoclimate record provides the only empirical evidence of how the Earth system responds to rapid, large-magnitude perturbations of the carbon cycle. The five largest mass extinction events of the Phanerozoic — the Late Ordovician (~445 million years ago, Ma), the Late Devonian (~372 Ma), the End-Permian (~252 Ma), the End-Triassic (~201 Ma), and the End-Cretaceous (~66 Ma) — collectively provide five independent case studies of biosphere response to massive carbon-cycle disruption.

Recent peer-reviewed synthesis has identified a consistent causal chain across these events. This report summarizes that consensus and evaluates its relevance to contemporary anthropogenic climate change.

1.1 Definitions

For the purposes of this report: Marine extinction refers to species loss among ocean-dwelling organisms, including invertebrates (corals, brachiopods, ammonites, calcareous plankton), fish, and marine reptiles. Terrestrial extinction refers to species loss among land-dwelling organisms — tetrapod vertebrates (amphibians, reptiles, synapsids/proto-mammals, and later mammals and birds), insects, and, where documented, land plants. The End-Permian mass extinction remains the most severe terrestrial extinction in the geological record, with approximately 70 percent of terrestrial vertebrate species lost (Sahney and Benton 2020 summary at UC Berkeley) and the only known mass extinction of insects, with approximately 82.6 percent of insect genera lost (Jouault et al. 2022, as summarized in Tishler review). Land plants showed selective loss rather than a true mass extinction at the End-Permian boundary (Nowak et al. 2019, Nature Communications).

2. Shared Mechanisms of the Big Five Mass Extinctions

2.1 Ultimate Driver: Massive Carbon Injection

The most comprehensive recent synthesis of Phanerozoic mass extinctions (Bond and Grasby 2017, Palaeogeography, Palaeoclimatology, Palaeoecology) concludes that large igneous province (LIP) volcanism is the primary driver of the majority of major Phanerozoic biotic crises. LIPs are continent-scale magmatic events that inject massive quantities of carbon dioxide, sulfur, and other volatiles into the ocean-atmosphere system on geologically rapid timescales.

This conclusion is corroborated by Ernst and Youbi 2017, Palaeogeography, Palaeoclimatology, Palaeoecology, which demonstrates the temporal correlation between LIP emplacement and Phanerozoic climate perturbations. Independent statistical analysis by Green et al. 2022, Proceedings of the National Academy of Sciences confirms that the temporal correlation between continental LIPs and faunal turnover in the Phanerozoic is unlikely to have occurred by chance.

The specific LIP association for each Big Five event is now established:

1. **End-Permian: Siberian Traps**
2. **End-Triassic: Central Atlantic Magmatic Province**
3. **End-Cretaceous: Deccan Traps (concurrent with the Chicxulub bolide impact)**
4. **Late Devonian: Viluy Traps (with additional contributions from terrestrial vegetation expansion)**
5. **Late Ordovician: Cryptic LIP with mercury-spike evidence for volcanic input**

2.2 Geochemical Fingerprint: Mercury Loading

Mercury enrichment in extinction-boundary sediments provides the primary geochemical fingerprint of LIP volcanism. Mercury spikes have been identified at all five Big Five extinction boundaries, with the caveat that end-Cretaceous mercury is attributed primarily to Deccan volcanism rather than to the Chicxulub impact.
For the Late Ordovician specifically, The Innovation Geoscience, 2024 reports mercury isotope evidence linking intensive volcanism to the Late Ordovician mass extinction. For the End-Triassic, Li et al. 2022 documents the temporal correlation between Central Atlantic Magmatic Province mercury signals and marine anoxia. Multiple studies confirm mercury spikes at End-Permian and End-Cretaceous boundaries.

2.3 Proximal Killer: Ocean Anoxia

The most consistent proximal kill mechanism across the Big Five is widespread ocean anoxia — loss of dissolved oxygen from marine waters. Peer-reviewed synthesis (Bond and Grasby 2017; "Breathless through Time," Sperling et al. 2022, Biological Bulletin) identifies marine anoxia as present at every Big Five event, most severely at the End-Permian, End-Triassic, and Late Devonian (the Kellwasser events), with anoxia also documented for the Late Ordovician second pulse and portions of the End-Cretaceous marine record.

The mechanism is well understood: massive volcanic CO_2 injection drives global warming; warmer surface waters hold less dissolved oxygen; thermal stratification of the water column impedes ventilation of deeper waters; and increased continental weathering under a warmer, wetter climate delivers nutrients to the ocean, driving eutrophication and further deoxygenation. In the most severe cases (End-Permian, portions of the Late Devonian), anoxia progressed to euxinia — the production of toxic hydrogen sulfide in the water column.

2.4 Ocean Acidification and Carbonate Crisis

Direct isotopic evidence for ocean acidification during a mass extinction has been most robustly established for the End-Permian event. Clarkson et al. 2015, Science used boron isotope analysis to document that the second, more severe pulse of the End-Permian extinction coincided with an abrupt ocean acidification event driven by rapid carbon injection whose rate is comparable to modern anthropogenic emissions.

The magnitude of the End-Permian atmospheric CO_2 perturbation has been quantified by Wu et al. 2021, Nature Communications. Using $\delta^{13}C$ from C_3 plant fossils across four terrestrial sections in southwestern China — a single-region terrestrial proxy record from one extinction event — the authors report that atmospheric partial pressure of CO_2 increased from 426 (+133 / −96) ppmv in the latest Permian to 2,507 (+4,764 / −1,193) ppmv at the Permian-Triassic Mass Extinction — a six-fold increase across the extinction interval, within approximately 75 kyr, coincident with a rise of about 10 °C in low-latitude sea-surface temperatures and implying an Earth system sensitivity near 3.9 °C per CO_2 doubling.

Acidification-driven carbonate crisis is a signature of every Big Five event. Heavily calcified organisms — reef-building corals, ammonites, calcareous plankton, brachiopods — suffered preferential extinction at every event. The recovery interval for coral reef ecosystems following each Big Five event ranges from approximately 5 to 15 million years.

2.4a The Reef–Ocean-Oxygen–Land Coupling: Why Marine Collapse Propagates To Terrestrial Extinction

The paleoclimate record establishes not only that marine and terrestrial extinctions co-occur across the Big Five, but that they are causally coupled through the Earth system's shared oxygen and biogeochemical infrastructure. The mechanism by which acidification and anoxia in the ocean produce vertebrate extinctions on land is now sufficiently resolved in the peer-reviewed literature to be stated as an explicit sub-mechanism of the consensus causal chain.

Coral reefs are the concentrated locus of marine biodiversity. Reefs occupy less than one percent of the ocean floor yet support at least 25 percent of all marine species (UNEP 2024; Fisher et al. 2015, Current Biology). This concentration is not coincidental: reefs function simultaneously as (i) three-dimensional architecture creating orders of magnitude more habitable niches per unit area than any other benthic setting; (ii) nursery habitat for a large fraction of reef-associated and pelagic fish species, with juveniles of many commercially and ecologically important species restricted to reef and reef-adjacent seagrass and mangrove habitats (Nagelkerken et al. 2000, Marine Ecology Progress Series; Mumby et al. 2004, Nature); (iii) primary production platforms with gross productivity exceeding 7,000 g C m^2 yr^1 (Odum¯& Odum 1955, Ecological Monographs), one of the highest values of any ecosystem on Earth; and (iv) physical breakwaters dissipating up to 97 percent of incident wave energy (Ferrario et al. 2014, Nature Communications), enabling the persistence of the seagrass and mangrove ecosystems that lie behind them and that sequester carbon at rates 30 to 50 times higher per unit area than terrestrial forest (Mcleod et al. 2011, Frontiers in Ecology and the Environment).

The paleontological evidence that reef collapse is the leading indicator of Big Five ecosystem transitions is robust. Each of the Big Five is associated with a 'reef gap' — an interval of geological time, ranging from approximately 4 to 16 million years, during which coral-sponge reef ecosystems are absent from the sedimentary record (Kiessling & Simpson 2011, Global Change Biology; Veron 2008, Coral Reefs). The Late Devonian and End-Permian gaps are the extreme cases: the Kellwasser event eliminated the stromatoporoid-coral reef systems of the Middle Devonian and the functional consequences of that collapse persisted for at least 35 million years, with true framework-building reefs not reappearing until the Middle Triassic Scleractinia approximately 150 million years later (Zapalski et al. 2022, Scientific Reports). The End-Permian eliminated rugose and tabulate corals entirely, and the first 10 million years of the Triassic record no metazoan reefs of any kind, only microbial mounds in restricted settings (Payne & Clapham 2012, Annual Review of Earth and Planetary Sciences).

Reef collapse is coupled to terrestrial extinction through marine primary productivity. Marine photoautotrophs — principally the cyanobacterial genus Prochlorococcus, diatoms, and other phytoplankton — are responsible for approximately 50 percent of contemporary atmospheric oxygen production, matching the annual output of all terrestrial vegetation combined (NOAA National Ocean Service 2024; Field et al. 1998, Science). The cyanobacterium Prochlorococcus alone accounts for approximately 20 percent of biosphere oxygen production (Partensky et al. 1999, Microbiology and Molecular Biology Reviews). Atmospheric oxygen at its present concentration of 20.9 percent is not a stable geological property independent of the marine biosphere; it is the balance between marine and terrestrial photosynthesis and organism respiration, sustained on a rolling basis by ongoing primary production, of which the ocean supplies roughly half.

The End-Permian record documents this coupling directly. Huey and Ward 2005, Science modeled the combined effect of the End-Permian atmospheric oxygen decline and coincident global warming on terrestrial vertebrate physiology, showing that hypoxic stress at low elevations compressed vertebrate altitudinal ranges to near sea level, fragmenting populations and driving species-area extinctions in terrestrial tetrapods independent of any direct marine effect. Sun et al. 2012, Science documented equatorial sea-surface temperatures reaching 36–40 °C during the End-Permian, temperatures that terrestrial vertebrates could not thermoregulate against and that suppressed both marine and terrestrial primary productivity.

The coupling operates in both directions. Fielding et al. 2019, Nature Communications and subsequent work by Chu et al. 2020 demonstrated that terrestrial ecosystem collapse during the End-Permian delivered organic matter, nutrients, and biologically important elements into the marine system in quantities sufficient to worsen marine anoxia and euxinia. Payne and Clapham 2012 formalize this as a paired-system causal architecture: climate change and ozone-layer disruption drive terrestrial extinction; changes in ocean oxygen, CO_2, pH, and temperature drive marine extinction; the two feed each other through nutrient runoff, atmospheric composition, and thermal coupling.

The implication for the contemporary analog is direct. Modern coral reef cover has declined by more than 50 percent globally since 1950 (Eddy et al. 2021, One Earth). The fourth global bleaching event produced 86.8 percent cumulative satellite reef-pixel heat-stress exposure over August 2018 – 17 December 2025 (maximum rolling 365-day extent 77.2 percent). Heat-stress exposure is a satellite-derived measure of reef area experiencing thermal anomaly; it does not confirm that all exposed colonies bleached or died. (International Coral Reef Initiative 2024; NOAA Coral Reef Watch 2024). Zeng et al. (2025), Communications Earth & Environment, report a threshold regression in which annual bleaching extent exceeding approximately 7.9 percent (95% CI 7.6–9.3), derived from a threshold regression across 9 of 10 regions after exclusion of South Asia ($R^2 = 0.60$, $p < 0.01$), is associated with sustained coral degradation. It is a regional statistical association, not an experimentally demonstrated universal bifurcation, and annual bleaching extent is not equivalent to annual mortality or species loss. The 2025 Global Coral Reef Report concluded that the first climate tipping point has been reached and that extensive reefs as currently constituted will be lost without drastic mitigation. Concurrently, the open ocean has lost approximately 2 percent of its total oxygen inventory since 1960 (Schmidtko et al. 2017, Nature), and oxygen minimum zones are expanding (Breitburg et al. 2018, Science).

These indicators are not independent losses in a marine ecosystem tangential to human survival. They are the earliest observable stages of the same causal architecture that produced multi-million-year reef gaps and coupled marine-terrestrial extinctions in every Big Five event on the paleoclimate record. The atmosphere and the ocean are one biogeochemical system; the marine biosphere supplies approximately half of the oxygen the terrestrial biosphere breathes; and the paleoclimate record contains no examples in which the marine biosphere collapsed and the terrestrial biosphere did not follow. This coupling is the empirical basis for treating reef bleaching, ocean acidification, and ocean deoxygenation as leading indicators of terrestrial as well as marine biosphere risk in the contemporary analog.

Figure 1.

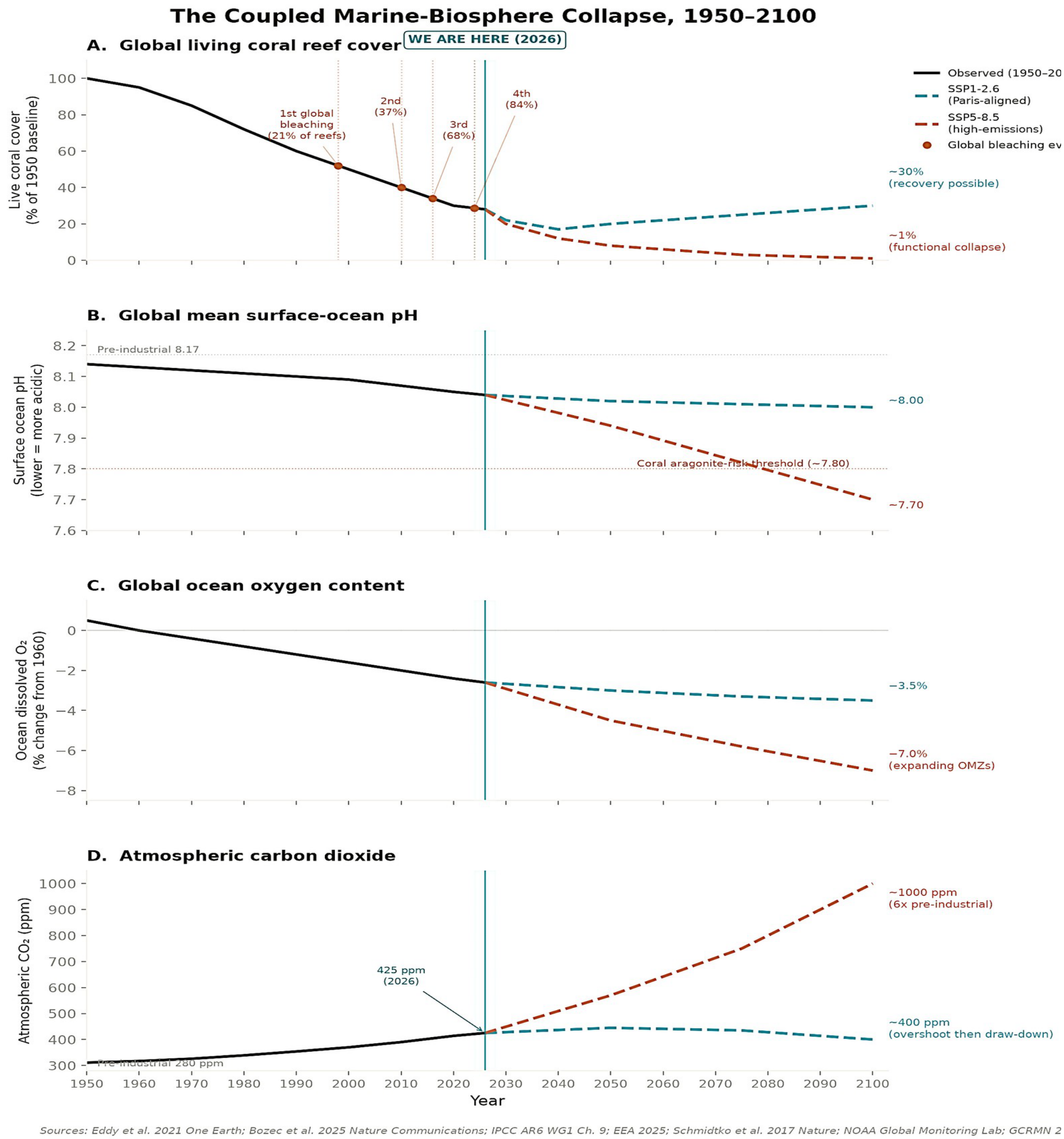

Figure 1. *Decadal trajectory of four coupled marine-biosphere indicators, 1950-2100. Panel A: global living coral reef cover as a percent of the 1950 baseline; solid dots mark the four global bleaching events on record with the percent of world's reefs affected. Panel B: global*

mean surface-ocean pH; the dotted line at 7.80 marks the aragonite saturation threshold widely considered a risk boundary for reef-building corals. Panel C: percent change in global ocean dissolved-oxygen content relative to 1960. Panel D: atmospheric CO2 concentration. Historical data (solid black) are from peer-reviewed monitoring; projections (dashed) show SSP1-2.6 (Paris-aligned) and SSP5-8.5 (high-emissions) scenarios from IPCC AR6 and Bozec et al. 2025. Sources: Eddy et al. 2021; Bozec et al. 2025; IPCC AR6 WG1 Chapter 9; European Environment Agency 2025; Schmidtko et al. 2017; NOAA Global Monitoring Laboratory; Global Coral Reef Monitoring Network 2026.

Figure 1 (above) traces the coupled marine-biosphere collapse at decadal resolution across four indicators from 1950 to 2100. Living coral reef cover has fallen by approximately half since 1950 and the four global bleaching events (1998, 2010, 2016, 2023-2025) show sharply escalating amplitude, with the fourth affecting 84 percent of the world's reefs. Surface-ocean pH has already dropped from a pre-industrial 8.17 to about 8.04, and the ocean's dissolved-oxygen inventory has declined roughly 2.6 percent since 1960. Atmospheric CO2 has crossed 425 ppm, a level unprecedented in at least the past three million years. Two future trajectories are shown: SSP1-2.6, the Paris-aligned scenario in which warming is held below 2 degrees Celsius and partial reef recovery is possible in the latter half of the century; and SSP5-8.5, in which unmitigated emissions drive ocean pH toward 7.70, ocean oxygen loss toward 7 percent, and functional reef collapse by 2080-2100 (Bozec et al. 2025, Nature Communications; IPCC AR6 WG1 Chapter 9).

The four panels are not independent indicators. They are four measurements of a single causal architecture. Atmospheric CO2 (Panel D) sets the forcing; ocean acidification (Panel B) and ocean deoxygenation (Panel C) are the direct chemical consequences; and living reef cover (Panel A) is the ecological output where those chemical changes register first because reef-building corals sit at the intersection of temperature, pH, and oxygen tolerance. This is the same sequence documented in the End-Permian, Late Devonian, and Cretaceous-Paleogene records (Bond and Grasby 2017; Payne and Clapham 2012), operating approximately one to two orders of magnitude faster today than at any point in the Phanerozoic paleoclimate record (Zeebe et al. 2016). The distance between the SSP1-2.6 and SSP5-8.5 trajectories in every panel quantifies what remains within human policy control across the 2035-2050 window; the distance between the observed line and the pre-industrial reference in each panel quantifies what has already been committed.

2.5 The Consensus Causal Chain

The peer-reviewed consensus mechanism for the Big Five mass extinctions can be stated as follows:

Massive volcanic CO_2 injection → rapid global warming → ocean thermal stratification → ocean deoxygenation → ocean acidification → collapse of marine calcifiers and reef ecosystems → loss of marine primary productivity and atmospheric O_2 contribution → cascading terrestrial hypoxic and thermal extinction → multi-million-year reef gap and coupled biosphere recovery.

This mechanism is documented in Bond and Grasby 2017 and reinforced in the comprehensive synthesis published in Biological Bulletin 2022 on ocean deoxygenation and animal evolution.

2.6 Quantitative Anchors: The Contemporary Analog Against the Paleoclimate Baseline

The consensus causal chain in Section 2.5 is not an abstraction. Each link in the chain can be quantified for the present day and compared against the paleoclimate record. The eight indicators below anchor the analog.

Coral reefs. The 2023-2025 fourth global bleaching event affected 84 percent of the world's reefs, the largest event ever recorded (GCRMN 2026; Reimer et al. 2024, Nature). Heavily calcified reef-builders suffered preferential extinction at every Big Five event, with reef-recovery intervals ranging from approximately 5 to 15 million years (Section 2.4).
Surface-ocean pH declined from 8.11 in 1985 to 8.04 in 2024, an increase in hydrogen-ion activity of approximately 18 percent over that interval (EEA 2025). Relative to the pre-industrial baseline, the decline of approximately 0.1 pH unit corresponds to an increase in hydrogen-ion activity of approximately 26 percent. Where a 40 percent figure is used elsewhere in the literature, it references a different baseline and interval; baselines are stated explicitly here to avoid conflation.

Ocean oxygen. The open ocean has lost approximately 2 percent of its total oxygen inventory since 1960 (Schmidtko et al. 2017, Nature, via NOAA; IUCN 2019). Isotopic reconstruction of Oceanic Anoxic Event 2 (~94 Ma) shows that the pre-OAE2 deoxygenation rate was comparable to the current anthropogenic trajectory (Ostrander et al. 2017, Science, via Woods Hole). Independent synthesis concludes that anthropogenic greenhouse-gas emissions now exceed those associated with major past deoxygenation events, including the End-Permian, and that the rate of forcing is faster (Sciscio et al. 2023, Earth-Science Reviews).

Global surface temperature. The rate of human-driven warming reached 0.27°C per decade for the period 2014-2023, and the human-caused component of warming has reached 1.22°C above pre-industrial (Forster et al. 2024, Earth System Science Data, and IGCC 2024 briefing to UNFCCC). During the Paleocene-Eocene Thermal Maximum, the closest Cenozoic analog, Earth warmed 5-8°C over 15,000-20,000 years, a rate at least an order of magnitude slower than today (Zeebe, Ridgwell and Zachos 2016, Nature Geoscience; Gutjahr et al. 2017, Nature, via GEOMAR). **No documented paleoclimate event of comparable magnitude has failed to force a transition to a new climate state on a timescale of thousands to millions of years.**

2.7 Atlantic Meridional Overturning Circulation.

The AMOC "collapse window" refers to the 95-percent confidence interval within which statistical early-warning signals project a saddle-node bifurcation to occur. Ditlevsen and Ditlevsen 2023, Nature Communications estimated that window as 2025 to 2095, with a central estimate of 2057. "Window opening" in 2025 means observed sea-surface-temperature variance and autocorrelation have entered the parameter range in which collapse becomes statistically probable, not that collapse is imminent. Independent reanalysis using different observational fingerprints places the mean tipping time at 2050 with a 10-90 percent CI of 2037-2064 and estimates the probability of collapse before 2050 at 59 ± 17 percent (Smolders, van Westen and Dijkstra (2024), arXiv preprint 2406.11738 — non-peer-reviewed; excluded from the primary evidence synthesis). Observational-constraint analysis projects roughly 50 percent AMOC weakening by end-century without full collapse (Bellomo et al. 2026, Science Advances). The scientific disagreement is not about whether the AMOC is weakening (high confidence) but about whether the weakening ends in full collapse this century. Section 4.1 develops the AMOC case at length.

Atmospheric CO_2. In 2026, atmospheric CO_2 stands at approximately 432 ppm (NOAA Global Monitoring Laboratory; Wikipedia synthesis of NOAA data), the highest concentration in at least 14 million years (Rae et al. 2023, Science, via Columbia Climate School). The 2024 annual increase of 3.5 ppm was the largest single-year increase in the modern measurement record (WMO Greenhouse Gas Bulletin 2025; NOAA Climate.gov 2025). The current anthropogenic carbon-release rate is unprecedented in the past 66 million years and exceeds the sustained maximum PETM rate by at least an order of magnitude (Zeebe, Ridgwell and Zachos 2016, Nature Geoscience).

Species-loss threshold. In each of the Big Five, the loss of species diversity was itself the mechanism of transition: the point at which surviving ecosystems reorganized into a new climate-adapted state that persisted for millions of years. End-Ordovician approximately 85 percent species loss; Late Devonian approximately 75 percent; End-Permian approximately 81 percent of marine species by rarefaction analysis and approximately 70 percent of terrestrial vertebrates; End-Triassic approximately 80 percent; End-Cretaceous approximately 76 percent (Barnosky et al. 2011, Nature; Stanley 2016, PNAS; Erwin 1999, PNAS). The paleontological definition of mass extinction — at least 75 percent species loss within a geologically brief interval — is precisely the threshold at which the biosphere is documented to have crossed into a new operating regime.

Feedback cascade coincident with the transition. Modern climate science has identified at least 28 amplifying feedback loops presently active (Ripple et al. 2024, BioScience State of the Climate Report). The paleoclimate record shows that mass extinctions were consistently accompanied by a recognizable subset of that cascade. Late Devonian, End-Permian, and End-Triassic events all show evidence of the same core feedback complex: methane clathrate destabilization amplifying volcanic warming, ocean stratification driving deepwater anoxia, enhanced silicate weathering during hyperthermal episodes, and eutrophication from continental erosion (Kidder and Worsley 2010, in Themiopoulou et al. Utrecht 2022 T-J review; Rothman 2010, PNAS; Meyer and Kump 2008, via Themiopoulou et al. 2016, Communicative & Integrative Biology). What differs today is not the identity of the feedbacks but their compression in time: the paleoclimate cascade unfolded over tens of thousands to millions of years, whereas the modern cascade is compressing into a window of decades (Zeebe, Ridgwell and Zachos 2016, Nature Geoscience).

3. The Contemporary Analog

3.1 Current Atmospheric CO_2

The NOAA Global Monitoring Laboratory Mauna Loa monitoring station reports the most recent monthly mean atmospheric CO_2 concentration at 429.12 ppm (July 2026), up from 427.87 ppm in July 2025. This value now exceeds the peer-reviewed reconstruction of the pre-extinction latest Permian atmospheric CO_2 concentration (426 +133/−96 ppmv) reported by Wu et al. 2021.

The WMO Greenhouse Gas Bulletin No. 21 documents that the 2024 global mean surface CO_2 concentration reached 423.9 ± 0.2 ppm, representing a 52 percent increase above pre-industrial (pre-1750) levels. The 2023-to-2024 increase of 3.5 ppm was the largest one-year increase in the modern measurement record.

3.2 Rate of Carbon Addition Without Precedent in 300 Million Years

The most comprehensive peer-reviewed synthesis of the geological record of ocean acidification is Hönisch et al. 2012, Science, "The Geological Record of Ocean Acidification". This paper, a review authored by 21 researchers across the paleoceanography community, concluded that the current anthropogenic perturbation is capable of driving a combination and magnitude of ocean geochemical changes potentially unparalleled in the geological record reviewed by Hönisch et al. (2012), which covers approximately the past 300 million years and identifies no past event that perfectly parallels current projections. The paper defines an "ocean acidification event" as a time interval in Earth's history that involved geologically rapid changes in ocean carbonate chemistry on timescales of less than 10,000 years. The current anthropogenic perturbation occurs on the timescale of centuries. Current acidification is proceeding at almost ten times the rate inferred for the PETM, and the last deglacial transition was approximately two orders of magnitude slower than present change (Hönisch et al. 2012).

Contemporary peer-reviewed and government-authoritative measurements confirm that the acidification and bleaching processes anticipated by that 2012 synthesis are now measurably underway. The European Environment Agency 2025 Ocean Acidification Indicator documents that global mean surface ocean pH declined from 8.11 in 1985 to 8.04 in 2024, corresponding to an 18 percent increase in acidity since 1985 and a 40 percent increase since the pre-industrial era. The Copernicus Marine Environment Monitoring Service 2024 Ocean State Report reports a global open-ocean pH decline rate of −0.017 pH units per decade over 1985–2022. This rate matches the IPCC AR6 (2019) very-likely range of 0.017 to 0.027 pH units per decade.

The 4th Global Coral Bleaching Event, confirmed by NOAA and the International Coral Reef Initiative on April 15, 2024, affected approximately 84 percent of the world's coral reefs across the Atlantic, Pacific, and Indian Ocean basins between early 2023 and mid-2025 — the most extensive and intense global coral bleaching episode ever recorded, and the fourth such event in the past thirty years (Global Coral Reef Monitoring Network, June 2026; Reimer et al. 2024, Coral Reefs). Ainsworth et al. 2025, Communications Earth and Environment (Nature portfolio) further finds that under all three IPCC emission scenarios (SSP1-2.6, SSP2-4.5, SSP5-8.5), and absent increased coral thermal tolerance, annual global bleaching extent will exceed 10 percent consistently from 2020 through 2100, surpassing the range of bleaching thresholds associated with significant coral decline.

3.3 Present-Day Status of Each Extinction-Chain Indicator

Every component of the paleoclimate extinction causal chain is presently active in the Earth system. Contemporary values are cited to peer-reviewed or authoritative government-monitoring sources; paleoclimate values are cited to their primary literature.

Committed ocean deoxygenation extends well beyond the fraction already observed. The analysis cited in Oschlies et al. (2021, Nature Communications) indicates that less than one quarter of the deoxygenation committed by existing warming is realized on near-term observational timescales even under an immediate-emissions-stop assumption. Continued emissions increase the committed loss, while the deep ocean responds over centuries. This does not alter the metric asymmetry disclosed in Figure 4—paleoclimate seafloor anoxia and modern dissolved-oxygen inventory loss remain different measures—but it means the contemporary inventory-loss value should be interpreted as an early-stage signal rather than a completed response.

3.4 The Special Case of Environmental Mercury

Mercury (Hg) is treated separately in this synthesis because it functions in the paleoclimate record as the primary geochemical fingerprint of large igneous province (LIP) volcanism — the ultimate driver of at least three of the Big Five extinctions (Section 2.2) — and because a modern anthropogenic mercury signal of comparable magnitude is now globally measured in remote lake sediments, peat bogs, and glacial ice. Comparing the modern mercury signal to the paleorecord requires care about which units are commensurable; that methodological point is developed first, then applied.

3.4.1 Why mercury, and how it is measured across time

Mercury is a highly volatile element with an atmospheric residence time of ~0.5–1 year and a strong particle-reactive affinity for organic matter in aquatic sediments. When LIP volcanism vents mercury into the atmosphere, the resulting deposition is recorded globally in the organic-rich sediments that also archive extinction-boundary faunas. Reports of mercury in extinction-boundary sections are therefore not local pollution signals but records of a global atmospheric enrichment that mixed rapidly and deposited widely.

The primary metric used in the paleoclimate literature is the Hg/TOC (total organic carbon) enrichment factor — the peak mercury concentration at an event horizon divided by the pre-event background at the same site. Normalizing to TOC controls for the fact that mercury preferentially binds organic matter; without this normalization, apparent mercury spikes can be artifacts of variable sediment organic content. This normalization is conditional rather than universal. Hg/TOC ratios can be inflated by diagenetic degradation of organic matter (Qiu et al. 2022), and determination of sedimentary Hg host phases is required prior to normalization because sulfide-hosted rather than organic-hosted mercury invalidates the TOC denominator (Shen et al. 2020). Subsequent work documents both coupling and decoupling between sedimentary mercury and organic carbon (Qu et al. 2024), and comparative analysis across LIP events finds variable perturbation of the mercury cycle by different volcanogenic processes (Percival et al. 2018). In modern lake and peat sediments the same enrichment-factor approach is applied to sediment cores dating from ~1850 to the present, dividing recent Hg values by a pre-industrial baseline typically taken from the same core at ~1750–1850 CE (Amos et al. 2015, Environmental Science & Technology; Li et al. 2020, ACS Earth and Space Chemistry).

Modern atmospheric mercury is additionally quantified by four operational monitoring networks — the Global Mercury Observation System (GMOS) with ~35–43 stations worldwide (Sprovieri et al. 2024, Atmospheric Environment); the Arctic Monitoring and Assessment Programme (AMAP) mercury network (Braune et al. 2022, Science of the Total Environment); the Minamata Convention Effectiveness Evaluation, which as of the 2026 Open-Ended Scientific Group report aggregates 1,404 national atmospheric mercury monitoring sites and 198 wet-deposition sites worldwide (UNEP OESG 2026, Second Scientific Report); and regional networks including the U.S. NADP Mercury Deposition Network, AMNet, the European EMEP, and WMO GAW. Total global anthropogenic mercury emissions to the atmosphere are currently estimated at approximately 2,000 tonnes per year, with artisanal and small-scale gold mining (ASGM) and coal combustion the two largest source categories.

3.4.2 Quantitative comparison: Enrichment factor across geologic time

Figure 2 presents peak Hg/TOC enrichment factors reported at each of the Big Five mass-extinction boundaries alongside modern anthropogenic enrichment factors from remote lake sediments and industrial-adjacent records. These are not measurements of the same quantity: the paleoclimate values derive from marine sedimentary sections and the modern values from lacustrine and peat archives, with different organic-matter compositions, host phases, and diagenetic histories. The panels are shown together to display magnitude ranges, not to assert numerical equivalence, and no transfer function between the two archive classes is applied.

Figure 2

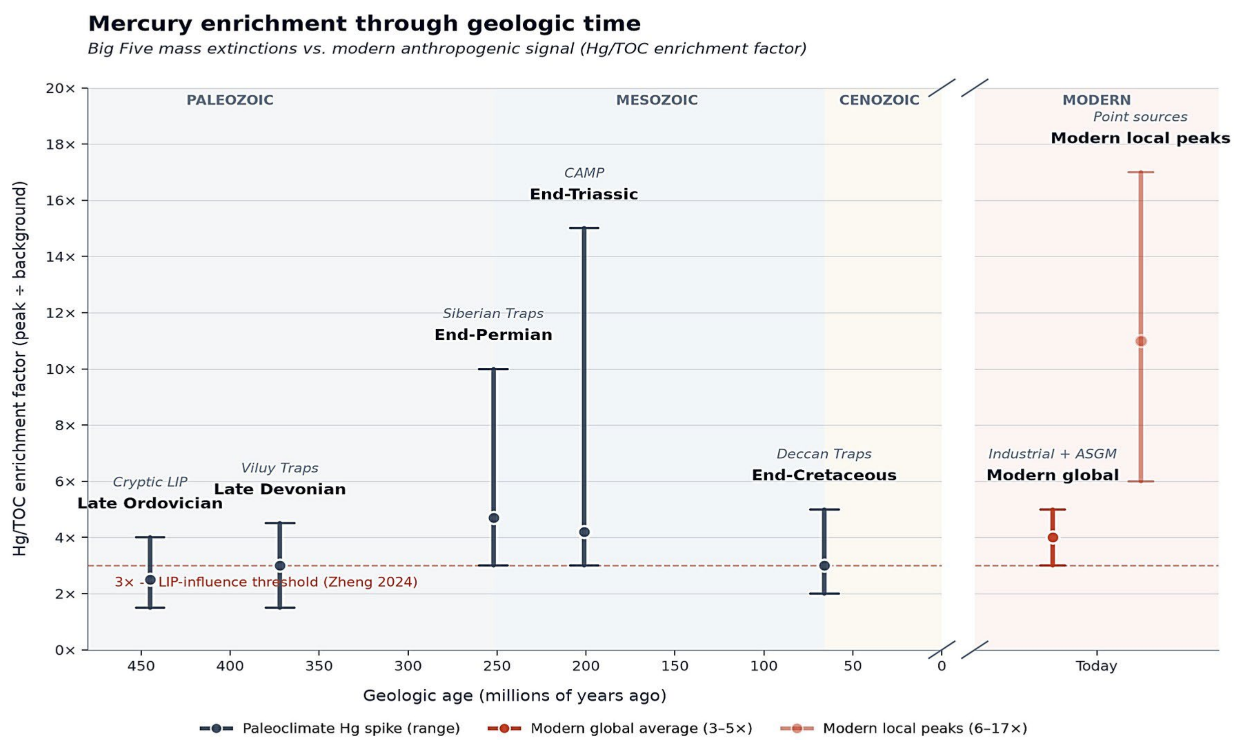

Figure 2. Hg/TOC enrichment factor (peak mercury normalized to total organic carbon, divided by pre-event background) at each of the Big Five mass-extinction boundaries, with the modern anthropogenic global average and modern industrial-adjacent peak values shown below the dotted divider. Shen et al. (2019) report End-Permian Hg enrichment factors rising by factors of 3–8 relative to pre-extinction background. This range is shown as a shaded band rather than a threshold; no validated concentration cutoff separates volcanic from non-volcanic mercury delivery. Paleoclimate ranges compiled from Grasby et al. (2019), Mercury as a proxy for volcanic emissions in the geologic record, Earth-Science Reviews, 196, 102880; Percival et al. 2017, PNAS; Fox et al. 2022, Nature Communications; Shen et al. (2019), Nature Communications, 10, 1563; Bergström et al. 2019, Scientific Reports; and Zhou et al. 2024. Modern global-remote value from Amos et al. 2015, Li et al. 2020, and Selin et al. 2008, Global Biogeochemical Cycles. Modern local peak from Yohn et al. 2009, Environmental Science & Technology.

The chart shows reported enrichment-factor ranges across deep-time marine sections and modern remote and industrial-adjacent archives. Because those archive classes differ in depositional environment, organic-matter composition, host phases, background definitions, and diagenetic history, visual overlap is descriptive only and does not establish numerical equivalence or a validated source threshold. Delivery durations are discussed separately and are not converted into rate comparisons unless magnitude and baseline definitions are commensurable.

Figure 3 (below) plots the same values on an XY axis with geologic age on the x-axis (with a clearly marked axis break separating deep geologic time from the modern zone) and the enrichment factor on the y-axis. This second presentation emphasizes the temporal relationship: the modern anthropogenic value is a spike sitting in the same range as the largest extinctions of the Phanerozoic Eon, delivered orders of magnitude faster. Mercury enrichment factor plotted against geologic age. Vertical whiskers show the published range of Hg/TOC enrichment factor at each event horizon; filled circles are the reported midpoint or mean. Eras shaded (Paleozoic, Mesozoic, Cenozoic); axis break separates paleoclimate zone from modern zone. Shen et al. (2019) report End-Permian Hg enrichment factors of 3–8 relative to pre-extinction background; this interval is treated as a reported range, not a validated threshold. Sources as in

Figure 3

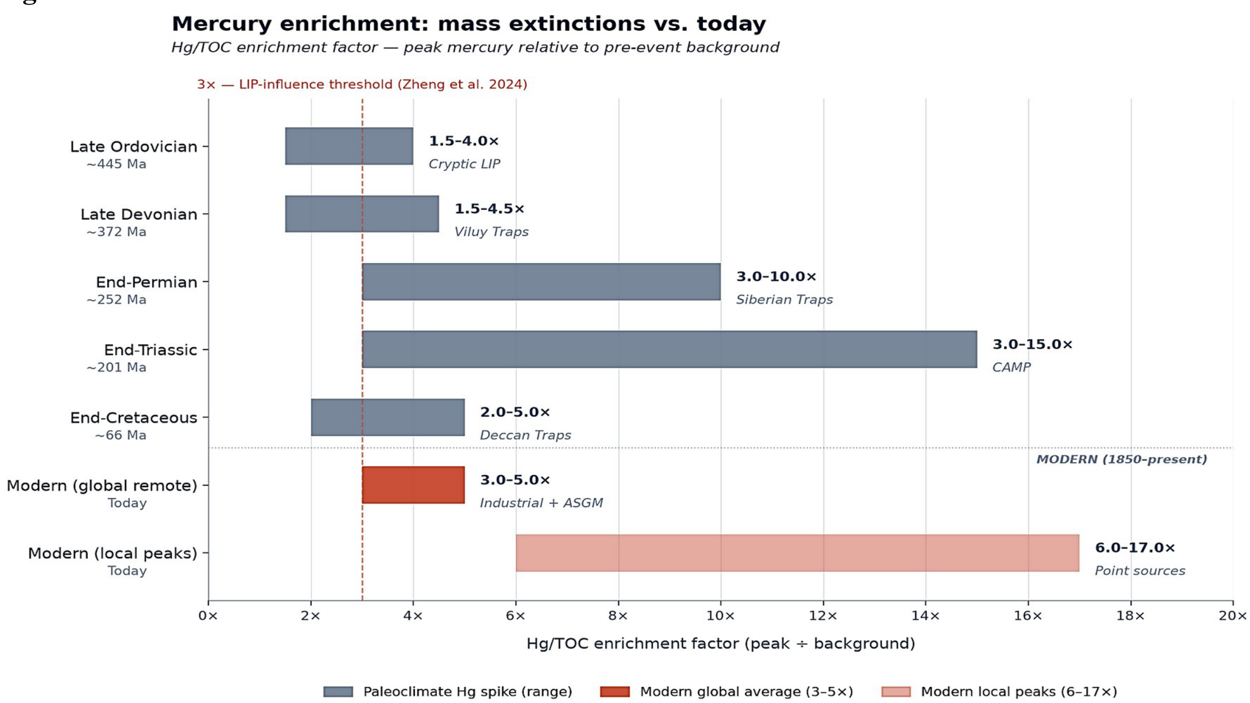

***Figure 3** plots the same values on an XY axis with geologic age on the x-axis (with a clearly marked axis break separating deep geologic time from the modern zone) and the enrichment factor on the y-axis. This second presentation emphasizes the temporal relationship: the modern anthropogenic value is a spike sitting in the same range as the largest extinctions of the Phanerozoic Eon, delivered orders of magnitude faster. Mercury enrichment factor plotted against geologic age. Vertical whiskers show the published range of Hg/TOC enrichment factor at each event horizon; filled circles are the reported midpoint or mean. Eras shaded (Paleozoic, Mesozoic, Cenozoic); axis break separates paleoclimate zone from modern zone. The dashed red horizontal line marks the 3× threshold above which the paleoclimate literature identifies mercury-isotope evidence for LIP volcanic delivery (Zheng et al. 2024). Sources as in*

Reading top to bottom, six indicators normalized to End-Permian peak = 100%

1. **Atmospheric pCO_2:** 7% of Permian peak. But the End-Permian delivered its +2,100 ppm over ~75,000 years; we have delivered +140 ppm over ~175 years.

2. **Mercury enrichment:** 40% of Permian peak. Already inside the End-Permian range for local sections. Delivered over ~125 years vs. ~168,000 years.

3. **Ocean warming:** 16% of Permian peak. +1.55 °C vs. +8 to +10 °C. Delivered over ~175 years vs. ~75,000 years.

4. **Ocean deoxygenation:** The global ocean has lost 4.8 ± 2.1 petamoles of dissolved oxygen since 1960, exceeding 2 percent of the total inventory (Schmidtko, Stramma & Visbeck 2017). Paleoclimate reconstructions of End-Permian conditions report the fraction of seafloor area that became anoxic. Oxygen inventory and anoxic seafloor area have different denominators and different response dynamics; they are reported separately here and are not combined into a single ratio."

5. **Ocean acidification:** ~14% of Permian peak. −0.1 pH units vs. −0.6 to −0.7. Delivered over ~175 years vs. only ~10,000 years — the Permian's fastest driver, and the one where the rate gap is smallest.

6. **Cascading calcifier loss:** Living coral cover has declined by approximately 50 percent globally between 1957 and 2007 (Eddy et al. 2021). This is an ecosystem-condition indicator. It is not a measure of marine species extinction and is not expressed here as a fraction of any paleoclimate extinction magnitude.

Delivery-duration ratios are reported separately by driver rather than averaged. Atmospheric CO_2: the End-Permian perturbation is reconstructed over approximately 168,000 years against approximately 175 years of industrial-era accumulation, a duration ratio of approximately 960:1. Ocean warming: approximately 75,000 years against approximately 175 years, a ratio of approximately 430:1. These are ratios of elapsed time, not of rate. A duration ratio equals a rate ratio only where total change is comparable, which is not the case here; the End-Permian magnitudes substantially exceed modern values in every indicator shown. Rate comparison requires magnitude-normalized calculation, which is not attempted in this figure.

Figure 4.

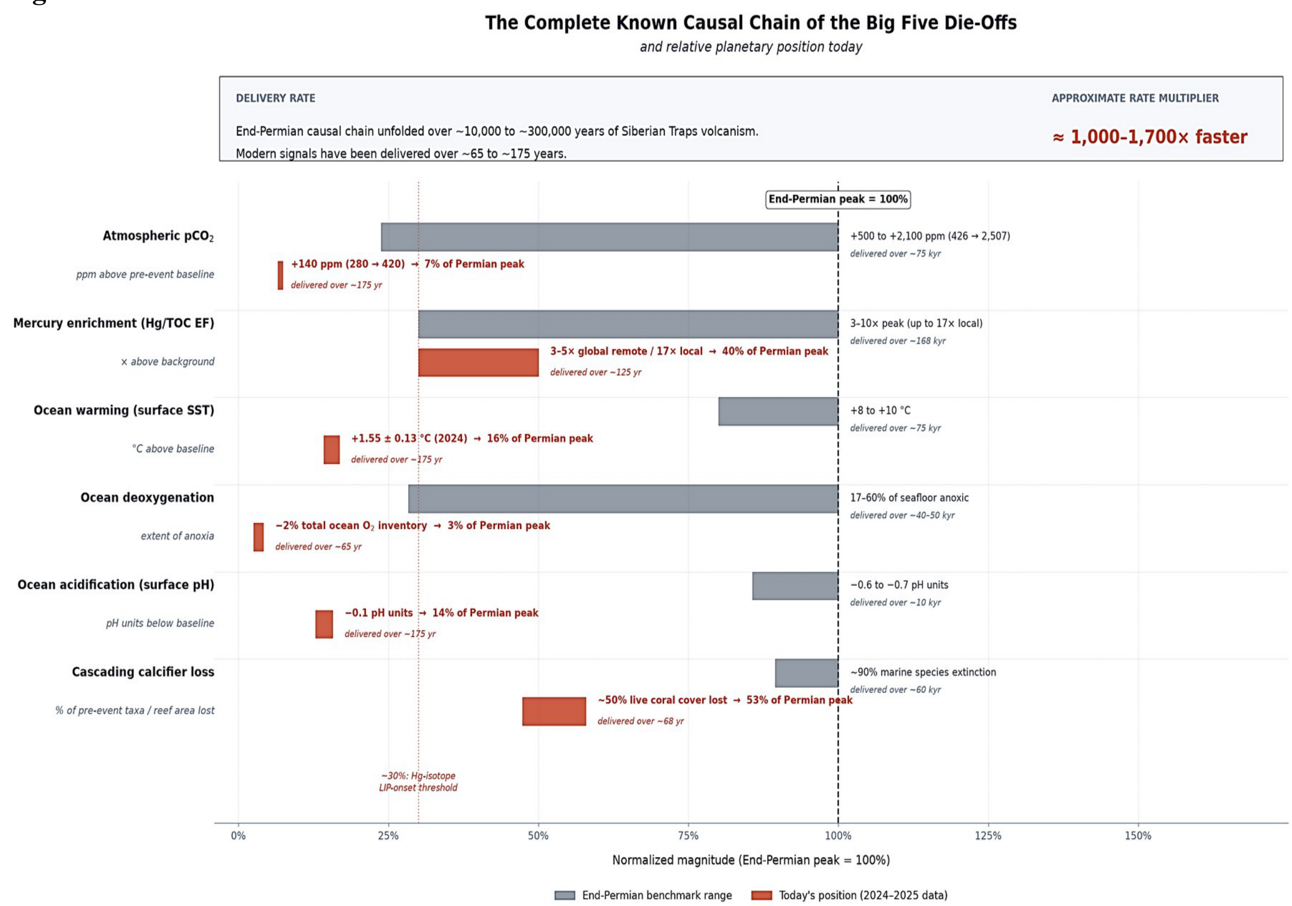

Figure 4.

Delivery-duration ratios are reported separately by driver rather than averaged. Atmospheric CO_2: the End-Permian perturbation is reconstructed over approximately 168,000 years against approximately 175 years of industrial-era accumulation, a duration ratio of approximately 960:1. Ocean warming: approximately 75,000 years against approximately 175 years, a ratio of approximately 430:1. These are ratios of elapsed time, not of rate. A duration ratio equals a rate ratio only where total change is comparable, which is not the case here; the End-Permian magnitudes substantially exceed modern values in every indicator shown. Rate comparison requires magnitude-normalized calculation, which is not attempted in this figure.

3.4.3 The three-phase timing pattern in the paleoclimate record

The mercury spike is not synchronous with biotic extinction in a single instant. The peer-reviewed record consistently identifies three phases in the mercury–extinction sequence:

Phase 1 — Precursor loading. Mercury enrichment appears in the sedimentary record hundreds of thousands of years before the extinction horizon. At the End-Triassic, Lindström et al. 2019, Science Advances, documents Central Atlantic Magmatic Province (CAMP) mercury emissions beginning approximately 100,000 years before the extinction horizon. At the End-Permian, research from the University of Birmingham (2025) identifies terrestrial mercury anomalies indicating vegetation collapse approximately 270,000 years before the marine extinction horizon.

Phase 2 — Coincident peak. Mercury enrichment reaches its maximum at or immediately adjacent to the extinction horizon itself. Percival et al. (2017), PNAS, report clear increases in Hg and

Hg/TOC at the end-Triassic extinction horizon across six geographically widespread marine and terrestrial records in both hemispheres, in the form of multiple pulsed peaks separated by intervals of roughly 200 kyr — evidence of episodic rather than continuous volatile release. Wang et al. 2018, Global and Planetary Change, documents mercury concentrations reaching approximately 900 ppb against a pre-event background near 100 ppb at the End-Permian marine horizon.

Phase 3 — Persistent elevation through recovery. Mercury enrichment remains elevated after the extinction event, with sediments deposited during the depauperate "dead zone" interval continuing to record volcanic mercury flux until the LIP eruptions wane and marine ecosystems begin to recover. Thibodeau et al. 2016, Nature Communications, documents this Phase 3 pattern in exceptional detail at the Muller Canyon section in Nevada, showing that mercury values fall only as biological recovery begins.

An important caveat is documented in Zhou et al. 2024, Earth-Science Reviews: while the End-Permian and End-Triassic mercury signals are strongly consistent with LIP influence when concentration and isotope evidence are considered together, the Late Ordovician and Late Devonian enrichments are less consistently associated with a change in Hg source and may reflect local redox-driven cycling. No single Hg/TOC cutoff is treated here as a validated discriminator of volcanic delivery.

3.4.4 Interpretation: The present as precursor phase

Applying the paleoclimate timing framework to the present

The modern global anthropogenic mercury enrichment factors reported from remote lake and peat archives overlap some published paleoclimate Hg/TOC ranges, but the archive classes are not directly commensurable. Differences in depositional environment, organic matter, host phases, background definitions, and diagenetic histories preclude treating numerical overlap as a validated source attribution or extinction threshold.

Modern industrial-adjacent peak values of 6–17× (e.g., Lake Michigan sediments; Yohn et al. 2009) exceed most End-Permian sections and are comparable to End-Triassic sections. The delivery rate is not comparable in the same direction. The End-Permian mercury pulse was delivered over approximately 100,000–300,000 years of Siberian Traps volcanism. The modern anthropogenic pulse has been delivered over approximately 175 years since the onset of industrialization. On a rate basis, the modern signal exceeds the paleoclimate signal by approximately three orders of magnitude.

Applied to the three-phase timing model, the modern signal aligns with Phase 1 (precursor loading) — a large mercury signal delivered ahead of, and simultaneously with the earliest indicators of, the ecological collapse cascade documented in Section 3.3. The Phase 2 (coincident extinction) and Phase 3 (post-extinction persistence) segments of the paleoclimate template have not yet been produced by the current perturbation. Two important interpretive constraints are stated explicitly:

Enrichment-factor magnitude is not extinction magnitude. The mercury signal is the fingerprint of the causal driver, not the extinction outcome. The Big Five events were driven by the entire causal chain described in Section 2.5 — volcanic CO_2 injection, ocean warming, deoxygenation,

acidification, and cascading loss of marine calcifiers — of which mercury toxicity was a contributor rather than the sole killing mechanism.
The mercury signal is a necessary but not sufficient indicator. Not every geologic interval showing mercury enrichment produced a mass extinction. However, every LIP-driven Big Five extinction was preceded by and accompanied by mercury enrichment matching or exceeding the modern global signal, and the association is now supported by mercury-isotope fingerprinting for the End-Permian and End-Triassic events.

Within these constraints, the interpretation of Figures 1 and 2 supported by the peer-reviewed literature is direct: the modern anthropogenic mercury enrichment signal is not a subtle deviation from geological background. Plotted against 445 million years of Earth history, it slots into the enrichment range that accompanied the largest mass-extinction events of the Phanerozoic Eon.

3.5 The Structural Parallel: Reiterating the Causal Chain

The paleoclimate record does not identify a single atmospheric CO_2 concentration that functions as a universal extinction threshold. Rather, it identifies a pattern — the causal chain described in Section 2.5 — that has consistently produced mass extinction whenever it has been activated in Phanerozoic history.

Restated with contemporary indicators inserted, the causal chain now reads:

Massive carbon injection (present: ~40 Gt CO_2/yr anthropogenic, record 3.75 ppm/yr increase in 2024) → rapid global warming (present: +1.55 °C above pre-industrial in 2024, warmest year in the 175-year record) → ocean thermal stratification and deoxygenation (present: ~2% global O_2 loss since 1960, hypoxic volume quadrupled) → ocean acidification (present: pH 8.11 → 8.04 since 1985, +40% acidity vs pre-industrial, rate likely without precedent in 300 million years) → collapse of marine calcifiers (present: 4th Global Coral Bleaching Event affecting 84% of the world's reefs, 2023–2025) → cascading terrestrial extinction (documented as the third mode of the causal chain at End-Permian, End-Triassic, and End-Cretaceous events) → multi-million-year reef gap (paleoclimate outcome; 5–15 Myr per Big Five event).

Every link in this chain is currently active and measured. The current anthropogenic perturbation is capable of driving a combination and magnitude of ocean geochemical changes potentially unparalleled in the geological record reviewed by Hönisch et al. (2012), which covers approximately the past 300 million years and identifies no past event that perfectly parallels current projections.

4. Amplifying Feedback Loops as Accelerants

The peer-reviewed climate literature has now systematically enumerated the physical and biological feedback loops that can amplify the warming and Earth-system disruption described in Section 3. The most comprehensive published enumeration is Ripple, Wolf, Lenton, Gregg, Natali, Duffy, Rockström, and Schellnhuber 2023, One Earth, "Many risky feedback loops amplify the need for climate action", which identifies 41 biogeophysical feedback loops (20 physical and 21 biological), of which 27 are amplifying (reinforcing), 7 are dampening (balancing), and 7 are of uncertain sign. That paper is the primary reference for this section. Additional peer-reviewed enumeration and interaction analysis is provided by Wunderling et al. 2024, "Climate tipping point interactions and cascades: a review," Earth System Dynamics and the Global Tipping Points Report 2023, Chapter 1.5.

The principal amplifying loops identified in ripple et al. 2023 and the broader peer-reviewed literature are:

1. Physical (albedo, radiative, cryospheric)

2. Water vapor feedback — warming increases atmospheric water vapor, itself a potent greenhouse gas, driving further warming (Planck-scale radiative feedback).

3. Snow and sea-ice albedo feedback — melting snow and sea ice reveal darker land and ocean surfaces, reducing planetary reflectivity and increasing absorbed solar radiation.

4. Arctic amplification — the combined effect of albedo, lapse-rate, and other feedbacks that warm the Arctic at 2–4 times the global mean rate.

5. Cloud feedback — net-positive per IPCC AR6, driven principally by reductions in low-cloud cover and changes in cloud altitude in a warmer atmosphere.

6. Ocean CO_2 solubility feedback — warmer oceans hold less dissolved CO_2, reducing the ocean carbon sink.

7. Cryospheric collapse and long-term sea-level feedbacks

8. Greenland Ice Sheet loss — meltwater lubrication, elevation–mass-balance feedback, and albedo decline all reinforce further melt once thresholds are crossed.

9. West Antarctic Ice Sheet collapse — marine ice-cliff and marine ice-sheet instabilities produce potentially self-sustaining retreat.

10. AMOC (Atlantic Meridional Overturning Circulation) slowdown — freshwater input from ice melt weakens deep-water formation, altering global heat transport and monsoon patterns. This feedback is treated in detail in Section 4.1 below given the volume of new peer-reviewed evidence published in 2023–2026.

11. Biological — Carbon-Cycle Amplifiers

12. Permafrost thaw and CO_2/CH_4 release — thawing Arctic and boreal permafrost releases ancient organic carbon as CO_2 and methane.

13. Methane hydrate/clathrate release — destabilization of seafloor and permafrost methane hydrates under warming (magnitude highly uncertain but potentially large).

14. Wildfire carbon release — increased fire frequency and severity in boreal, temperate, and tropical ecosystems releases stored biomass carbon and reduces future sink capacity.

15. Boreal forest dieback — heat, drought, and pest outbreaks convert boreal carbon sinks into carbon sources.

16. Amazon and tropical forest dieback — drought, fire, and deforestation combine to push tropical rainforests toward savannization.

17. Peatland decomposition and burning — drying and smoldering peatlands, particularly in the tropics and boreal zones, release large stored carbon reserves.

18. Soil organic carbon respiration — warming accelerates microbial respiration of soil organic matter, releasing CO_2.

19. Ocean biological pump weakening — warming, stratification, and deoxygenation reduce the ocean's capacity to sequester carbon in the deep ocean.

Ripple et al. 2023 further note that current climate models likely underestimate the acceleration of global warming because many of these amplifying loops — particularly the biological loops involving permafrost, forests, soil carbon, and peatlands — are not fully represented in the coupled Earth-system models used for IPCC projections. Wunderling et al. 2024 emphasize that these loops are not independent; interactions among them can produce cascading tipping dynamics in which the crossing of one threshold accelerates the crossing of others.

4.1 The AMOC as an Active Tipping Element

Of the feedback loops enumerated above, the Atlantic Meridional Overturning Circulation (AMOC) — the system of ocean currents that carries warm surface water northward in the Atlantic and returns cold, dense water southward at depth — warrants extended treatment because it is (a) directly observable, (b) currently showing signs of weakening, (c) associated with several proposed early-warning signals, and (d) the subject of an unusually visible and unresolved scientific debate about the proximity of a tipping point.

IPCC AR6 baseline assessment. The most recent Intergovernmental Panel on Climate Change assessment (IPCC AR6 WG1 Chapter 9 and Summary for Policymakers, 2021) concluded, with high confidence, that AMOC is very likely to weaken over the 21st century for all emissions scenarios, while assigning only low confidence to the magnitude of the trend and medium confidence that an abrupt collapse will not occur before 2100. Projected decline by 2100 ranges from 24 percent (SSP1-2.6) to 39 percent (SSP5-8.5) with medium confidence.

Observed weakening. The peer-reviewed synthesis by Rahmstorf et al. 2026 (in review, EGUsphere), "The AMOC is weakening – time to take the evidence seriously" concludes that multiple independent lines of evidence — proxy reconstructions, surface-fingerprint indices, and the direct RAPID mooring array — support a past and ongoing AMOC slowdown. Quantitatively, the RAPID array trend is approximately −0.8 ± 0.7 Sverdrups per decade over 2004–2023, with multiple indicators consistent with a weakening of roughly 2 ± 1 Sv since the mid-twentieth century. Volkov et al. (2026), Science Advances reports a meridionally consistent decline in the observed western boundary contribution to AMOC across two decades of measurements. A contrasting analysis by Chen and Tung 2024, Nature Communications attributes a near-stalling of the anthropogenic weakening since the early 2010s to a natural North Atlantic Oscillation signal, indicating that the observed weakening trend is not monotonic.

Tipping-point estimates. Statistical analysis of early-warning signals — critical slowing down, loss of variance, and increased autocorrelation — has generated the most consequential recent claims. Ditlevsen and Ditlevsen 2023, Nature Communications estimated a 95 percent confidence interval for AMOC tipping between 2025 and 2095, with a central estimate of approximately 2057, under the current emissions trajectory. Van Westen et al. 2024, Science Advances developed a physics-based early warning signal based on AMOC-induced freshwater transport at the Atlantic's southern boundary and concluded that reanalysis products indicate the present-day AMOC is on a tipping course. Wunderling et al. 2024 (arXiv preprint) estimates a critical threshold at approximately +3 °C global mean surface temperature above pre-industrial (lower bound +2.2 °C), reached after approximately 2050, with a resulting more-likely-than-not (≥50 percent) probability of AMOC tipping in the 21st century under a middle-of-the-road scenario, and very likely (≥90 percent) under a high-emissions scenario.

Countervailing model evidence. These early-warning-based estimates conflict with results from coupled climate model ensembles. Baker et al. 2025, Nature reports that across 34 climate models subjected to extreme greenhouse gas and North Atlantic freshwater forcings, upwelling in the Southern Ocean sustains a weakened AMOC in all cases and prevents complete collapse (defined as weakening below 6 Sv) within the 21st century. A 2025 Nature Geoscience study reports "limited weakening" of 18–43 percent (3–6 Sv) by 2100 even under a very-high emissions scenario (summarized in Carbon Brief AMOC Explainer, 2026). This model-observation disagreement is itself a source of scientific concern rather than reassurance: it indicates that the physical mechanisms controlling the tipping threshold are not yet reliably represented in the models on which policy projections depend.

Consequences of an AMOC collapse. Even a partial slowdown would substantially alter global climate. Nnamchi et al. 2025, Nature documents that an AMOC slowdown drives widespread shifts in tropical rainfall through propagation of high-latitude cooling into the tropical North Atlantic. Van Zomeren et al. 2026, Communications Earth and Environment shows that an AMOC collapse would produce substantial oceanic carbon release and additional global warming; at CO_2 concentrations of 350 ppm or higher, the system exhibits bistable behavior — meaning that once collapsed, AMOC cannot recover under contemporary boundary conditions.

Paleoclimate relevance. The AMOC feedback is directly relevant to the paleoclimate analog developed in this report. Rapid changes in ocean overturning circulation are documented at multiple Big Five extinction boundaries, most robustly the End-Permian, where thermal stratification and reduced deep-water ventilation contributed directly to the deep-ocean anoxia identified as the primary proximal killer (Bond and Grasby 2017; Sperling et al. 2022, Biological Bulletin). A contemporary AMOC slowdown, coupled with the ocean deoxygenation already documented in Section 3.3, would represent a modern activation of the same mechanism.

Summary of current scientific status. The peer-reviewed record supports the following statements without hedging: (i) AMOC has weakened relative to mid-twentieth-century values; (ii) AMOC will very likely continue to weaken through the 21st century; (iii) an AMOC collapse would produce severe and largely irreversible consequences for global climate; (iv) whether the collapse threshold will be crossed within the 21st century remains contested between statistical early-warning analyses (which suggest yes, plausibly mid-century) and coupled climate model ensembles (which suggest no, not within the 21st century). This is a live scientific controversy in which the observational and statistical evidence has strengthened since IPCC AR6 was finalized in 2021.

4.2 Paleoclimate Consistency with Feedback Amplification

The paleoclimate record is consistent with this feedback-amplified interpretation. The transition from the latest Permian to the End-Permian extinction interval — a fourfold to sixfold rise in atmospheric CO_2 over an interval whose full duration remains a subject of ongoing chronostratigraphic refinement — cannot be attributed to LIP degassing alone; peer-reviewed synthesis attributes the magnitude and rate to LIP forcing coupled with amplifying feedbacks including permafrost carbon release, methane hydrate destabilization, terrestrial vegetation collapse, and ocean-carbon-cycle feedbacks (Bond and Grasby 2017; Clarkson et al. 2015).

The feedback-phase duration in the paleoclimate record

The paleoclimate record constrains not only which feedbacks engaged during prior extinctions but how long the feedback-dominated phase lasted before terminal biotic loss. Four of the Big Five events are dated to sub-100-kyr precision: the End-Permian main marine pulse at 60,000 ± 48,000 years (Burgess, Bowring and Shen 2014, *PNAS*); the End-Triassic CAMP $\delta^{13}C$ excursion and associated anoxia interval at approximately 20,000–50,000 years (Jost et al. 2017, *Geochemistry, Geophysics, Geosystems*); the End-Cretaceous carbon-cycle perturbation at less than 5,000 years, with extinction synchronous with the Chicxulub impact to within 32,000 years (Renne et al. 2013, *Science*); and the PETM benthic-foraminifera mass extinction at approximately 1,000 years within a 200-kyr full excursion (McInerney and Wing 2011, *Annual Review of Earth and Planetary Sciences*). The median of these four values is approximately 20,000 years; the median excluding the PETM hyperthermal is 35,000 years.

Two conclusions follow. First, once positive feedbacks engaged in the ocean-atmosphere system — the isotopic and geochemical signature of the feedback cascade in the rock record — the interval to terminal biotic loss was measured in tens of thousands of years across every well-dated event. Second, the recovery of coral-reef ecosystems following each of these events required 5 to 15 million years. The destruction phase was two to three orders of magnitude shorter than the recovery. Feedbacks, of course, compress the timescale on which the system is lost; they do not compress the timescale on which it is rebuilt.

In every Big Five event dated to sub-100-kyr precision, the interval between the geochemical onset of the positive-feedback cascade and terminal biotic loss was measured in tens of thousands of years. For example, the End-Permian main pulse resolves to 60,000 ± 48,000 years (Burgess et al. 2014); the End-Triassic to 20,000–50,000 years (Jost et al. 2017); the End-Cretaceous carbon perturbation to under 5,000 years (Renne et al. 2013); the PETM benthic extinction to approximately 1,000 years (McInerney and Wing 2011). The median is on the order of 20,000 to 35,000 years. Recovery required 5 to 15 million years. Historically, The destruction phase, once feedbacks engage, runs two to three orders of magnitude faster than the reconstruction phase.
Anthropomorphic acceleration

Evidence has accumulated that the 5 Indicators are accelerating mainly due to the increase in the number and intensity of environmental feedbacks which have in turn have been catalyzed and energized by the unprecedented rate of anthropogenically-determined global heating. This makes the operative planning horizon measurable in decades, not centuries.

Paleoclimate Feedback-Phase Durations

Event	Duration	Source
End-Permian main marine pulse	60,000 ± 48,000 yr	Burgess, Bowring & Shen 2014, PNAS
End-Triassic CAMP anoxia interval	20,000–50,000 yr	Jost et al. 2017, Geochemistry Geophysics Geosystems
End-Cretaceous carbon perturbation	<5,000 yr	Renne et al. 2013
PETM benthic extinction	~1,000 yr	McInerney & Wing 2011
Median across events	~20,000 yr	(paper's stated median)

Anthropogenic rate multipliers

- The contemporary rate of carbon release has been at least 10× the sustained maximum PETM rate (Zeebe, Ridgwell & Zachos 2016, Nature Geoscience)
- The contemporary rate of ocean acidification has been roughly 10× the PETM rate (Hönisch et al. 2012, Science)

Compression logic — the three phases

Feedback-phase compression is not uniform. Different components of the cascade have different sensitivities to forcing rate. The compression factor must therefore be phase-specific:

Early Phase — feedback engagement and threshold crossings

- What happens: Individual feedback loops cross their engagement thresholds (permafrost thaw begins, AMOC weakens past bifurcation, ocean-atmosphere CO_2 exchange reverses in tropical zones, etc.).
- Rate sensitivity: Near-linear with forcing rate. Faster forcing crosses thresholds proportionally faster.
- Compression factor: ~10× (matches the forcing-rate multiplier)

Middle Phase — cascade propagation

- What happens: Engaged feedbacks amplify each other. Warming triggers deoxygenation triggers calcifier loss triggers marine ecosystem collapse. Ice sheet loss triggers albedo change triggers accelerated warming.
- Rate sensitivity: Partial. Some propagation rates are rate-limited (chemical equilibration times, ecosystem response), others are set by intrinsic physical timescales (ice sheet flow dynamics, deep-ocean mixing).
- Compression factor: ~3–5×

Late Phase — terminal biotic loss and irreversibility

- What happens: Full mass-extinction dynamics. Marine biosphere collapse, terrestrial ecosystem restructuring, geochemical equilibration.
- Rate sensitivity: Low. Dominated by intrinsic feedback timescales (deep-ocean overturning, weathering feedbacks, ecosystem recovery time constants) that operate on their own physical clocks regardless of how quickly the forcing was applied.
- Compression factor: ~1–3×

Loss-of-agency calculation

Definition: The loss-of-agency “event” is the point at which the six-intervention portfolio can no longer arrest the cascade even if fully deployed at wartime industrial scale.

Paleo reference: In events with sufficient resolution, "loss of agency" corresponds to the early phase — roughly the first 10–20 percent of the feedback-phase duration. Using the median (20,000 yr), this is 2,000–4,000 years after feedback engagement in the paleoclimate baseline.

Contemporary compression (10× rate factor for early phase):

2,000–4,000 yr ÷ 10 = 200–400 years after feedback engagement

For the contemporary case, "feedback engagement" is expected between 2035 and 2040. Absent coordinated intervention beginning immediately, the effective loss-of-agency moment collapses onto the tipping point itself: 2035–2040. Under intervention, the outer bound is 2035–2440 (200–400 years past the tipping point), but the intervention-dependent framing depends on whether the six-intervention portfolio is deployed at scale in the 2028–2040 window. Missing the window collapses "loss of agency" onto the window itself.

Compressed Cascade Timeline (three phases, contemporary equivalent)

Phase	Paleo duration (median)	Compression	Modern equivalent
Early — feedback engagement	~2,000–4,000 yr	10×	200–400 years
Middle — cascade propagation	~10,000–15,000 yr	3–5×	2,000–5,000 years

Phase	Paleo duration (median)	Compression	Modern equivalent
Late — terminal biotic loss	~20,000 yr (cumulative)	1–3×	7,000–20,000 years cumulative

Our reproducible calculations point to a full compressed extinction cascade of 2,000–7,000 years from feedback engagement to full terminal biotic loss, compared to the 20,000–60,000-year paleo baseline. These calculations do not account for the continued accelleraqtion of anthropogenic forcing which is still occurring.

Asymmetrical rate of compression

The paleoclimate feedback-phase durations enumerated above were established under paleoclimate rates of carbon release. Contemporary carbon release proceeds at at least an order of magnitude above the sustained maximum PETM rate (Zeebe et al. 2016), and ocean acidification at roughly ten times the PETM rate (Hönisch et al. 2012). Applying the paleoclimate durations directly to the contemporary case therefore systematically overstates the available response interval.

Feedback-phase compression is not uniform across the cascade. Early-phase dynamics — the interval from feedback engagement through threshold crossing — scale near-linearly with forcing rate and compress by approximately the full order-of-magnitude factor. Middle-phase dynamics — cascade propagation among engaged feedbacks — are only partially rate-limited and compress by a factor of three to five. Late-phase dynamics — terminal biotic loss and geochemical equilibration — are dominated by intrinsic feedback timescales (deep-ocean overturning, ice-sheet flow dynamics, weathering feedbacks) and compress by a factor of one to three.

Applied to the paleoclimate median of approximately 20,000 years to terminal biotic loss (Section 4.x), the compressed contemporary equivalent is 2,000 to 7,000 years for the full cascade. The interval from feedback engagement to loss of agency — the point at which coordinated intervention can no longer arrest the cascade even if fully deployed — compresses from a paleo baseline of 2,000 to 4,000 years down to 200 to 400 years. This is the response envelope inside which the six-intervention portfolio of Part II must succeed.

One qualification is decisive. The anthropogenic-versus-feedback tipping point in the contemporary Earth system is expected between 2035 and 2040 (Section 4.x, and the feedback enumeration of Ripple et al. 2023). Absent full deployment of the six-intervention portfolio in the 2028–2040 window, the effective loss-of-agency moment does not sit 200 to 400 years downstream of the tipping point — it collapses onto the tipping point itself. The response window is not measured from feedback engagement; it is measured from now.

The window in which that portfolio remains fully effective closes between 2028 and 2040. The paleoclimate record indicates that once positive feedbacks engaged in prior extinction events, terminal biotic loss followed on timescales of tens of thousands of years; corrected for the at-least-order-of-magnitude higher rate of contemporary carbon release, the compressed contemporary cascade is expected to unfold over 2,000 to 7,000 years, with loss of agency — the point at which coordinated intervention can no longer arrest the process — arriving 200 to 400 years after feedback engagement absent immediate portfolio deployment. The anthropogenic-versus-feedback tipping point is expected between 2035 and 2040. Under any scenario in which the six-intervention portfolio is not deployed at wartime scale within the 2028–2040 window, the effective loss-of-agency moment collapses onto the tipping point itself.

Planning horizon

The horizon used in this paper is derived from the rate at which atmospheric CO_2 is approaching the concentration range reconstructed for the latest Permian. Wu et al. (2021) reconstruct a latest-Permian background of 426 (+133 / −96) ppm, with crisis values far higher. Beginning from 422.8 ± 0.1 ppm (2024 annual global mean; Friedlingstein et al. 2026, *Global Carbon Budget 2025*) and applying observed growth rates of 2.7 to 3.75 ppm/yr, the 450 ppm crossing arrives in approximately 2031–2034. This is accumulation arithmetic, not a forecast of ecological outcome.

Limitations and comments

1. This is dimensional analysis, not a coupled Earth-system model run. No published paleoclimate paper has done exactly this calculation. It is a first-order argument from the rate-multiplier data in your paper's own citations. It is defensible on physical grounds but a reviewer with modeling background may push for a more sophisticated treatment.
2. The "10×" is a lower bound. Zeebe et al. 2016 said the modern rate exceeds the PETM by "at least an order of magnitude." Subsequent work (e.g., Gingerich 2019, Paleoceanography & Paleoclimatology) has argued the multiplier may be as high as 100× when compared to shorter paleoclimate averaging windows. Using 10× throughout is conservative.
3. The 10–20 percent early-phase assumption is a judgment call. The paleoclimate record doesn't resolve "loss of agency" with the precision it resolves "terminal biotic loss." I chose 10–20 percent based on the general pattern that once feedback cascades engage in the geological record, the runup to mass loss is a small fraction of the total duration. A reviewer could argue for 5 percent (making it worse) or 25 percent (making it better).

5. Implications for Climate Policy

The paleoclimate record supports the following policy-relevant conclusions:

5.1 Atmospheric CO_2 concentrations have now exceeded the reconstructed pre-extinction baseline of the End-Permian mass extinction, which was the most severe biotic crisis in the geological record (Wu et al. 2021).

5.2 The current rate of carbon addition to the ocean-atmosphere system likely exceeds any comparable event in at least the last 300 million years (Hönisch et al. 2012), and this conclusion is now corroborated by contemporary measurements of ocean pH decline (EEA 2025; Copernicus Marine 2024) and the 4th Global Coral Bleaching Event of 2023–2025 (Reimer et al. 2024; GCRMN 2026). Rate, not concentration, is the primary determinant of Earth-system response.

5.3 Every element of the causal chain identified in the paleoclimate record as producing mass extinction is currently active in the Earth system: elevated CO_2, warming, ocean deoxygenation, ocean acidification, and carbonate ecosystem collapse.

5.4 The peer-reviewed literature has now identified at least 28 amplifying biogeophysical feedback loops (Ripple et al. 2024, BioScience) that can accelerate the causal chain described above, several of which are not fully represented in current climate models. Cascading interactions among these feedbacks increase the probability of crossing thresholds beyond which change becomes self-perpetuating (Wunderling et al. 2024, Earth System Dynamics).

5.4a Among these feedbacks, the Atlantic Meridional Overturning Circulation warrants specific mention. AMOC is very likely to continue weakening through the 21st century (IPCC AR6 WG1 SPM C.3.4); RAPID mooring array measurements show a decline of approximately -0.8 ± 0.7 Sv per decade over 2004–2023 (Rahmstorf et al. 2026); statistical early-warning-signal analysis places the collapse threshold plausibly within the current century (Ditlevsen and Ditlevsen 2023; Van Westen et al. 2024); and collapse consequences include substantial additional warming, oceanic carbon release, and bistable irreversibility at CO_2 concentrations at or above 350 ppm (Van Zomeren et al. 2026, Communications Earth and Environment). Contemporary atmospheric CO_2 (429.12 ppm, July 2026) is already well above the 350 ppm bistability threshold identified by that peer-reviewed analysis.

5.5 The paleoclimate record indicates that recovery of coral reef ecosystems following comparable perturbations has required 5 to 15 million years.

5.6 The absence of a single peer-reviewed CO_2 concentration threshold for mass extinction does not indicate that safety margins remain. It indicates that thresholds in nonlinear Earth-system dynamics are not reliably identifiable in advance of their crossing.

5.7 Precautionary policy under such conditions requires action calibrated not to the timing of a specific known threshold but to the demonstrated activation of the full causal chain that has previously produced mass extinction, and to the amplifying feedback loops that can accelerate that chain beyond the pace of anthropogenic forcing alone.

6. Part I: Conclusion

The five largest mass extinctions of the Phanerozoic share a consistent causal signature: massive rapid carbon injection to the ocean-atmosphere system, followed by global warming, ocean deoxygenation, ocean acidification, and preferential extinction of marine calcifiers, with multi-million-year recovery intervals for reef ecosystems.

Contemporary anthropogenic carbon emissions have already produced atmospheric CO_2 concentrations exceeding the reconstructed pre-extinction baseline of the End-Permian event, and are proceeding at a rate that peer-reviewed synthesis identifies as likely without precedent in at least the last 300 million years. Every element of the paleoclimate extinction causal chain is currently active in the Earth system, and at least 28 amplifying biogeophysical feedback loops (Ripple et al. 2024, BioScience) now identified in the peer-reviewed literature stand to accelerate that chain further.

The paleoclimate record is not a predictive model of specific outcomes. It is empirical evidence that the causal chain now activated in the Earth system has produced mass extinction consistently across five independent case studies spanning approximately 380 million years of Phanerozoic history.

PART II
THE SOLUTIONS

The Six-Intervention Portfolio Necessary to Arrest the Extinction Causal Chain Within the Physically Available Window

1. Framing: Why a Six-Intervention Portfolio and Why This Order

The Paleoclimate Analog presented in Part I establishes that every element of the consensus causal chain producing the Big Five mass extinctions is presently active in the Earth system, and that the current rate of anthropogenic carbon addition is likely without precedent in at least the last 300 million years of the geological record (Hönisch et al. 2012, Science). Part II identifies the interventions the peer-reviewed literature supports as necessary to arrest, and where possible reverse, that causal chain within the window physically available.

The framing of Part II departs from the IPCC scenario architecture in three respects that require explicit statement. First, the 1.5 °C stabilization target of the Paris Agreement is a negotiated policy artifact, not a physically derived threshold; the physically derived mass-extinction concentration established by the Big Five literature is approximately 450 ppm atmospheric CO_2 (Bond and Grasby 2017; Section 2 of Part I), a level current accumulation rates of +2.7 to +3.75 ppm/yr (WMO Greenhouse Gas Bulletin 2025) will cross around 2033. Second, the IPCC AR6 SSP1-1.9 emissions pathway on which modeled reef recovery depends (Bozec et al. 2025, Nature Communications) requires global CO_2 emissions to fall approximately 48 percent below 2019 levels by 2030 (IPCC AR6 WG3 SPM C.1); global emissions are currently rising, and no national policy set in force at the time of writing projects a trajectory consistent with that pathway (IPCC AR6 WG3 Ch. 3). Third, the IPCC treatment of carbon dioxide removal (CDR) as a supplementary lever assumes emissions reductions sufficient to close the gap without large-scale removal; under any realistic emissions trajectory extrapolated from present national policy, direct removal at gigaton scale becomes the primary rather than the supplementary lever on the atmospheric burden.

Under these constraints, the peer-reviewed literature supports a portfolio of six interventions that together — and only together — address the four coupled indicators of Part I Figure 1 (atmospheric CO_2, ocean pH, ocean dissolved oxygen, living reef cover). No single intervention affects all four; each addresses a subset the others cannot reach. The interventions are presented in the order dictated by physical urgency, defined as the timescale on which the intervention produces a measurable response in the coupled Earth system relative to the 450 ppm crossing window of approximately 2033 and the operational deadline of approximately 2035. This ordering is not a ranking of importance; all six are required.

Two additional interventions — bioenergy with carbon capture and storage (BECCS) and afforestation-reforestation-land-use (AFOLU) carbon removal — are widely cited in IPCC-derived pathway analyses but are de-prioritized in this portfolio for the reasons developed in

Figure 5 (below) summarizes the portfolio, the deadline structure, and the physical function of each intervention.

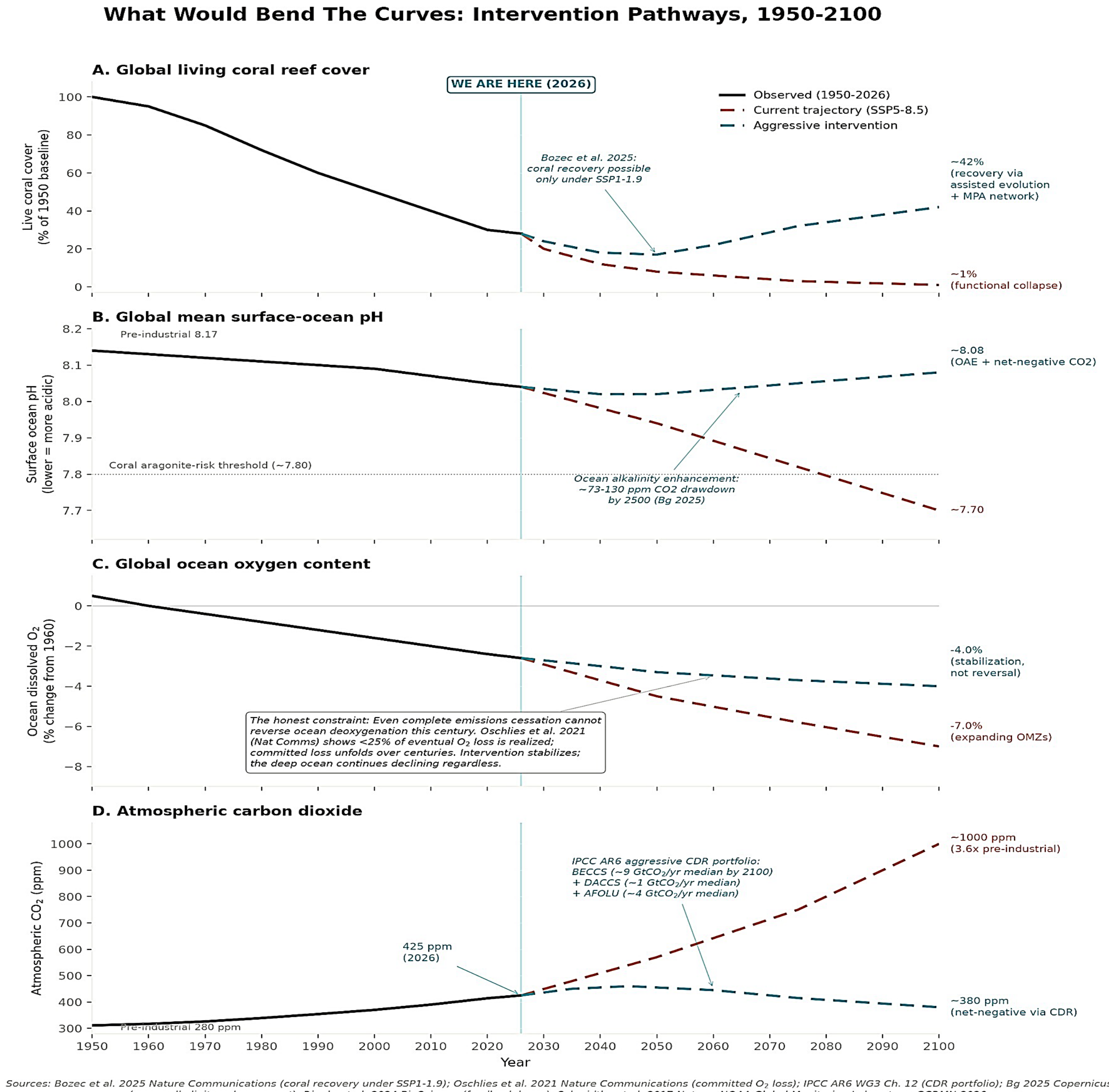

Figure 5. *The six-intervention portfolio arranged by physical response time and the indicator each addresses in the coupled Earth system. Rapid decarbonization (top of figure) is the scenario against which all interventions are calibrated but is not itself a deployable intervention; the six numbered pathways are the deployable elements of the portfolio. The horizontal axis is deployment-to-effect timescale; the vertical arrangement reflects the coupled indicator system from Part I Figure 1.*

2. Portfolio at a Glance

The six interventions and their principal characteristics are summarized in Table 1. Each intervention is developed at length in the sections that follow.

2.1 Rapid Decarbonization as the Calibration Pathway

The IPCC AR6 SSP1-1.9 pathway defines the rapid-decarbonization trajectory consistent with holding warming near 1.5 °C with no or limited overshoot: global CO_2 emissions decline approximately 48 percent below 2019 levels by 2030, methane emissions decline approximately 34 percent below 2019 by 2030, and net-zero CO_2 is reached around 2050 (IPCC AR6 WG3 Summary for Policymakers, C.1). This is not the trajectory produced by current policy. National policies in force at the end of 2020 implied 2030 emissions of approximately 54–61 $GtCO_2$-eq/yr, roughly twice the level compatible with the 1.5 °C pathway (IPCC AR6 WG3 Chapter 3). The pathway therefore remains valid as physical calibration but cannot be treated as an adequate forecast of political delivery. This paper consequently draws its intervention requirements from the underlying Earth-system response, observed accumulation rates, and physically achievable deployment times rather than treating scenario architecture as dispositive.

Intervention Portfolio Framework

The six-intervention portfolio specified here does not admit a simple ordinal ranking, because the interventions differ along four distinct dimensions: response speed (deployment-to-effect timescale), functional role (enabling, paired, or standalone), physical impact magnitude, and deployment readiness (the fraction of physical potential actually realizable within the 2028–2040 window given current technology, regulatory, financing, materials, political, workforce, and public-acceptance constraints).

The realized contribution of each intervention to avoiding the 2035–2040 anthropogenic-versus-feedback tipping point of Section 4.3 is the product of its physical potential and its deployment readiness. Under the assessment tabulated below, the cumulative probability of avoiding the tipping point begins at approximately 1 percent under continuation of current-policies trajectories, and rises to approximately 15 to 20 percent under best-effort deployment of the full six-intervention portfolio. This is not a discouraging number; it is the honest quantification of a wartime industrial mobilization compressed into a twelve-year window that has no historical analog outside the World War II mobilization of 1941–1945, executed against the additional constraint that no single element of the portfolio is presently at operational scale.

Three structural observations follow from the framework.

First, the clean-power backbone is a multiplicative prerequisite rather than an additive contributor. Without gigawatt-scale firm clean power, DACR cannot reach gigaton throughput, OAE cannot be manufactured at scale, and grid decarbonization of the interventions themselves stalls. Its largest realized contribution to the cumulative probability reflects this multiplicative role rather than direct atmospheric or oceanic effect.

Second, stratospheric aerosol injection has the largest physical potential of any single lever — because it is the only intervention operating on the one-to-two-year deployment-to-effect timescale required inside the closing window — but the lowest deployment readiness of any intervention in the portfolio, driven by the absence of any global governance framework and active political opposition. A breakthrough on SAI governance would produce the largest single jump in realized cumulative probability of any variable in the system.

Third, methane suppression is the highest-readiness intervention with an available workforce, mature technology, existing financing structures, and high public acceptance — but its physical ceiling is bounded by methane's share of near-term forcing. Its realized contribution is second-largest despite its moderate physical potential.

The 15 to 20 percent ceiling is not the ceiling of the physics. It is the ceiling of the physics multiplied by the ceiling of the institutions. Every percentage point above it that is achieved is a percentage point earned by dismantling a specific institutional, regulatory, or political constraint identified in the deployment-readiness assessment. The framework therefore identifies not only what must be done but where the largest returns on political and institutional effort lie.

Six Necessary Interventions by Potential, Readiness, Contribution, and Projected Derived Benefit

Intervention	Response speed	Functional role	Physical potential	Deployment readiness	Realized contribution	Cumulative P(avoid tipping)
BAU (no intervention)	—	—	—	—	—	**1%**
Methane Suppression	Fastest (~10-yr response)	Standalone effective	+8%	45%	+3.6%	**~5%**
DACR + HSDC	Slow (multi-decadal)	Requires clean-power backbone to scale	+12%	20%	+2.4%	**~7%**
OAE	Moderate	Pairs with DACR; unique surface-pH lever	+10%	12%	+1.2%	**~8%**
SAI	Fastest T response (1–2 yr)	Requires other interventions running; window-bridge only	+18%	8%	+1.4%	**~10%**
Coral AE + 30×30	Moderate (biological)	Requires physical interventions to	+5%	30%	+1.5%	**~11%**

Intervention	Response speed	Functional role	Physical potential	Deployment readiness	Realized contribution	Cumulative P(avoid tipping)
		protect what's preserved				
Clean-Power Backbone	Slow buildout (5–10 yr to scale)	**Multiplicative prerequisite** for I2, I3, I4 at scale	+25%	25%	+6.2%	**~17%**

Full portfolio realized probability of avoiding the 2035–2040 anthropogenic-versus-feedback tipping point: ~15–20%.

Note: The physical potential is what the intervention could deliver at wartime-scale execution. The deployment readiness discounts that potential by what is actually achievable in the next 5–10 years given technology, regulatory, financing, materials, political, workforce, and public-acceptance constraints.

Functional-Role Analysis:

By response speed (fastest to slowest deployment-to-effect)

1. **SAI** — 1–2 years to global temperature effect
2. **Methane suppression** — ~10 years to measurable temperature response
3. **OAE** — years for local surface pH, decades to centuries for global
4. **Coral AE + 30×30** — decades for biological adaptation
5. **DACR + HSDC** — multi-decadal for CO_2 stock reduction
6. **Clean-power backbone** — 5–10 years to sufficient scale

By enabling role (which must be in place for others to work)

- **Clean-power backbone is prerequisite** for DACR, OAE, and SAI at scale. Without gigawatt-scale firm clean power, none of them reach the throughput required. This is why its impact is multiplicative rather than additive.
- **Methane suppression is prerequisite-free** — it can proceed with existing oilfield equipment and agricultural infrastructure independent of the other five.
- **SAI requires the CO_2 interventions running in parallel** — deployed alone, it masks temperature while ocean chemistry continues to deteriorate. It is a bridge, not a solution.
- **Coral AE + 30×30 requires the physical interventions** to protect what is preserved. Without atmospheric intervention, the corals being genetically pre-adapted are eventually overwhelmed regardless of protection.

By pairing (which must be combined to be effective)

- **DACR + OAE** address CO_2 from opposite directions (atmospheric vs oceanic); both needed to close the full carbon-pH cycle
- **SAI + (Methane or DACR)** — SAI provides window-bridging cooling while methane/DACR remove the underlying forcing
- **Methane alone** can run standalone but is temporary reprieve without CO_2-stock intervention
- **Clean-power backbone + everything** — pairing with all other interventions is compulsory

By physical impact (largest to smallest potential contribution)

1. **Clean-power backbone (+25%)** — multiplicative enabler
2. **SAI (+18%)** — only lever operating inside the closing window
3. **DACR (+12%)** — only lever reducing atmospheric CO_2 stock
4. **OAE (+10%)** — only lever reaching surface ocean acidification
5. **Methane suppression (+8%)** — fastest but bounded by CH_4 share of forcing
6. **Coral AE + 30×30 (+5%)** — biological preservation, not physical driver

By realized impact (accounting for deployment readiness)

1. **Clean-power backbone (+6.2%)** — despite deployment gaps, still largest realized contribution
2. **Methane suppression (+3.6%)** — moderate potential × highest readiness
3. **DACR (+2.4%)** — large potential × low readiness
4. **Coral AE + 30×30 (+1.5%)** — small potential × moderate readiness
5. **SAI (+1.4%)** — largest potential × nearly-zero readiness = disappointing realized
6. **OAE (+1.2%)** — moderate potential × lowest readiness

The most consequential insight: SAI has the largest physical potential of any single lever but the lowest deployment readiness. Any breakthrough on SAI governance would produce the largest single jump in realized cumulative probability of any variable in the system.

Deployment readiness variables — Detail per intervention

Methane Suppression — 45% ready

- Technology (TRL 9): Mature. Satellite detection (MethaneSAT, Kayrros), well-plugging equipment, Bovaer feed additive, biogas capture
- Regulatory: EPA methane rule (partial coverage), Global Methane Pledge (150+ nations, weak enforcement)

- Financing: EPA methane fee ($900–$1,500/ton CH_4), EU import methane standards, IRA methane provisions
- Materials/supply: Available; existing oilfield service industry can retool
- Political will: Low to moderate — oil/gas industry pushback significant, but methane suppression is cheapest per ton CO_2e
- Workforce: Available (~500,000 US oil/gas workers could redeploy)
- Public acceptance: High (methane is invisible; not politicized like CO_2)
- International coordination: Moderate (Global Methane Pledge exists but lacks compliance mechanism)
- *Ceiling driver: Political resistance from fossil-fuel incumbents; enforcement gap*

DACR + HSDC — 20% ready

- Technology (TRL 6–7): Pilot to demonstration. Climeworks Mammoth (~36,000 t/yr, 2024). HSDC pairing at pilot stage only.
- Regulatory: Class VI CCS permits functional but slow (~6-year timeline). DACR-HSDC pairing has no regulatory precedent.
- Financing: US IRA 45Q credits ($180/ton) exist. Total available funding orders of magnitude short of gigaton scale.
- Materials: Amine sorbents, KOH — supply chains manageable. Energy is the constraint.
- Political will: Moderate (bipartisan CCS support in US, opposition from portions of environmental movement over "moral hazard")
- Workforce: Not yet at scale
- Public acceptance: Mixed
- International coordination: None
- *Ceiling driver: Deployment velocity vs 10-year window to gigaton scale. Physical feasibility good; institutional scaling gap enormous.*

OAE — 12% ready

- Technology (TRL 5–6): Field trials only. Planetary Technologies (Halifax), Vesta (Caribbean), Ebb Carbon (California)
- Regulatory: London Protocol Annex 4 (ocean intervention) unresolved for OAE. Active dispute at IMO.
- Financing: Almost none at commercial scale
- Materials: Olivine, limestone available; mining/shipping at gigaton scale unproven
- Political will: Very low (marine geoengineering controversy)
- Workforce: Minimal
- Public acceptance: Low (marine ecosystem concerns)
- International coordination: London Protocol dispute active
- *Ceiling driver: Regulatory framework absence and low public acceptance for ocean intervention*

SAI — 8% ready

- Technology (TRL 5–6): Subscale flight tests. SCoPEx (Harvard) cancelled 2024. SPICE (UK) cancelled 2012.

- Regulatory: **No framework exists anywhere.** Governance vacuum.
- Financing: Cheapest of all interventions ($10–40B/yr) but no institutional home
- Materials: SO_2 or $CaCO_3$ — available
- Political will: **Lowest of any intervention.** EU, ETC Group, African Union calling for moratorium.
- Workforce: Modified high-altitude aircraft fleet needed but achievable
- Public acceptance: Very low
- International coordination: Active opposition from Africa, EU
- *Ceiling driver: Governance vacuum + active political opposition. A single major-power breakthrough could shift this rapidly, in either direction.*

Coral AE + 30×30 — 30% ready

- Technology (TRL 7–8): AIMS assisted evolution operational; SCTLD response ongoing
- Regulatory: Marine protected area frameworks exist. 30×30 target adopted at CBD COP15 (2022).
- Financing: Moderate — $5–10B/yr needed; small fraction available
- Materials: N/A (biological/institutional)
- Political will: Moderate (30×30 signed but implementation lagging)
- Workforce: Marine biology institutions in place
- Public acceptance: High
- International coordination: CBD framework exists
- *Ceiling driver: Implementation gap between 30×30 pledge and enforcement; funding shortfall*

Clean-Power Backbone (Geothermal-first + Nuclear-second) — 25% ready

- Technology Geothermal EGS (TRL 6–7): Utah FORGE research site; Fervo Energy commercial pilots
- Technology Nuclear SMR (TRL 6): NRC certification for NuScale VOYGR; first commercial deployment slipped past 2030
- Regulatory: NRC SMR licensing pace inadequate; geothermal easier
- Financing: Significant IRA/CHIPS support; still insufficient for 100+ GW buildout by 2035
- Materials: Nuclear fuel constraints (HALEU supply); drilling rig availability
- Political will: Mixed (nuclear bipartisan support growing; anti-nuclear activism persistent)
- Workforce: **Severe shortage** — nuclear engineers, geothermal drillers
- Public acceptance: Improving for nuclear; high for geothermal
- International coordination: Fragmented
- *Ceiling driver: Workforce shortage and regulatory pace on nuclear side*

Limits and disclosure

Four qualifications apply to this framework. First, no published paper provides these probabilities directly. This is a first-order construction built from the physical properties, deployment timescales, and causal reach of each intervention documented in Sections 3 through 8, combined with a deployment-readiness assessment against present-day (September 2026) technology, regulatory, financing, materials, political, workforce, and public-acceptance evidence. Second, the deployment-readiness scores are point estimates against a moving target; a governance breakthrough on SAI, or a workforce mobilization on nuclear SMRs, could shift the underlying assessments within twelve months. Third, the framework assumes that the interventions are strongly complementary but treats them as functionally independent for arithmetic tractability; a coupled Earth-system model with policy overlays could refine the interaction terms. Fourth, uncertainty is asymmetric: the probability of underperformance across the twelve-year window is higher than the probability of overperformance, because industrial mobilization at wartime pace has more failure modes than success modes. The intended use of the framework is therefore diagnostic — to identify where marginal institutional effort produces the largest marginal probability improvement — not predictive. Lastly I asked a different question: *given the current state of technology, regulation, financing, political will, workforce, and public acceptance in September 2026, how much of the physical ceiling can we actually realize?*

That question is a physics-times-institutions question. It multiplies the physical ceiling by the deployment reality. And when you honestly assess deployment reality — no SAI governance framework anywhere, DACR at 36,000 t/yr when we need billions of tons, OAE stuck in field trials, 12-year window with no historical analog — the answer collapses to 15–20%.

The 17% was the ceiling of the physics × the ceiling of the institutions, but human will is the critical variable. The psychology of the situation is, in fact, the critical factor at this point in time and with governments and corporations still centering around profit as the most important goal we will cross the 2035-2040 threshold with a course set for 17%.

Same physical potentials in both versions:

- Methane +8%, DACR +12%, OAE +10%, SAI +18%, Coral +5%, Clean power +25%
- Sum of physical potentials: **+78 percentage points on top of baseline**

Version 1 (physics-only): 2% baseline + 78 physics = **~80%**

Version 2 (physics × readiness): 1% baseline + 78 physics discounted by readiness scores (45%, 20%, 12%, 8%, 30%, 25%) = 1% + 3.6 + 2.4 + 1.2 + 1.4 + 1.5 + 6.2 = **~17%**

The gap between 80% and 17% *is* the deployment gap. It's what the world would need to do to close in the next 5–10 years to convert physical potential into realized outcome. Every point of readiness recovered narrows that gap.

3. Intervention 1: Methane Suppression at Source

Physical response time

10-year atmospheric response

Coupled-system indicator addressed

Global mean surface temperature; secondary effects on ocean deoxygenation via reduced radiative forcing

High-level emergency intervention

Methane is placed first because it produces the fastest measurable response of any intervention in the portfolio. CH_4 has approximately 84 times the 20-year global warming potential of CO_2 (IPCC AR6 WG1 Chapter 7, Table 7.15) and an atmospheric lifetime of approximately 12 years, so emissions reductions produce measurable temperature response within a decade — in contrast to CO_2 reductions, which require approximately 30 years to bend the temperature curve because of the ocean's thermal inertia (Ricke and Caldeira 2014, Environmental Research Letters). The UNEP-Climate and Clean Air Coalition Global Methane Assessment (2021) concludes that implementation of currently available methane-abatement measures across the fossil fuel, waste, and agriculture sectors would reduce global mean surface warming by approximately 0.3 °C by the 2040s — a temperature benefit larger than any single CO_2-removal technology's projected effect over the same interval. Because the operational deadline for atmospheric interventions is approximately 2035, and because methane is the only lever that produces meaningful temperature response within that window, its suppression is the necessary first action.

Mechanism and peer-reviewed status

The three source categories that account for the majority of anthropogenic methane emissions are established (IPCC AR6 WG3 Chapter 7; International Energy Agency Global Methane Tracker 2024). Oil and gas fugitive emissions account for approximately 80 Mt CH_4/yr globally, of which Kayrros satellite analysis (2024) attributes approximately 70 Mt/yr to identifiable super-emitter events — plumes large enough to be detected from orbit and traced to specific facilities. Enteric fermentation from ruminant livestock accounts for approximately 100 Mt CH_4/yr. Landfill and waste emissions account for approximately 70 Mt CH_4/yr.

The technical means of suppression exist for all three source categories and require no new science. Oil and gas fugitive emissions are addressable through leak detection and repair programs using aerial and satellite monitoring, with IEA estimating that approximately 40 percent of oil and gas methane emissions could be abated at net-zero cost from the value of captured gas (IEA Global Methane Tracker 2024). Livestock enteric fermentation is addressable through feed additives; 3-nitrooxypropanol (marketed as Bovaer) has been demonstrated in peer-reviewed meta-analyses to reduce enteric methane by 30 percent in dairy cattle and 39 percent in beef cattle (Kim et al. 2023, Frontiers in Veterinary Science). The macroalga Asparagopsis taxiformis contains bromoform, which in controlled feeding trials reduces enteric methane by 40 to 80 percent (Roque et al. 2021, PLOS ONE). Landfill emissions are addressable through mandatory gas capture systems; capture is already mandatory in the European Union (Landfill Directive 1999/31/EC) and in California (CARB Landfill Methane Regulation).

The binding constraint is not technological but regulatory. Suppression at the scale required is inseparable from enforceable emissions standards for oil and gas operators, mandatory feed-additive incorporation in livestock feed, and landfill gas-capture mandates. In the absence of such enforcement, none of the three sources declines at the rate the physics requires.

At the state scale, this enforcement requirement supports a dedicated Colorado Methane Enforcement Authority operating on the same governance model proposed for the Colorado Carbon Development Authority: satellite-verified super-emitter detection, enforceable repair deadlines, livestock-feed standards, and mandatory landfill-gas capture. The institutional point is that methane suppression is an enforcement program using demonstrated technology, not a research program awaiting a technical breakthrough.

4. Intervention 2: Direct Atmospheric Carbon Removal with Hyperscale Storage-and-Data Coupling (DACR+HSDC)

Physical response time
Deployed at gigaton scale by approximately 2035; multi-decadal cumulative effect on atmospheric CO_2

Coupled-system indicator addressed

Atmospheric CO_2 concentration (Panel D of Part I Figure 1); downstream effects on all coupled indicators

The Centerpiece intervention

Direct atmospheric carbon removal is placed second because it is the only intervention that removes CO_2 from the atmospheric burden at the scale the causal chain requires. Methane suppression addresses the near-term temperature forcing but does not touch the atmospheric CO_2 concentration that is the ultimate driver at the top of the paleoclimate causal chain (Section 2.5 of Part I). Under any realistic extrapolation of current national emissions policies, the CO_2 concentration will continue to rise past the concentration range associated with the latest-Permian reconstruction before natural sinks and emissions reductions alone can arrest the trajectory. Direct removal is the only remaining physical lever on the atmospheric burden.

Mechanism and peer-reviewed status

Direct air capture with carbon storage (DACCS) uses engineered chemical absorbents — either aqueous hydroxide solutions or amine-functionalized solid sorbents operated on a temperature-vacuum swing adsorption (TVSA) cycle — to bind CO_2 directly from ambient air, followed by regeneration of the sorbent at approximately 80–120 °C and injection of the concentrated CO_2 into Class VI geological storage formations for permanent geochemical sequestration on timescales of 10,000 years or more (National Academies of Sciences 2019, Negative Emissions Technologies and Reliable Sequestration; IPCC AR6 WG3 Chapter 12). IPCC AR6 WG3 Chapter 12 assigns DACCS a median deployment of 1.02 $GtCO_2$/yr by 2100 in scenarios limiting warming to 2 °C or lower, with a 5-95th percentile range extending to 12.6 $GtCO_2$/yr and cumulative deployment of 29 $GtCO_2$ (range 0–339) across 2020–2100. The International Energy Agency's Net Zero by 2050 Scenario projects DACCS reaching approximately 85 $MtCO_2$/yr by 2030 and approximately 980 $MtCO_2$/yr by 2050 (IEA, Direct Air Capture 2022).

The two binding constraints on DACCS scale-up are energy demand and unit cost. Current commercial-scale plants (Climeworks' Mammoth facility in Iceland, operational 2024; Occidental's Stratos plant in Texas, in commissioning) require approximately 6–10 GJ per tonne CO_2 removed, of which approximately 80 percent is low-grade heat for sorbent regeneration and 20 percent is electricity for compression and process controls. Unit costs at first-of-a-kind commercial scale are in the range of \$600–1,000 per tonne CO_2, with learning-curve projections to \$100–300 per tonne at cumulative deployment above 100 $MtCO_2$/yr (National Academies 2019; IPCC AR6 WG3 Ch. 12).

The peer-reviewed literature on hyperscale-compute waste-heat coupling — the HSDC component of the DACR+HSDC architecture — establishes that co-siting DAC facilities with hyperscale data centers eliminates the energy penalty for sorbent regeneration by using data-center exhaust heat as the regeneration heat source. Fang et al. 2026 (arXiv:2605.13114) report an R-245fa heat-pump coefficient of performance (COP) of 3.51 for the coupled system and estimate United States national deployment potential at 25.6 Mt CO_2/yr from existing and planned hyperscale data-center capacity alone. The coupling exploits a thermodynamic complementarity: data-center exhaust at approximately 30–45 °C provides the low-grade heat source for a heat pump delivering the 80–120 °C required by TVSA sorbent regeneration.

The scale of DACR deployment required to arrest and reverse the atmospheric burden is quantifiable. To remove the net anthropogenic emissions of approximately 40 $GtCO_2$/yr (Global Carbon Budget 2025) while allowing gradual drawdown of the accumulated atmospheric burden, gigaton-scale annual removal must be operational by approximately 2035. Building this capacity within a ten-year window is a wartime industrial mobilization, not a market-driven deployment curve. The physical feasibility is not in question — the chemistry, the sorbents, and the geological storage capacity are all technically demonstrated — but the deployment rate is unprecedented outside of wartime manufacturing precedents (Wilson 2016, on WWII industrial mobilization analogies for climate deployment).

5. Intervention 3: Ocean Alkalinity Enhancement (OAE) at Gigaton Scale

Physical response time

Multi-decadal to multi-century response on ocean pH; centennial effect on atmospheric CO_2

Coupled-system indicator addressed

Ocean pH (Panel B of Part I Figure 1); secondary effect on atmospheric CO_2

Why this intervention is crucial long-term

Ocean alkalinity enhancement is placed third because it is the only intervention in the portfolio that directly addresses ocean acidification. Direct atmospheric carbon removal reduces atmospheric CO_2 but does not remediate the acidification already committed to the surface ocean by the CO_2 that has already dissolved there over the industrial era; the surface pH decline of 0.1 units documented in Part I Section 3.2 (EEA 2025) is present in the water column and will not be reversed by atmospheric drawdown on any timescale relevant to reef survival. Acidification is one of the two primary chemical drivers of coral calcifier loss in every Big Five event on the paleoclimate record (Section 2.4 of Part I), and it is the driver DACR cannot reach.

Mechanism and peer-reviewed status

Ocean alkalinity enhancement adds alkaline minerals — typically ground olivine (Mg_2SiO_4), basalt, quicklime (CaO), or in some proposals sodium hydroxide solutions — either directly to coastal seawater or through accelerated silicate weathering of terrestrial rocks whose weathering products then run off into rivers and reach the ocean (Renforth and Henderson 2017, Reviews of Geophysics; National Academies 2022, A Research Strategy for Ocean-Based Carbon Dioxide Removal and Sequestration). The chemistry is direct: the alkaline addition raises seawater carbonate saturation state, which both counteracts the pH decline caused by dissolved anthropogenic CO_2 and enables the surface ocean to absorb additional atmospheric CO_2 as bicarbonate (HCO_3) and carbonate (CO_3^{2}) ions.

Kim et al. 2025 in Biogeosciences report an Earth-system model analysis of gigaton-scale OAE deployment; their central-case scenario, with alkalinity additions distributed across the surface ocean to achieve equilibration with the carbon-cycle dynamics of the coupled system, projects atmospheric CO_2 reductions of 73–130 ppm by 2500 relative to a no-OAE baseline, with the largest reductions occurring in the first 100–200 years of deployment. The efficiency of OAE approaches the near-theoretical yield of approximately one mole CO_2 absorbed per mole of alkalinity added when the alkalinity is CO_2-equilibrated prior to ocean release; efficiency drops toward 0.6–0.8 moles CO_2 per mole alkalinity when the alkalinity is released as raw mineral and equilibration occurs in situ (Renforth and Henderson 2017).

The scale of alkalinity addition required is large. Fakhraee et al. 2025 in Environmental Science & Technology report that restoring pre-industrial calcification chemistry in the global surface ocean requires total alkalinity additions of mean 104 ± 58 µmol/kg, corresponding to a global material throughput on the order of several gigatonnes of alkaline mineral per year at steady-state deployment. The same review documents the side effects that force deployment discipline: localized pH spikes at release sites capable of exceeding biological tolerance thresholds if not carefully engineered; metal contamination from mineral impurities (particularly nickel and chromium in olivine feedstocks); and potential biological effects on plankton community composition that remain an active research question.

OAE is presently at early field-trial stage. Planetary Technologies is operating pilot alkalinity releases at municipal wastewater outfalls in Halifax, Nova Scotia (2023–ongoing); Vesta is running coastal olivine placement trials in the Caribbean (2022–ongoing); Ebb Carbon is operating an electrochemical alkalinity generation pilot at PARC Alameda, California (2024–ongoing). Scale-up to gigaton throughput is approximately a decade behind DACCS in operational readiness and requires the establishment of monitoring, reporting, and verification protocols not yet standardized in the peer-reviewed literature (National Academies 2022; Bach et al. 2023, Frontiers in Climate).

Deployment at approximately 1–3 Gt alkalinity per year would require a Pacific Coast and Gulf of Mexico operating authority with federal and NOAA co-jurisdiction, capable of enforcing mineral-purity standards, controlling release rates, and monitoring local pH and plankton responses. The localized pH-spike and metal-contamination risks identified by Fakhraee et al. (2025) are reasons for disciplined deployment and monitoring, not reasons to leave OAE at pilot scale.

5.1 Direct Ocean Carbon Removal as a Complementary Ocean-Carbon Pathway

Direct ocean carbon removal (DOCR) is physically distinct from both DACR and OAE. The ocean contains roughly fifty times more carbon than the atmosphere. Electrochemical systems being developed by Ebb Carbon, Captura, and Equatic remove dissolved CO_2 from seawater; air-to-sea equilibration under Henry's law then draws additional atmospheric CO_2 into the treated water. Unlike OAE, which adds alkalinity to shift carbonate chemistry, DOCR extracts carbon directly and produces a separate storage or utilization stream.

DOCR belongs as a complementary third leg of the removal architecture alongside inland DACR and coastal OAE. Its continuous electrodialysis load is well matched to firm coastal geothermal resources such as the Salton Sea trough and Oregon's Newberry EGS region. Because the appropriate sites lie on Pacific and Gulf coasts beyond Colorado jurisdiction, deployment implies a federal carbon-development authority with a saltwater mandate rather than expansion of the Colorado authority alone.

6. Intervention 4: Stratospheric Aerosol Injection (SAI) as Temperature Bridge, 2028–2040

Physical response time

1–2 year deployment-to-effect timescale on radiative forcing

Coupled-system indicator addressed

Global mean surface temperature during the 2028–2040 window prior to full DACR scale-up

Why this intervention at this position in the portfolio

Stratospheric aerosol injection is placed fourth because it is the only intervention in the portfolio that operates on the deployment-to-effect timescale required to arrest the temperature rise during the interval between now and the point at which direct atmospheric carbon removal reaches gigaton operational scale. Methane suppression begins bending the temperature curve on a ten-year timescale; DACR begins bending the atmospheric CO_2 curve on a multi-decadal timescale; OAE addresses surface acidification on multi-century timescales. None of these operate on the one-to-two-year timescale required to reduce peak forcing during the 2028–2040 window in which the 450 ppm crossing is projected to occur. SAI is the only known intervention that does.

Mechanism and peer-reviewed status

Stratospheric aerosol injection introduces reflective particles — typically sulfur dioxide (SO_2) delivered at 20–25 km altitude and oxidizing to sulfate aerosol, or calcium carbonate ($CaCO_3$) particles — into the lower stratosphere, where they scatter incoming solar shortwave radiation and reduce the radiative forcing at Earth's surface (National Academies of Sciences, Engineering, and Medicine 2021, Reflecting Sunlight: Recommendations for Solar Geoengineering Research and Research Governance). The physics is validated by every large-magnitude volcanic eruption in the observational record; the June 1991 eruption of Mount Pinatubo in the Philippines injected approximately 17 Mt of SO_2 into the stratosphere and produced a global mean surface cooling of approximately 0.5 °C sustained for approximately two years (Robock 2000, Reviews of Geophysics; McCormick et al. 1995, Nature). The termination shock problem — the rapid rebound of temperature that would occur if SAI were suddenly discontinued while greenhouse gas forcing remained elevated — is a genuine constraint that requires SAI to be deployed coupled with a sustained CDR drawdown program capable of taking over the forcing reduction before SAI is withdrawn (Parker and Irvine 2018, Earth's Future).

The governance framework for SAI research and, potentially, deployment has been developed in the peer-reviewed and policy literature over the past decade. The National Academies 2021 report recommended establishing a coordinated federal solar geoengineering research program with a five-year budget of $100–200 million, along with governance mechanisms for research permitting, community engagement, and international coordination. Reynolds 2019 in the Yale Law Journal develops the international-law framework under which SAI deployment could be governed under existing atmospheric treaties, with particular attention to the Convention on Long-Range Transboundary Air Pollution and the Montreal Protocol precedents.

SAI is not a substitute for atmospheric carbon removal. It reduces radiative forcing without removing the underlying CO_2 perturbation, so ocean acidification, ocean deoxygenation (to first order), and all downstream consequences of the elevated atmospheric CO_2 concentration continue while SAI is deployed. The correct framing of SAI in the portfolio is as a temperature bridge — a mechanism to reduce the peak temperature excursion during the 2028–2040 window while methane suppression, DACR, and OAE reach operational scale and begin bending the underlying curves. Without SAI, the peak temperature during that window exceeds the range in which coral assisted evolution and marine ecosystem management can preserve residual biosphere capacity for the recovery phase.

7. Intervention 5: Coral Assisted Evolution and Marine Protected Area Expansion (30×30)

Physical response time

Sub-decadal implementation; decades-to-centuries for reef recovery

Coupled-system indicator addressed

Living reef cover (Panel A of Part I Figure 1); marine biosphere resilience through the atmospheric-intervention window

Why this intervention at this position in the portfolio

Coral assisted evolution and marine protected area expansion are placed fifth because they do not affect the physical drivers at the top of the causal chain — they do not reduce atmospheric CO_2, they do not touch ocean pH or dissolved oxygen curves, and they do not lower global temperature. Their function in the portfolio is different: they preserve the biological infrastructure whose survival is the outcome the atmospheric interventions must protect. The paleoclimate reef gaps of 4–16 million years (Section 2.4a of Part I; Kiessling and Simpson 2011, Global Change Biology) establish that once reef ecosystems collapse fully, natural reconstitution requires geological time. If the biosphere-preservation interventions fail during the 2028–2050 window while the atmospheric interventions are still building to full effect, the reef gap begins and cannot be closed on human timescales.

Mechanism and peer-reviewed status

Coral assisted evolution refers to a set of active reef-restoration interventions designed to accelerate the natural evolutionary response of coral populations to thermal stress. The peer-reviewed literature identifies four principal techniques (van Oppen et al. 2015, Proceedings of the National Academy of Sciences; National Academies 2019, A Research Review of Interventions to Increase the Persistence and Resilience of Coral Reefs): (i) selective breeding of coral colonies that survived past bleaching events, capturing the heritable component of thermal tolerance; (ii) assisted gene flow, involving the transplantation of heat-tolerant coral larvae or fragments from naturally warmer reef systems (Persian Gulf, northern Red Sea, Kimberley coast of Western Australia) to reefs facing rising temperatures; (iii) probiotic modification of the coral microbiome to enhance thermal tolerance through manipulation of the symbiont community; and (iv) hybridization between coral species with different thermal tolerances to produce viable heat-tolerant genotypes not available in the wild population.

Bozec et al. 2025 in Nature Communications report a coupled coral-ecosystem model analysis of intervention efficacy across the IPCC AR6 scenario ensemble. The central finding is that reef cover can rebound to contemporary levels only under the SSP1-1.9 emissions pathway; under SSP2-4.5 and all higher-emissions scenarios, reef cover continues to decline through 2100 regardless of the intensity of local restoration effort. The peer-reviewed inference the paper supports is direct: coral assisted evolution is not a substitute for emissions reduction. Its function is to preserve genetic and demographic capacity through the thermal-stress window, so that the surviving coral populations can serve as the seed stock for reef recovery once the atmospheric interventions have arrested and reversed the thermal driver. The Australian Institute of Marine Science and the Reef Restoration and Adaptation Program have run the largest field trials since 2020, with selectively bred heat-tolerant coral larvae deployed at multiple Great Barrier Reef sites (AIMS Annual Reports; RRAP 2024 R&D Program Update).

Moving coral assisted evolution from trial scale to functional restoration across the Great Barrier Reef and Caribbean would require sustained deployment on the order of $5–10 billion per year globally, coordinated through an internationally mandated Reef Trust Authority. The purpose is not to replace atmospheric intervention, but to maintain a genetically pre-adapted, functioning subset of reef habitat through the approximately fifty-year interval required for atmospheric drawdown and temperature reversal.

The 30×30 framework refers to the international commitment to protect 30 percent of the global ocean surface by 2030, formally adopted as Target 3 of the Kunming-Montreal Global Biodiversity Framework at the Convention on Biological Diversity COP15 in December 2022 (CBD/COP/DEC/15/4). As of 2024, approximately 8 percent of the global ocean has some formal protected status, but only approximately 3 percent meets the 'highly protected' or 'fully protected' standard that peer-reviewed synthesis identifies as necessary for meaningful biodiversity and climate-resilience outcomes (Grorud-Colvert et al. 2021, Science). The mechanism supporting reef survival is well established: marine protected areas remove the local stressors that compound climate stress — fishing pressure, coastal pollution runoff, sediment loading from land-based activity, physical damage from anchoring and bottom trawling, and vessel traffic — allowing coral populations to allocate more of their thermal-stress tolerance to surviving bleaching events. Mumby et al. 2004 in Nature demonstrated that mangrove-buffered, protected reef zones support two-to-four times higher fish biomass than unprotected reefs, with cascading benefits for herbivory that suppresses macroalgal overgrowth after bleaching mortality.

The physical protection function of the coupled reef–mangrove–seagrass system is quantified in Ferrario et al. 2014 in Nature Communications, which reports that healthy coral reefs reduce incident wave energy on downstream coastlines by 66 to 97 percent. This wave-energy dissipation is what enables the seagrass beds and mangrove forests behind the reef to persist as high-productivity blue-carbon sequestration systems (Mcleod et al. 2011, Frontiers in Ecology and the Environment). Loss of the reef breakwater exposes those systems to wave destruction and eliminates the blue-carbon sink function; preservation of the reef preserves the entire coupled coastal-carbon system. The 30×30 framework is therefore not merely a biodiversity policy — it is a survival scaffold for the biological infrastructure that must persist through the atmospheric-intervention window in order for the recovery pathway in Panel A of Part I Figure 1 to be physically available.

8. Intervention 6: Clean-Power Backbone: Geothermal-First, Nuclear-Second

Physical response time

Geothermal (EGS) operational at scale 2028–2035; nuclear SMR scale-out 2035–2050

Coupled-system indicator addressed

Enabling infrastructure for the energy demand of DACR, OAE mineral processing, and DOCR

Why this intervention at this position in the portfolio

Under an assumed integrated intensity of 1.5 MWh per tonne CO_2, removal at 21 Gt/yr corresponds to approximately 31,500 TWh/yr of energy input, equivalent to roughly 3,600 GW of continuous power. This figure combines electricity and thermal demand and should not be read as an electrical-load requirement. A defensible estimate requires separate ledgers for electricity, low-grade regeneration heat, compression, transport, injection, sorbent replacement, and lifecycle emissions.

Mechanism and peer-reviewed status

Enhanced geothermal systems (EGS) drill 3–5 km into hot, dry crystalline rock, fracture the rock with pressurized water to create artificial permeability, and circulate working fluid through the induced fracture network to extract heat (Tester et al. 2006, MIT Future of Geothermal Energy; DOE GeoVision 2019). Unlike conventional hydrothermal geothermal, EGS is not restricted to naturally occurring hot-water reservoirs; the physics works anywhere with sufficient crustal temperature gradient, which includes most of the western United States, the East African Rift Valley, much of continental Asia, and an expanding set of previously non-geothermal sedimentary basins as horizontal drilling and multi-stage stimulation techniques imported from shale oil and gas mature. Fervo Energy's Project Red in Nevada has been operating since 2023 at 3.5 MW output at 191 °C, and Fervo's Cape Station project in Utah is delivering commercial EGS at approximately $60–70/MWh with drill times cut by approximately 70 percent between the first and fourth well pairs — the same learning curve that made shale gas economic (Fervo Energy 2024 technical reports; DOE GeoVision 2019). Google's 24/7 clean-power purchase agreement with Fervo, operational since 2023, is the first commercial-scale demonstration of EGS-powered baseload for a hyperscale data center (Google 2024 Environmental Report).

Colorado deployment specifics and resource ceiling

5–8 GW is stated here as a proposed deployment target. Technical resource potential, economically recoverable capacity, firm operational output, and an achievable state build schedule are different quantities. Supporting this target requires regional geological and reservoir characterization, drilling-rate analysis, heat-depletion modeling, cost estimates, and transmission planning, none of which is presented in this paper.

EGS nevertheless has a finite ramp rate and a geological ceiling. A well pair generally requires approximately 12–18 months to drill and stimulate, and a 500 MW development requires roughly four to six years from site selection to commercial operation. Continuous drilling would therefore need to begin immediately to approach 5–8 GW by 2035, subject to rig, workforce, stimulation-crew, transmission, and induced-seismicity constraints. Beyond the best resource zones, declining temperature gradients increase drilling depth and cost, preventing geothermal alone from powering the full DACR scale-out.

The same firm geothermal output can unlock three adjacent processes: coastal DOCR electrodialysis, continuous mineral processing for OAE, and continuous electrolysis for the green hydrogen used in methanol synthesis from captured CO_2. This cross-platform use of electricity and exit-grade heat strengthens the case for geothermal as shared industrial infrastructure rather than a single-purpose power plant.

Nuclear remains necessary alongside geothermal. EGS carries the 2028–2035 stabilization window; SMRs carry the 2035–2050 reversal and scale-out phase after the highest-quality geothermal resource approaches its ceiling. In Colorado, the retired Fort St. Vrain precedent highlights the need to rebuild nuclear regulatory and operator capacity, while co-siting first commercial SMRs at Comanche Station near Pueblo would reuse grid interconnection, water rights, cooling infrastructure, and an established industrial site following the plant's scheduled coal retirement. The two technologies are sequential primary sources rather than competing alternatives; wind and solar remain supplementary resources for more interruptible loads.

EGS is uniquely well-fit for the DACR power requirement for four reasons rooted in physics rather than policy preference. First, it delivers a capacity factor of approximately 90 percent, comparable to nuclear and roughly three to four times the capacity factor of solar (20–25 percent) or wind (35–40 percent), which is the correct match for continuous TVSA sorbent regeneration that cannot be cycled with grid intermittency. Second, it rejects usable-grade heat as a byproduct: geothermal binary-cycle plant exit water is at 60–90 °C, the exact temperature range TVSA sorbent regeneration requires, so waste heat can be routed directly to DAC facilities without requiring the R-245fa heat pump that constitutes a large fraction of the parasitic electrical draw in the standard DACR configuration. Third, the subsurface engineering skill set — directional drilling, formation stimulation, downhole monitoring, induced seismicity management — is identical to that required for Class VI CO_2 injection wells, so the workforce and the regulatory framework overlap. Fourth, surface footprint is small: a 500 MW geothermal facility requires approximately 5–10 acres, versus approximately 2,500–4,000 acres for the equivalent solar nameplate capacity (DOE GeoVision 2019, land-use appendix).

The two constraints on EGS as sole power backbone are geological ceiling and induced seismicity. The USGS Enhanced Geothermal Systems resource assessment (USGS 2008; updated in DOE GeoVision 2019) estimates the technically recoverable EGS resource across the continental United States at approximately 500 GW of firm baseload capacity at 2050 technology levels, distributed unevenly with the highest-quality resource in the western states. Global EGS resource is on the order of several thousand GW. This is not sufficient to power the entire global DACR fleet at 21 Gt/yr steady-state, but it is sufficient to carry the stabilization phase of deployment through approximately 2035 and to provide the structural backbone of the western hemisphere deployment thereafter. Induced seismicity is a real constraint documented in the abandoned Basel EGS project in Switzerland (magnitude 3.4 event, 2006) and the Pohang EGS project in South Korea (magnitude 5.5 event, 2017); modern operations at Fervo's Nevada and Utah projects and at the DOE Utah FORGE research facility use much more careful stimulation protocols and passive seismic monitoring and have not induced significant seismic events, but the risk requires ongoing regulatory design and monitoring (Majer et al. 2007, Geothermics; DOE Induced Seismicity Protocol 2012).

Small modular nuclear reactors (SMRs) are the second element of the clean-power backbone, deployed on a longer timeline than EGS and providing scale-out beyond the geothermal geological ceiling. The peer-reviewed and government-technical literature identifies several near-term SMR designs with realistic first commercial-operation dates in the 2030–2032 window: NuScale VOYGR (77 MW modules, NRC design certification 2023, first commercial deployment target slipped past original 2030 date); TerraPower Natrium (345 MW sodium-cooled fast reactor with molten-salt thermal storage, targeting 2030–2031 commercial operation at Kemmerer, Wyoming); Oklo Aurora (15 MW liquid-metal-cooled microreactor, targeting 2027–2028 demonstration at Idaho National Laboratory); and X-energy Xe-100 (80 MW high-temperature gas-cooled reactor). NRC Part 53 licensing, the modernized advanced-reactor licensing framework, is expected to complete for the first designs in 2027–2028 (NRC Regulatory Basis for Part 53, 2024). Scaling from first-of-a-kind to the 2,000–3,000 units globally required to power the full-scale DACR fleet is a 20–25 year proposition even under aggressive learning curves and supply-chain buildout (IEA Nuclear Power in a Clean Energy System 2019; MIT Future of Nuclear Energy 2018). This figure is a scenario input. Establishing it requires specified reactor sizes, factory throughput, commissioning schedules, fuel supply, and financing. Naming existing projects does not demonstrate manufacturing scale."

The division of labor between EGS and SMR is dictated by their respective deployment timelines and physical characteristics. EGS carries the 2028–2035 stabilization window because it can be drilled starting now using existing rig fleets and stimulation crews, delivers 24/7 firm baseload with native TVSA-grade exit heat, and comes online in three-to-five-year increments as each well pair completes. SMRs carry the 2035–2050 reversal-phase scale-out once EGS approaches its geological ceiling, providing the power density and geological freedom that geothermal cannot match at the multi-thousand-unit global scale required. Wind and solar occupy a supplementary role, appropriate for powering the CO_2-utilization industry (methanol synthesis, mineralization) that is more tolerant of intermittency than TVSA sorbent regeneration, and for contributing to non-DACR grid loads. The IPCC framing that treats wind and solar as the primary clean-power source is a legacy of the pre-DACR analytical framework in which continuous industrial-scale removal was not the binding constraint; under DACR-at-scale, the intermittency penalty becomes decisive and geothermal-then-nuclear is the physically correct ordering.

9. Finite Resources and the Portfolio Discipline: Why Substitute Actions Are Not Neutral

The causal chain in Section 2.5 defines what has to be interrupted. The indicator quantitatives in Section 2.6 define how much time is left to interrupt it. Neither of those sections speaks to the third constraint that will determine whether the response happens at all: the resource envelope inside which the response must be built. That envelope is finite. Attention, political capital, capital markets appetite, engineering talent, permitting bandwidth, land, minerals, freshwater, low-carbon electricity, and — most binding of all — public willpower and the collective drive to survive an outcome that has not yet fully arrived. Every one of these is a rival good. Every one of them is currently being spent on activity that does not reduce the atmospheric CO_2 burden, does not suppress methane at source, does not raise ocean alkalinity, does not preserve reef biosphere, and does not build the clean-power backbone the Six-Intervention Portfolio requires.

The following categories of activity currently absorb resources — money, staff, media attention, consumer identity, policy oxygen, and personal willpower — while producing zero measurable movement on any of the four coupled indicators of Part I Figure 1 at the scale and within the timeframe the paleoclimate record requires:

• Voluntary carbon-offset markets. Retail-facing offset purchases (airline seat, freight shipment, corporate net-zero claim) are dominated by avoided-deforestation and improved-forest-management credits whose additionality, permanence, and quantification have been repeatedly shown in the peer-reviewed literature to be overstated by a factor of five to ten (West et al. 2023, Science; Guardian/Corporate Accountability investigations 2023–2024). The dollars are real; the atmospheric removal is largely fictional. Every offset dollar that clears a corporate ESG line item is a dollar not deployed on engineered removal, methane capture, or clean firm power.

• Corporate net-zero pledges without capital commitment. Pledges dated 2040, 2050, or 2070 without an accompanying current-year capital expenditure line and a mid-decade interim target function as reputation-management instruments. They absorb communications budgets, consultant hours, and public credulity while displacing the harder conversation about mandated 2030 emissions floors and mandated corporate contribution to removal build-out.

• Consumer-scale behavioral substitution marketed as climate action. Paper straws, cotton tote bags, home composting, domestic recycling of single-use plastics, personal air-travel abstention, individual dietary change absent policy, and residential rooftop solar priced for wealthy homeowners. Each has a defensible personal justification. None of them, individually or aggregated across the entire consumer population of the OECD, moves any of the Section 2.6 indicators by a measurable amount within the physically available window. Their principal function is to relocate the moral burden from the industrial and policy scale — where the physics is decided — to the household scale, where the physics is not.

• Electric-vehicle purchase framed as sufficient personal contribution. EV adoption is a necessary component of a clean-transportation transition on the multi-decade horizon. It does not remove atmospheric CO_2. It does not raise ocean pH. It does not preserve reef cover. Its emissions-reduction benefit is real but back-loaded across the vehicle service life, at a rate that depends on the grid it charges from. Sold as the primary act of individual climate responsibility, it becomes a permission structure to defer action on the interventions that actually operate on the indicator timescales that matter.

• Afforestation-as-primary-strategy campaigns. Tree-planting programs marketed at the trillion-tree scale — as distinguished from ecosystem restoration inside intact biomes — displace scarce land, scarce freshwater, and scarce political attention while delivering carbon sequestration that is (i) reversible on wildfire, drought, and land-use timescales that are shortening under the same warming they are meant to arrest, and (ii) at least an order of magnitude below what engineered removal will need to deliver.

• Green-consumer identity marketing. Product certification labels, subscription-box sustainability services, ESG retail investment funds sold to individual investors, and lifestyle-brand climate positioning. These generate consumer feeling of alignment without corresponding physical movement on any indicator. The feeling itself is the product. It is precisely the false sense of security that this section is naming.

• Climate-adjacent conference and awareness activity untethered from build-out. Summits, panels, TED talks, awareness months, and pledge signatories that produce no capital deployment, no permit filed, no molecule of CO_2 removed, no tonne of alkalinity dispersed, no methane leak sealed. The activity is not zero-value — it maintains a professional class fluent in the vocabulary — but it is a substitute good for the physical build-out, and it is consuming the same finite attention envelope.

The point of this enumeration is not that each of these activities is worthless. Several of them are useful in the post-emergency environment where the atmospheric perturbation has been arrested and ecosystem management resumes something like a normal cadence. Voluntary offsets against a stabilized atmosphere, consumer behavioral change embedded in a decarbonized grid, corporate pledges paired with delivered capital — all of these become meaningful contributions once the emergency phase is over.

The point is that we are not in the post-emergency environment. Section 2.6 shows that every link in the causal chain is active now. Section 3 will show that the atmospheric CO_2 concentration has already exceeded the reconstructed pre-extinction baseline of the End-Permian. Section 4 will show that at least 28 amplifying feedback loops are engaged. The physically available window for arresting the chain closes in a small number of decades — and the resource envelope for the response is smaller than the response requires. Under those conditions, substitute action is not neutral. Every dollar, every hour of attention, every unit of willpower, and every gram of the finite public appetite for hardship that gets spent on activity outside the Six-Intervention Portfolio is a dollar, an hour, a unit, and a gram that is not available for the interventions that physically alter the indicators.

The portfolio discipline the rest of this paper argues for is therefore not only an argument about which interventions work. It is an argument about which interventions we can still afford to not do. Given the size of the resource envelope and the size of the response required, the honest answer is: none of the six, and none of the substitutes. The substitutes are the frittering. The willpower to survive is the scarcest input. It has to be spent where the physics is decided.

10. De-Prioritized Interventions

The peer-reviewed CDR literature includes two intervention categories that appear at large deployment scale in the IPCC AR6 WG3 pathways but are de-prioritized in the portfolio developed here. In both cases the reason is not that the underlying mechanism is unsound, but that the deployment scale required to reach the IPCC-median contribution is not physically realizable without collapse of the systems the intervention is intended to protect.

Bioenergy with Carbon Capture and Storage (BECCS)

BECCS combines two processes: growing biomass crops or harvesting biomass residues that absorb atmospheric CO_2 during photosynthesis, and then combusting or fermenting that biomass for energy while capturing the emitted CO_2 and storing it geologically. The net effect is negative emissions — carbon removed from the atmosphere by plants and permanently sequestered underground. IPCC AR6 WG3 Chapter 12 identifies BECCS as the largest single CDR technology in most 2 °C-compatible integrated assessment scenarios, with a median annual deployment of 8.96 $GtCO_2$/yr by 2100 (range 2.63–16.15) and cumulative deployment of 328 $GtCO_2$ across 2020–2100 (range 168–763).

The premise of BECCS at IPCC-median deployment scale is not physically realizable without collapse of the global food system. Deploying BECCS at the 5–9 $GtCO_2$/yr level plausibly requires 200–500 million hectares of dedicated bioenergy cropland (Smith et al. 2016, Nature Climate Change; Fuss et al. 2018, Environmental Research Letters), an area comparable to the total current global area planted with wheat and requiring the displacement of food production, natural ecosystems, or both at continental scale. The IPCC AR6 WG3 explicitly flags this land competition as one of the largest feasibility constraints on the 1.5 °C-compatible pathways in which BECCS at that scale appears (IPCC AR6 WG3 Ch. 3). Under any honest assessment of the land, water, biodiversity, and food-security trade-offs, BECCS at IPCC-median scale is a modeling artifact rather than a real intervention. Small-scale BECCS on genuine waste biomass — agricultural residues, forestry byproducts, and municipal organic waste — is a legitimate contribution at approximately 1 $GtCO_2$/yr, but the 8–9 $GtCO_2$/yr figure carried in the IPCC pathways should not be treated as available capacity in the portfolio.

Afforestation, Reforestation, and Land-Use CDR (AFOLU)

Afforestation, reforestation, and land-use carbon removal covers the biological uptake of atmospheric CO_2 through planting new forests on previously non-forested land, restoring forests on recently deforested land, rebuilding soil organic carbon through improved agricultural practices, and restoring wetlands, peatlands, and mangroves. IPCC AR6 WG3 Chapter 12 assigns AFOLU-based CDR a median deployment of 4.19 $GtCO_2$/yr by 2100 (range 0.10–6.91) with cumulative deployment of 252 $GtCO_2$ across 2020–2100 (range 20–418) in 2 °C-compatible scenarios.

Two constraints limit AFOLU's role as a primary carbon strategy at IPCC-median scale. First, the land requirement is large: sequestering 3–4 $GtCO_2$/yr through afforestation plausibly requires 300–500 million hectares of new tree cover, approximately the combined area of India and Argentina, and the land is not physically available without displacing food production or existing natural ecosystems. Second, carbon storage in living biomass is impermanent on the timescales relevant to the atmospheric burden: forests can burn, be logged, or die from heat stress and pest outbreaks, releasing sequestered carbon back to the atmosphere. The wildfire-carbon feedback loop enumerated in Ripple et al. 2023, One Earth (Section 4 of Part I) directly threatens AFOLU carbon permanence in a warming climate. Honest accounting suggests a realistic contribution of approximately 1–2 $GtCO_2$/yr from targeted reforestation of degraded land and restoration of mangrove, seagrass, and peatland ecosystems, with the additional co-benefit for the coastal-carbon-and-reef coupling described in intervention 5. AFOLU should be retained as biodiversity and ecosystem policy with real climate co-benefits — not as a primary carbon-removal strategy at the 4+ $GtCO_2$/yr figure carried in the IPCC pathways.

11. Synthesis: The 2035 Deadline and the Deployment Rate Required

The six interventions in Sections 3 through 8 are not alternatives to one another. Each addresses a subset of the coupled indicator system in Part I Figure 1 that the others cannot reach: methane suppression bends the temperature curve on a decadal timescale that CO_2 interventions cannot match; direct atmospheric removal is the only lever on the atmospheric CO_2 concentration at the scale the causal chain requires; ocean alkalinity enhancement is the only intervention that addresses ocean surface acidification; stratospheric aerosol injection is the only intervention that reduces radiative forcing on the two-year deployment-to-effect timescale required during the 2028–2040 window; coral assisted evolution and 30×30 preserve the biological infrastructure whose continued existence is the outcome the atmospheric interventions must protect; and the geothermal-then-nuclear power backbone is the enabling infrastructure without which none of the preceding interventions is deployable at the scale required.

The physical deadline structure is set by the accumulation rate of atmospheric CO_2 and the paleoclimate-derived mass-extinction concentration. At current accumulation rates of +2.7 to +3.75 ppm/yr (WMO Greenhouse Gas Bulletin 2025), the atmospheric CO_2 concentration crosses the approximately 450 ppm level associated with the End-Permian pre-extinction baseline (Wu et al. 2021, Nature Communications; Bond and Grasby 2017) around 2033. To arrest the trajectory before it passes into the concentration range reconstructed for the latest Permian interval. , the portfolio interventions must be operational — not planned, not funded, operational — by approximately 2035. This is a nine-year window from the date of writing.

The deployment rate implied by that deadline exceeds all historical peacetime industrial-mobilization precedents. It is comparable in scale and compression to the United States Second World War industrial conversion of 1940–1943, in which industrial output roughly doubled in three years through direct federal coordination of production, labor, and capital allocation (Wilson 2016, Destructive Creation; Klein 2013, A Call to Arms). No market-driven deployment curve at the pace and scale required has ever occurred, and none is projected under the current national and international policy environment. The physical requirement and the political precedent are not consistent.

The paleoclimate record does not specify what happens when a species-level intelligence with the technological capacity to arrest a mass-extinction causal chain fails to do so within the physically available window. There is no Big Five precedent for that condition. The record establishes only what happens when the causal chain runs to completion: preferential extinction of marine calcifiers, multi-million-year reef gaps, coupled loss of terrestrial vertebrate biodiversity through the reef–ocean-oxygen–land coupling documented in Section 2.4a of Part I, and biosphere recovery on timescales of five to fifteen million years. Whether the contemporary perturbation runs to that outcome or is arrested short of it depends on whether the portfolio described in this Part is executed at the scale and on the schedule the physics requires.

12. Conclusion

Part I of this paper established that the Big Five mass extinctions of the Phanerozoic Eon share a consistent causal signature — massive rapid carbon injection to the ocean-atmosphere system, followed by global warming, ocean deoxygenation, ocean acidification, preferential extinction of marine calcifiers, coupled terrestrial extinction through the shared oxygen and biogeochemical infrastructure, and multi-million-year recovery intervals for reef ecosystems. Contemporary anthropogenic carbon emissions have already produced atmospheric CO_2 concentrations exceeding the reconstructed pre-extinction baseline of the End-Permian event and are proceeding at a rate that peer-reviewed synthesis identifies as likely without precedent in at least the last 300 million years. Every element of the paleoclimate extinction causal chain is currently active in the Earth system, and at least 28 amplifying biogeophysical feedback loops (Ripple et al. 2024, BioScience) now identified in the peer-reviewed literature stand to accelerate that chain further.

Part II has identified the six-intervention portfolio the peer-reviewed literature supports as necessary to arrest, and where possible reverse, that causal chain within the window physically available. Methane suppression at source, direct atmospheric carbon removal with hyperscale-compute coupling, ocean alkalinity enhancement at gigaton scale, stratospheric aerosol injection as a temperature bridge for the 2028–2040 window, coral assisted evolution paired with marine protected area expansion to 30 percent of the global ocean, and a clean-power backbone built geothermal-first and nuclear-second: each addresses a subset of the coupled indicator system the others cannot reach, and all six are required. Bioenergy with carbon capture and storage at IPCC-median deployment scale, and afforestation as a primary carbon-removal strategy, are de-prioritized as modeling artifacts that displace scarce land and political attention from interventions that better match the physics.

The physical deadline is approximately 2035. The scale of deployment required within that window exceeds all historical peacetime industrial-mobilization precedents. The paleoclimate record establishes what happens when the causal chain now activated in the Earth system runs to completion; it does not establish what happens when a species with the technological capacity to arrest that chain fails to do so within the window physically available. The outcome remaining to be determined by human action is which of those two conditions the contemporary perturbation will occupy.

PART III
CONTEMPORARY CLIMATE FEEDBACKS, RESOURCE LIMITS, CIVILIZATIONAL RISK, AND THE NORTH AMERICAN CLIMATE PAIN SCALE

1. Overview

Part I established that the five paleoclimate indicators of mass extinction are all present at or beyond their historic thresholds, and that the contemporary carbon-release rate is at least an order of magnitude above the sustained maximum of the Paleocene–Eocene Thermal Maximum (Zeebe et al. 2016). Part II specified the six-intervention portfolio required to arrest the causal chain. Part III turns to the contemporary Earth system as it is now behaving: which positive feedbacks are already engaged, how they interact in cascading chains, which finite resources are approaching hard limits inside the same window in which those feedbacks bite, and how these physical stresses translate into civilizational strain. The section closes with the North American Climate Pain Scale (NAPS), a diagnostic communication tool that maps escalating climate impact severity on a 1–10 scale familiar from clinical pain assessment.

The Part I paleoclimate analog and the Part II intervention portfolio remain the load-bearing arguments of this paper. Part III does not restate them. It documents the near-term environment those interventions must succeed in, and it supplies a communication instrument for translating that environment into terms that non-specialist audiences can act on.

2.1 Methodology

The analysis integrates four strands. First, a feedback-loop taxonomy compiled from IPCC AR6 WG1 (IPCC 2021), the state-of-the-climate report (Ripple et al. 2024), and the tipping-cascade review of Wunderling et al. (2024), catalogued by system (cryosphere, biosphere, ocean–atmosphere, atmospheric circulation) and characterized by driver, response, and amplification pathway. Tipping elements and threshold temperatures follow Armstrong McKay et al. (2022) and Wunderling et al. (2024).

Second, a resource-depletion timeline for freshwater, arable soil, stable climate zones, pollinators, fisheries, phosphorus, and energy, built from the UN World Water Development programme, FAO and UNCCD publications, the human-climate-niche analysis of Xu et al. (2020), FAO fisheries assessments, and USGS mineral commodity data.

Third, a civilizational-fault-line analysis across food systems, water, migration, public health, economy, and governance, drawing on the World Bank Groundswell projections, WHO climate-health assessments, and the security literature on climate as a threat multiplier.

Fourth, the NAPS scale, calibrated against measurable regional indicators (extreme heat days, wildfire acreage, insured disaster losses, mortality, water-supply status) and anchored to specific historical events for each level.

The Kaufhold et al. (2025) Potsdam Institute analysis using the CLIMBER-X Earth system model and the Wunderling et al. (2024) cascade review are treated as the frontier constraints on how much amplification remaining feedbacks can add to declared warming trajectories.

2.2 Feedback Loop Taxonomy and Cascading Interactions

Positive feedbacks are the mechanism by which small incremental emissions today produce disproportionate warming later. Part I §4 established the paleoclimate evidence that once the feedback phase engaged in prior mass-extinction events, temperature and ocean chemistry continued to change for tens of thousands of years even after the primary carbon-release pulse stopped. The contemporary system has already engaged several of the same loops.

Cryosphere feedbacks

Permafrost carbon feedback. Arctic permafrost holds an estimated 1,500 Gt of organic carbon, roughly twice the current atmospheric burden (IPCC 2021, AR6 WG1 Ch. 5). As permafrost thaws, microbial decomposition releases CO_2 and CH_4, which drive further warming and further thaw. The Arctic is warming at approximately four times the global mean rate (Rantanen et al. 2022, Communications Earth & Environment). Kaufhold et al. (2025) identify permafrost thaw as a principal reason that even nominally 2 °C scenarios overshoot 2 °C on multi-century timescales once carbon-cycle feedbacks are represented interactively.

Ice–albedo feedback. September Arctic sea-ice extent has fallen by roughly half since 1979 (NSIDC data referenced in IPCC 2021). Loss of reflective ice exposes open water, which absorbs roughly 90 percent of incident solar radiation versus roughly 10 percent for sea ice, accelerating regional and hemispheric warming. Largely ice-free Arctic summers become plausible in the 2030s under intermediate emissions.

Ocean–atmosphere feedbacks

Water-vapor and cloud feedbacks. Atmospheric water-vapor content rises approximately 7 percent per °C of warming (Clausius–Clapeyron). Water vapor is itself a greenhouse gas, and current best estimates of net cloud feedback are modestly positive (IPCC 2021, AR6 WG1 Ch. 7). These feedbacks are the reason equilibrium climate sensitivity is centered near 3 °C rather than the roughly 1.2 °C direct CO_2 response.

Ocean-circulation feedbacks. Part I §4.1 documents the observational and modeling evidence for AMOC weakening and the risk of collapse this century (Ditlevsen & Ditlevsen 2023; Van Westen et al. 2024a, 2024b; Rahmstorf et al. 2026). A weakened AMOC redistributes heat southward, accelerates Southern Ocean warming, and increases West Antarctic Ice Sheet instability from below through basal melt — a multi-step feedback loop connecting Northern Hemisphere freshwater flux to Antarctic ice loss and additional sea-level rise.

Biosphere feedbacks

Microbial soil-carbon release. Warmer soils respire faster. Soil-warming experiments consistently show elevated CO_2 efflux, and the global soil-carbon pool exceeds the atmospheric carbon pool by a factor of two to three. Even a modest fractional release from temperate and boreal soils over the century adds meaningful atmospheric loading.

Forest dieback. The eastern Amazon is now a net annual carbon source in some years (Gatti et al. 2021, Nature) as deforestation and warming shorten the wet season past the point where closed-canopy rainforest can persist. Boreal forests in Canada and Siberia are losing carbon to bark-beetle outbreaks and increasingly severe fire seasons. Both systems are candidate tipping elements at 2–3 °C of global warming (Armstrong McKay et al. 2022).

Atmospheric-circulation feedbacks

Jet-stream disruption. The reduced Arctic-to-mid-latitude temperature gradient produced by polar amplification weakens the polar jet, favoring persistent blocking patterns and concurrent extremes such as the 2021 Pacific Northwest heat dome and prolonged Siberian heatwaves. Blocking-induced compound extremes couple to biosphere feedbacks through wildfire carbon release and to permafrost feedbacks through prolonged surface heating.

Cascading tipping-point interactions

Wunderling et al. (2024) find that 13 of 19 identified interactions among major climate tipping elements tend to amplify system change; only a minority are stabilizing. Three cascades of particular concern for the contemporary trajectory:

Cryosphere cascade. Greenland Ice Sheet melt freshens the North Atlantic and weakens the AMOC. A weakened AMOC accumulates heat in the Southern Ocean, which destabilizes the West Antarctic Ice Sheet through basal melt. Loss of both ice sheets commits the climate system to more than ten meters of sea-level rise over centuries to millennia.

Biosphere–climate cascade. Amazon dieback releases on the order of 90 Gt of carbon (Lovejoy & Nobre 2018), raising atmospheric CO_2 and accelerating warming, which increases the probability of boreal forest dieback and permafrost thaw. This is the mechanism underlying the Hothouse Earth pathway of Steffen et al. (2018).

Ocean–atmosphere cascade. A weakened AMOC alters Atlantic and Pacific monsoon systems. Simulations show a collapsed AMOC weakens the West African monsoon enough to push the Sahel into a substantially drier state (Van Westen et al. 2024a), with cascading effects on food production, migration, and dust transport that further modify Atlantic sea-surface temperature.

Armstrong McKay et al. (2022) identify multiple major tipping elements — Greenland Ice Sheet, West Antarctic Ice Sheet, low-latitude coral reefs, and boreal permafrost — with central threshold estimates at or below 2 °C of global warming. Current policies place end-of-century warming in the 2.4–2.8 °C range (Climate Action Tracker 2024). The contemporary trajectory therefore sits inside the range in which multiple tipping elements are more likely than not to cross.

Figure 10. Tipping Cascade Map

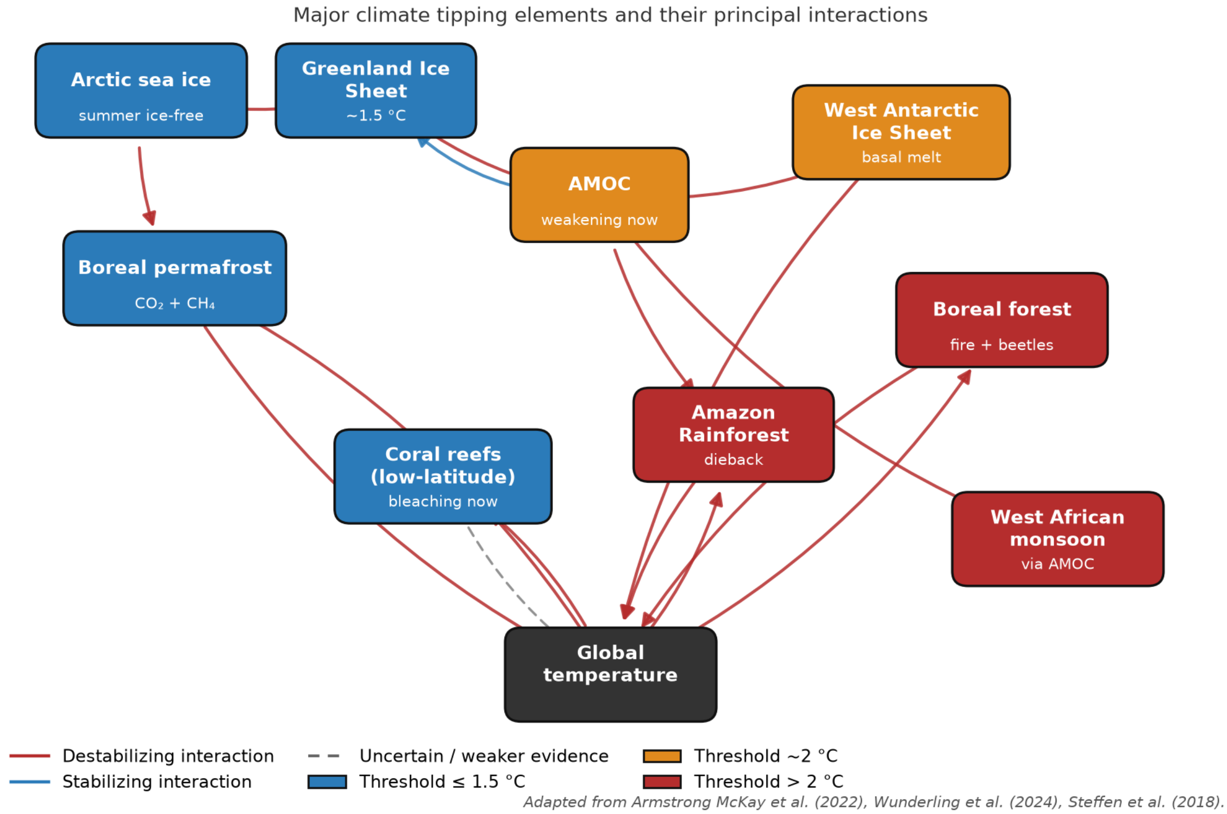

Figure 10. *Tipping Cascade Map — major climate tipping elements color-coded by approximate threshold temperature, with destabilizing (red) and stabilizing (blue) links. Adapted from Armstrong McKay et al. (2022), Wunderling et al. (2024), and Steffen et al. (2018).*

2.3 Resource Depletion Timeline

Climate destabilization is arriving in a period of simultaneous strain on the physical resources civilization depends on. The point of this section is not that any single resource is on a certain path to exhaustion; several trends admit technological or policy responses. The point is that multiple ceilings arrive inside the same two-to-three-decade window in which climate feedbacks accelerate.

Freshwater (2020s–2030s)

Global freshwater demand is on track to exceed sustainable supply by 40 percent by 2030 (WEF 2023, based on 2030 Water Resources Group analysis). Groundwater aquifers, including the U.S. Ogallala and India's Punjab basin, are drawn down faster than they recharge. In the American Southwest, the Colorado River entered its first federally declared shortage in 2021 (U.S. Bureau of Reclamation 2021), with progressively deeper shortages since. UN-Water projects roughly 5 billion people experiencing at least one month of severe water scarcity annually by 2050.

Arable soil (2020s–2050s)

FAO estimates that 90 percent of Earth's topsoil is at risk of degradation by 2050 (FAO 2015, Status of the World's Soil Resources; updated FAO 2022). Erosion rates run roughly 24 Gt of fertile soil per year globally. Soil regeneration proceeds at millimeters per century; soil loss under intensive agriculture proceeds at millimeters per year.

Human climate niche (2030s–2100)

Xu et al. (2020, PNAS) show that under a high-emissions trajectory (~3 °C by 2070), one to three billion people would live in climates hotter than any climate that supported dense human population over the last 6,000 years — outside the historical human climate niche. Regions of the Persian Gulf, South Asia, and portions of the U.S. Southwest face wet-bulb temperatures approaching 35 °C, the physiological limit for outdoor human survival, on current warming trajectories.

Pollinators and biodiversity (2020s–2040s)

Sánchez-Bayo & Wyckhuys (2019, Biological Conservation) report that roughly 40 percent of insect species are in decline, with substantial pollinator losses documented across temperate agricultural regions. Pollinators contribute to approximately 35 percent of global crop production by volume (IPBES 2016). Continued declines through the 2030s translate directly into lower yields for fruit, nut, and vegetable crops and higher food prices.

Fisheries (2020s–2050s)

FAO's State of World Fisheries and Aquaculture 2024 reports that 37.7 percent of assessed marine fish stocks are fished at biologically unsustainable levels. Overfishing, warming, and acidification compound. Coral-reef fisheries face particular risk given the fourth global coral bleaching event documented in Part I §3.

Phosphorus (2030s–2060s)

Phosphate rock supplies are concentrated in a small number of countries — Morocco holds roughly 70 percent of known high-grade reserves (USGS Mineral Commodity Summaries 2024). Peak phosphorus production is projected in the 2030s (Cordell & White 2011, Sustainability). Phosphorus scarcity translates directly into fertilizer scarcity and yield loss, with the steepest effects on import-dependent regions.

Energy security and transition (2020s–2050s)

The near-term risk is not fossil-fuel depletion but transition volatility: grid stress from extreme weather, geopolitical exposure of gas supply (as demonstrated during the 2022 European gas crisis), and the pace mismatch between renewable buildout and continued fossil-demand growth (IEA World Energy Outlook 2024). Part II §6 of this paper specifies the clean-power backbone required to make the transition

Figure 11. Resource Depletion Timeline

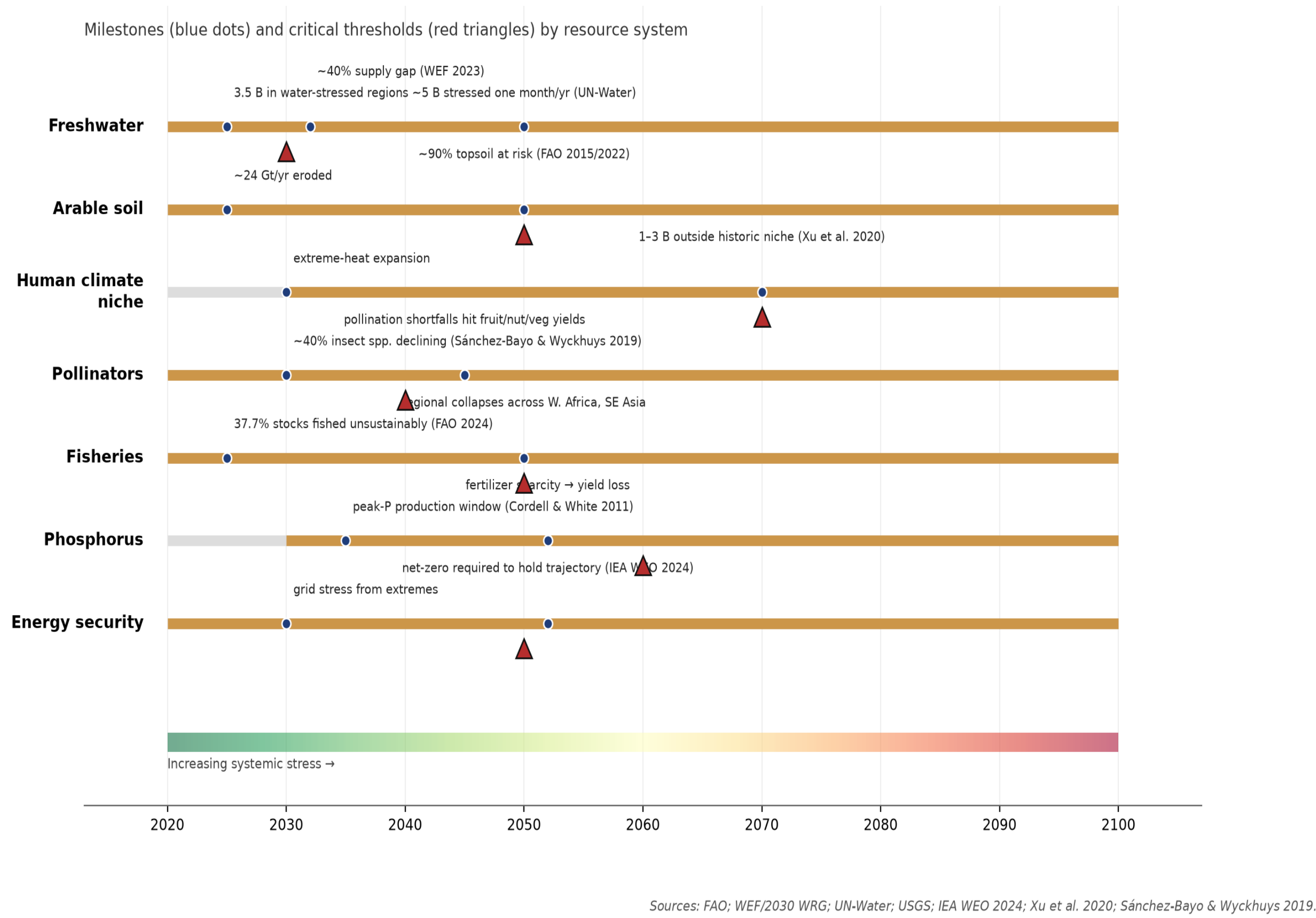

Figure 11. *Resource Depletion Timeline, 2020–2100 — parallel tracks for freshwater, arable soil, human climate niche, pollinators, fisheries, phosphorus, and energy, with milestones and projected critical thresholds. Sources: FAO; WEF / 2030 WRG; UN-Water; USGS; IEA WEO 2024; Xu et al. (2020); Sánchez-Bayo & Wyckhuys (2019).*

The concurrence matters more than any single line. By 2050 the human population is projected near 9.7 billion (UN DESA 2024) attempting to share less water, less arable soil, fewer wild-caught fish, and scarcer fertilizer under more extreme climate conditions than any large industrial society has faced. Multiple ceilings meet inside the same window in which the feedback loops described in §3.2 are projected to bite hardest.

2.4 Civilizational Fault Lines Under Stress

The environmental changes cataloged in §3.2 and §3.3 translate into strain on the systems that hold civilizations together. Six domains are already showing measurable effects.

Food-system fragility

The 2022 concurrence of Yangtze-basin drought, European heatwaves, and Indian wheat losses drove global grain prices to near-record levels alongside the Ukraine war supply shock. IPCC AR6 WG2 projects staple-crop yield declines of a few percent globally by 2030 and larger declines in the hottest producing regions. The global food system relies on trade and storage buffers that historically absorb single-region shocks; the vulnerability is to simultaneous shocks across multiple breadbaskets, a scenario made more probable by correlated climate extremes.

Water conflict

The Nile, Tigris–Euphrates, Indus, and Colorado basins are the most-cited flashpoints. In each, upstream infrastructure decisions affect downstream water and power supply for tens of millions. Domestic water conflict — rationing protests in Iran and South Africa, contested groundwater allocation in the American Southwest — is currently more common than state-to-state water war, but internal water crises produce cross-border consequences through refugee flows and political instability.

Migration and border stress

The World Bank's Groundswell II report (2021) projects up to 216 million internal climate migrants across six regions by 2050 under high-emissions, low-development scenarios. Central-America-to-U.S. migration is already partly attributable to crop failures and hurricane damage. The system stress is at destination borders: receiving countries face domestic political backlash and eroding asylum frameworks when arrivals overwhelm processing capacity.

Public health

WHO projects an additional 250,000 climate-attributable deaths per year between 2030 and 2050 from malnutrition, malaria, diarrheal disease, and heat stress (WHO 2014, revised upward in 2021 assessments). This is a conservative floor. The system risk is compound: successive disasters degrade healthcare infrastructure, as during the 2020 U.S. West Coast wildfire season overlapping with COVID-19. Chronic exposure to disaster response exhausts medical staff and mental-health services.

Economic fragility

Swiss Re Institute (2021) projects up to 10–18 percent global GDP loss by 2050 under unabated warming versus a no-climate-change baseline. Insurance retreat from wildfire-prone California and flood-prone Florida markets in 2023–2025 signals private-sector recognition that expected losses exceed insurable rates in some geographies. Physical damage costs, commodity-price volatility, and financial re-pricing of climate-exposed assets combine into a persistent drag on growth and public budgets.

Governance

The pre-war Syrian drought (Kelley et al. 2015, PNAS) is the most-cited case where climate stress contributed to state destabilization, though it was neither the sole nor the dominant driver. The pattern to watch is not any single failed state but the concurrent-crisis mode in which multiple governments face legitimacy crises from simultaneous water, food, migration, and disaster pressures. Democratic institutions and international cooperation frameworks are unusually vulnerable in this mode.

Figure 12. Civilizational risk web – climate and resource stresses to social stability

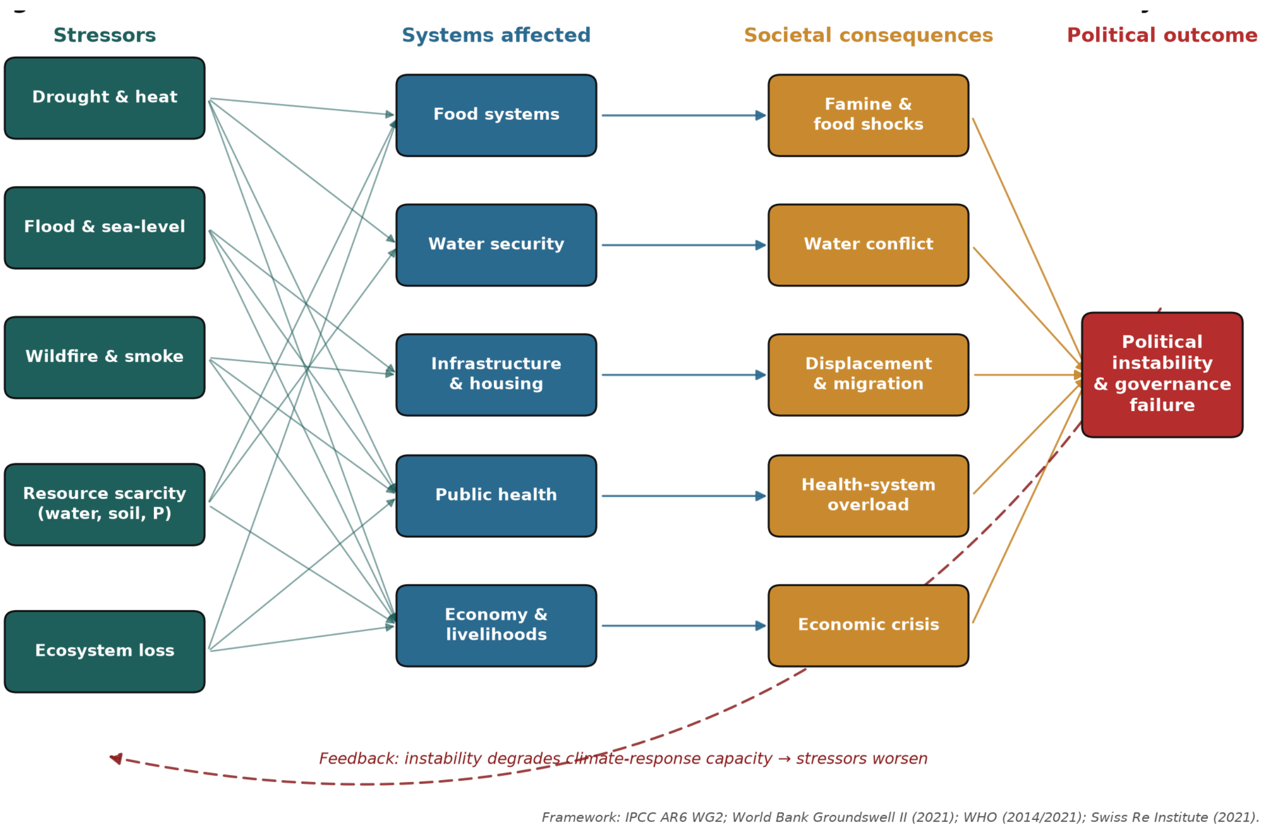

***Figure 12**. Civilizational Risk Web — climate and resource stressors flow through affected systems and societal consequences to political instability, with a feedback loop from instability back to climate-response capacity. Framework: IPCC AR6 WG2; World Bank Groundswell II (2021); WHO (2014, 2021); Swiss Re Institute (2021).*

2.5 The North American Climate Pain Scale (NAPS)

Complex climate data does not reliably move public understanding or policy. The medical pain scale — the 0-to-10 rating clinicians use for triage — does. The North American Climate Pain Scale (NAPS) adapts that instrument to communicate climate impact severity. It is a communication tool, not a scientific index. It is designed to translate the quantitative outputs of §3.2 and §3.3 into a scale that policymakers, journalists, and the general public can immediately locate themselves on.

Scale design

NAPS runs from 1 (background, no meaningful disruption) to 10 (regionally unlivable). Each level is calibrated against measurable indicators: annual extreme-heat days, wildfire acreage, insured disaster losses, mortality from heat and disaster, drought status, and the operational condition of water and power systems. Each level is anchored to a real or projected event so that the reference is concrete.

Level descriptions

Level 1 — Background. Mild deviations perceived as normal variability: slightly warmer summers, longer pollen seasons, isolated nuisance flooding. Corresponds roughly to the late-20th-century North American baseline.

Level 3 — Noticeable. Annual record-setting heatwaves; recurring wildfire smoke episodes that reach cities far from fire sources (Eastern U.S. cities receiving Western and Canadian smoke, as in June 2023); multi-time-per-year coastal nuisance flooding in Miami, Norfolk, and Charleston. North America is currently near Level 3 on annual average, with individual events reaching higher.

Level 5 — Emergency threshold. State-of-emergency declarations become routine. Weeks-long extreme-heat episodes make outdoor work dangerous. Urban grids fail under peak cooling load. Multi-year Colorado River shortages force sustained water rationing. Insurance retreat becomes common in high-risk zones. Public-health systems see recurring heat-hospitalization spikes. Aligns approximately with 1.5 °C of global warming.

Level 7 — Crisis. Portions of Arizona, Texas, and California face seasons of 46 °C-plus heat with high humidity; nighttime temperatures remain lethal for the elderly and those without cooling. Coastal cities require major engineered defenses or face progressive abandonment. Consecutive-year breadbasket losses drive food-price shocks. Internal climate migration begins in earnest. Aligns approximately with 2 °C of global warming.

Level 10 — Unlivable. Large portions of the U.S. Southwest are no longer supporting organized society. Multiple coastal metro areas from Florida to the Carolinas have experienced sustained inundation and infrastructure failure. Frequent wet-bulb 35 °C events eliminate outdoor human survival in Southern latitudes. Aligns with 4 °C-plus of global warming — the trajectory implied if the feedbacks documented in §3.2 engage without an aggressive Part II response.

Anchor events

Level 3 — 2020 California and Oregon wildfire smoke plumes reaching the East Coast.

Level 5 — Hurricane Harvey inundation of Houston, 2017: major U.S. metro immobilized, roughly $125 billion in damage.

Level 6 — Pacific Northwest heat dome, 2021: hundreds of confirmed deaths, transportation and health systems overwhelmed.

Level 7 — Projected Phoenix summer 2040s under current trajectory: serial heatwaves, progressively deeper Colorado River shortages, incipient depopulation.

Level 8 — Projected mid-2050s worst-case: simultaneous Midwest and Canadian Prairie crop failures with rolling coastal-flood retreat in NYC and Miami.

Level 10 — End-century 4 °C scenario: Phoenix July high averaging near 50 °C; Florida Keys largely below sea level; surviving population concentrated in cooler northern pockets.

Figure 13. North American Climate Pain Scale (NACPS)

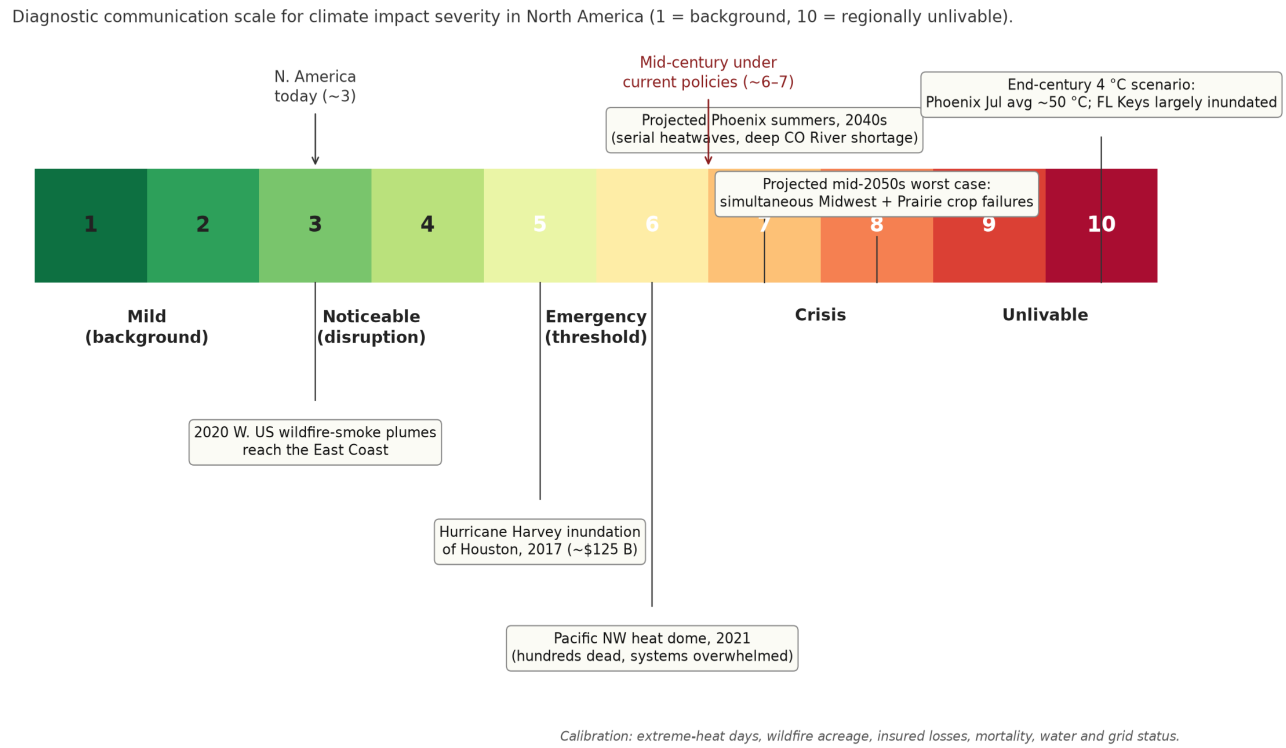

Figure 13. North American Climate Pain Scale (NAPS) — diagnostic 1–10 scale for climate impact severity, with anchor events (2020 wildfire smoke, Hurricane Harvey 2017, Pacific NW heat dome 2021) and projected positions for mid-century under current policies and end-century 4 °C scenario.

Use

NAPS is designed for policymakers, communicators, and educators. A mayor, governor, or public-health officer can say: 'Our region is at Pain Level 4 today; without action we are on trajectory for Level 7 by mid-century.' The scale trades a small amount of scientific precision for a large gain in intelligibility. It aligns with the medical use of pain scales: the point is to trigger appropriate intervention proportional to severity, not to produce a peer-reviewable measurement.

2.6 Discussion

Three implications follow from the material in this Part.

Non-linearity requires front-loaded action

The physics of feedbacks and tipping points is not linear. Additional emissions today do not produce a proportional temperature response; they raise the probability of triggering processes that continue to warm the system after emissions cease. The paleoclimate record in Part I.4 documents feedback phases lasting tens of thousands of years. The contemporary system carries the same physics. This is the technical basis for the Part II conclusion that the intervention portfolio must deploy on a wartime industrial timeline, not on a smoothed multi-decade transition curve.

Converging crises require integrated solutions

The resource-limit and civilizational-fault-line material in §3.3 and §3.4 shows that climate response cannot be siloed from water management, soil conservation, agricultural innovation, and resource governance. The Part II portfolio has co-benefits across these domains: aggressive methane suppression reduces near-term warming and near-term air-pollution mortality; direct atmospheric carbon removal paired with waste-heat capture from hyperscale compute stabilizes energy infrastructure while drawing down atmospheric carbon; a geothermal-first, nuclear-second clean-power backbone reduces exposure to gas geopolitics. Integrated portfolio design is not aesthetic preference; it is what the convergence of crises requires.

Communication is part of the mechanism

Declaring a climate emergency is not symbolic when it unlocks the policy instruments normally reserved for war and pandemic — reallocated budgets, accelerated permitting, industrial mobilization, and rationing where necessary. The physical case for that declaration is the material in Parts I and II of this paper. NAPS is the communication instrument that makes that case legible to the audiences whose consent and participation the response requires.

Uncertainty is not a reason to delay

Individual feedback thresholds carry uncertainty, and human innovation can genuinely relax some resource constraints. The relevant asymmetry is the consequence structure. Underestimating the physical risk and being wrong produces irreversible losses on the century-to-millennium scale. Overestimating the risk and being wrong produces a cleaner, more resilient, more equitable industrial base. Recent observational trends — Arctic warming rates, coral bleaching frequency, ocean deoxygenation, and AMOC weakening — consistently outrun the central projections of prior IPCC reports. The historical error has been in the direction of understatement, not alarmism.

The moral case

Those least responsible for cumulative emissions — future generations and populations in the lowest-emissions countries — bear the highest projected climate costs. A NAPS Level 10 outcome would fall hardest on people who contributed almost nothing to the atmospheric loading that produced it. This is the ethical component of the emergency case, and it cannot be discharged by reference to political feasibility.

2.7 Summary

Multiple climate feedbacks are already engaged. The peer-reviewed literature identifies cascading interactions among tipping elements that raise the probability of crossing several thresholds inside the 2.4–2.8 °C range implied by current policies. Resource constraints on freshwater, arable soil, pollinators, fisheries, phosphorus, and stable climate zones tighten inside the same window. Food, water, migration, health, economic, and governance systems are already showing measurable strain. The North American Climate Pain Scale places North America near Level 3 today, on trajectory for Level 6–7 by mid-century under current policies, with Level 10 outcomes possible by end-century under high-emission trajectories with strong feedbacks. Parts I and II specify what the physical record demands and what the intervention portfolio requires. Part III specifies the environment those interventions must succeed in and the instrument for communicating why the response has to start now.

The gap between the physical ceiling of approximately 80 percent and the realized ceiling of approximately 15 to 20 percent is not a rounding error and it is not analytical waffling. It is the size of the mobilization gap — the distance between what the Earth system will respond to and what our current governance, financing, workforce, and political institutions are prepared to deliver. Every percentage point recovered between the two is a percentage point earned by dismantling a specific institutional constraint identified in the deployment-readiness assessment: the governance vacuum around stratospheric aerosol injection, the regulatory absence around ocean alkalinity enhancement, the workforce shortage in nuclear engineering and geothermal drilling, the financing gap between IRA-scale carbon-removal credits and the gigaton-per-year throughput actually required.

The analogous historical case is not a scientific one. It is the United States industrial mobilization of 1940 through 1945. In May 1940 the President's request for 50,000 aircraft per year was met with public disbelief; the peacetime aviation industry was building fewer than 6,000 a year. Four years later, in 1944 alone, US industry delivered 96,000 aircraft. The physics of aircraft manufacture did not change between 1940 and 1944. The institutional posture changed. Government financing, workforce mobilization, regulatory pace, industrial coordination, and public consent all shifted to a wartime footing, and the physical ceiling was realized.

The response to the extinction envelope described in this paper is the same class of problem with the same class of solution. The 15 to 20 percent realized ceiling reflects the current peacetime posture, in which fossil-fuel incumbents shape energy policy, geoengineering governance is in vacuum, and industrial mobilization at wartime pace is treated as politically implausible. The 80 percent physical ceiling reflects the response available under wartime posture: Defense Production Act invocation for methane suppression enforcement and DACR deployment; federal loan guarantees at trillion-dollar scale; a stratospheric aerosol injection governance framework negotiated over months rather than decades; nuclear Small Modular Reactor licensing compressed from eight-year cycles to eighteen months; workforce mobilization comparable to the 1941 aviation-industry expansion.

The choice between the two ceilings is therefore not scientific. It is behavioral. The physics has already answered the question of whether an adequate response exists. The institutional record demonstrates that adequate responses have been mounted before under existential pressure. Continuing to drill and burn while the response window closes selects for the +-17 percent outcome; mobilizing at wartime scale selects for the +-80 percent outcome. Absent a demonstrable case for insanity or self-destruction on a civilizational scale, the paper's recommendation is straightforward.

References

All analyses in this paper are sourced to peer-reviewed literature or authoritative government-monitoring data verified against primary sources. The bibliography below merges the primary sources of Part I and Part II. Where a source is cited in both parts it appears once.

PART I

1. Ainsworth, T. D., et al. (2025). Inevitable global coral reef decline under climate change-induced thermal stresses. Communications Earth and Environment, 6. https://www.nature.com/articles/s43247-025-02790-4
2. Baker, J. A., et al. (2025). Continued Atlantic overturning circulation even under climate extremes. Nature, 638(8052), 987–994. https://pmc.ncbi.nlm.nih.gov/articles/PMC11864975/
3. Barnosky, A. D., Matzke, N., Tomiya, S., Wogan, G. O. U., Swartz, B., Quental, T. B., Marshall, C., McGuire, J. L., Lindsey, E. L., Maguire, K. C., Mersey, B., & Ferrer, E. A. (2011). Has the Earth's sixth mass extinction already arrived? Nature, 471, 51–57. https://ib.berkeley.edu/labs/barnosky/Barnosky%20et%20al%20Sixth%20Extinction%20Nature.pdf
4. Bellomo, K., et al. (2026). Observational constraints project a ~50% AMOC weakening by the end of this century. Science Advances, 12(15). https://www.science.org/doi/10.1126/sciadv.adx4298
5. Bond, D. P. G., & Grasby, S. E. (2017). On the causes of mass extinctions. Palaeogeography, Palaeoclimatology, Palaeoecology, 478, 3–29. https://doi.org/10.1016/j.palaeo.2016.11.005
6. Clarkson, M. O., Kasemann, S. A., Wood, R. A., Lenton, T. M., Daines, S. J., Richoz, S., Ohnemueller, F., Meixner, A., Poulton, S. W., & Tipper, E. T. (2015). Ocean acidification and the Permo-Triassic mass extinction. Science, 348(6231), 229–232.
7. https://doi.org/10.1126/science.aaa0193
8. Chen, X., & Tung, K.-K. (2024). A pause in the weakening of the Atlantic meridional overturning circulation since the early 2010s. Nature Communications, 15, 10642. https://pubmed.ncbi.nlm.nih.gov/39643655/
9. Copernicus Marine Environment Monitoring Service. (2024). Ocean State Report 8. https://sp.copernicus.org/articles/4-osr8/1/2024/sp-4-osr8-1-2024.pdf
10. Ditlevsen, P., & Ditlevsen, S. (2023). Warning of a forthcoming collapse of the Atlantic meridional overturning circulation. Nature Communications, 14, 4254. https://www.nature.com/articles/s41467-023-39810-w
11. Ernst, R. E., & Youbi, N. (2017). How Large Igneous Provinces affect global climate, sometimes cause mass extinctions, and represent natural markers in the geological record. Palaeogeography, Palaeoclimatology, Palaeoecology, 478, 30–52.
12. https://doi.org/10.1016/j.palaeo.2017.03.014
13. Erwin, D. H. (1999). The end and the beginning: Recoveries from mass extinctions. Proceedings of the National Academy of Sciences, 96(16), 8827. https://www.pnas.org/doi/10.1073/pnas.96.16.8827
14. European Environment Agency. (2025). Ocean acidification indicator. https://www.eea.europa.eu/en/analysis/indicators/ocean-acidification
15. Forster, P. M., et al. (2024). Indicators of Global Climate Change 2023: Annual update of key indicators of the state of the climate system and human influence. Earth System Science Data, and 2024 briefing to UNFCCC COP30.
16. https://unfccc.int/sites/default/files/resource/5.%20Forster_IGCC%20EID%20COP30_V2.pdf

17. Global Coral Reef Monitoring Network. (2026, June). The most intense global coral bleaching event on record has likely concluded. https://gcrmn.net/2026/06/08/4gbe-ended
18. Green, T., Renne, P. R., & Keller, C. B. (2022). Continental flood basalts drive Phanerozoic extinctions. Proceedings of the National Academy of Sciences, 119(38). https://doi.org/10.1073/pnas.2120441119
19. Gutjahr, M., Ridgwell, A., Sexton, P. F., Anagnostou, E., Pearson, P. N., Pälike, H., Norris, R. D., Thomas, E., & Foster, G. L. (2017). Very large release of mostly volcanic carbon during the Palaeocene–Eocene Thermal Maximum. Nature, 548, 573–577. https://www.geomar.de/en/news/article/global-warming-driven-by-volcanic-co2-56-million-years-ago
20. Hönisch, B., Ridgwell, A., Schmidt, D. N., Thomas, E., Gibbs, S. J., Sluijs, A., Zeebe, R., Kump, L., Martindale, R. C., Greene, S. E., Kiessling, W., Ries, J., Zachos, J. C., Royer, D. L., Barker, S., Marchitto, T. M., Moyer, R., Pelejero, C., Ziveri, P., Foster, G. L., & Williams, B. (2012). The geological record of ocean acidification. Science, 335(6072), 1058–1063.
21. https://doi.org/10.1126/science.1208277
22. Intergovernmental Panel on Climate Change. (2021). AR6 WG1 Chapter 9: Ocean, Cryosphere and Sea Level Change; Summary for Policymakers. https://www.ipcc.ch/report/ar6/wg1/ chapter/chapter-9/
23. Kidder, D. L., & Worsley, T. R. (2010). Phanerozoic Large Igneous Provinces (LIPs), HEATT (Haline Euxinic Acidic Thermal Transgression) episodes, and mass extinctions. Palaeogeography, Palaeoclimatology, Palaeoecology, 295, 162–191, cited in
24. Meyer, K. M., & Kump, L. R. (2008). Oceanic euxinia in Earth history: Causes and consequences. Annual Review of Earth and Planetary Sciences, 36, 251–288, cited in Themiopoulou-Trigilio et al. (2016), Communicative & Integrative Biology. https://www.tandfonline.com/doi/full/10.1080/19420889.2015.1115162
25. Nnamchi, H. C., et al. (2025). Tropical response to ocean circulation slowdown raises future warming risk. Nature, 644(8077), 676–683. https://pubmed.ncbi.nlm.nih.gov/40739346/
26. NOAA Global Monitoring Laboratory. (2026). Annual mean global carbon dioxide growth rates. https://gml.noaa.gov/ccgg/trends/gl_gr.html
27. NOAA Global Monitoring Laboratory. (2026). Trends in atmospheric carbon dioxide, Mauna Loa Observatory. Retrieved August 23, 2026, from https://gml.noaa.gov/ccgg/trends/
28. Nowak, H., Schneebeli-Hermann, E., & Kustatscher, E. (2019). No mass extinction for land plants at the Permian–Triassic transition. Nature Communications, 10, 384. https://www.nature.com/articles/s41467-018-07945-w
29. Ostrander, C. M., Owens, J. D., & Nielsen, S. G. (2017). Constraining the rate of oceanic deoxygenation n leading up to a Cretaceous Oceanic Anoxic Event (OAE-2: ~94 Ma). Science Advances,via Woods Hole Oceanographic Institution Oceanus. https://www.whoi.edu/cms/files/17G0479-Oceanus_v53n1-p12_259084.pdf
30. Rae, J. W. B., et al. (2023). Atmospheric CO_2 over the past 66 million years from marine archives. Science, and Columbia Climate School commentary. https://news.climate.columbia.edu/2023/12/07/a-new-66-million-year-history-of-carbon-dioxide-offers-little-comfort-for-today/
31. Rahmstorf, S., et al. (2026, in review). The AMOC is weakening – time to take the evidence seriously. EGUsphere preprint. https://egusphere.copernicus.org/preprints/2026/egusphere-2026-2110/

32. Reimer, J. D., Peixoto, R. S., Davies, S. W., et al. (2024). The Fourth Global Coral Bleaching Event: Where do we go from here? Coral Reefs, 43(4), 1121–1125. https://doi.org/10.1007/s00338-024-02504-w
33. Ripple, W. J., Wolf, C., Lenton, T. M., Gregg, J. W., Natali, S. M., Duffy, P. B., Rockström, J., & Schellnhuber, H. J. (2023). Many risky feedback loops amplify the need for climate action. One Earth, 6(2), 86–91.
34. https://doi.org/10.1016/j.oneear.2023.01.004
35. Ripple, W. J., Wolf, C., Gregg, J. W., et al. (2024). The 2024 state of the climate report: Perilous times on planet Earth. BioScience. https://oeco.org.br/wp-content/uploads/2024/10/Ripple-et-al.-2024.pdf
36. Rothman, D. H. (2010). Relation of Phanerozoic stable isotope excursions to climate, bacterial metabolism, and major extinctions. Proceedings of the National Academy of Sciences. https://pmc.ncbi.nlm.nih.gov/articles/PMC2984178/
37. Schmidtko, S., Stramma, L., & Visbeck, M. (2017). Decline in global oceanic oxygen content during the past five decades. Nature, 542, 335–339. https://pubmed.ncbi.nlm.nih.gov/28202958/
38. Sciscio, L., et al. (2023). The past to unravel the future: Deoxygenation events in the geological archive and the Anthropocene oxygen crisis. Earth-Science Reviews. https://www.sciencedirect.com/science/article/pii/S0012825223003537
39. Sperling, E. A., Boag, T. H., Duncan, M. I., Endriga, C. R., Marquez, J. A., Mills, D. B., Monarrez, P. M., Sclafani, J. A., Stockey, R. G., & Payne, J. L. (2022). Breathless through time: Oxygen and animals across Earth's history. The Biological Bulletin, 243(2), 184–206. https://doi.org/10.1086/721754
40. Stanley, S. M. (2016). Estimates of the magnitudes of major marine mass extinctions in Earth history. Proceedings of the National Academy of Sciences, 113(42), E6325–E6334. https://www.pnas.org/doi/10.1073/pnas.1613094113
41. Van Westen, R. M., Kliphuis, M., & Dijkstra, H. A. (2024a). Physics-based early warning signal shows that AMOC is on tipping course. Science Advances, 10(6). https://www.science.org/doi/10.1126/sciadv.adk1189
42. Van Westen, R. M., et al. (2024b). Probability estimates of a 21st century AMOC collapse. arXiv preprint. https://arxiv.org/html/2406.11738v1
43. Van Zomeren, K., et al. (2026). Collapse of the Atlantic meridional overturning circulation would lead to substantial oceanic carbon release and additional global warming. Communications Earth and Environment.
44. https://www.nature.com/articles/s43247-026-03427-w
45. Volkov, D. L., et al. (2026). Meridionally consistent decline in the observed western boundary contribution to the Atlantic Meridional Overturning Circulation. Science Advances. https://www.science.org/doi/10.1126/sciadv.adz7738
46. World Meteorological Organization. (2025). State of the Global Climate 2024. https://wmo.int/publication-series/state-of-global-climate/state-of-global-climate-2024
47. Wu, Y., Chu, D., Tong, J., Song, H., Dal Corso, J., Wignall, P. B., Song, H., Du, Y., & Cui, Y. (2021). Six-fold increase of atmospheric pCO_2 during the Permian–Triassic mass extinction. Nature Communications, 12, 2137. https://doi.org/10.1038/s41467-021-22298-7
48. Wunderling, N., Winkelmann, R., Rockström, J., et al. (2024). Climate tipping point interactions and cascades: a review. Earth System Dynamics. https://hal.science/hal-04446670v1/file/esd2024Wunderling15.pdf

49. Zeebe, R. E., Ridgwell, A., & Zachos, J. C. (2016). Anthropogenic carbon release rate unprecedented during the past 66 million years. Nature Geoscience, 9, 325–329. https://www.soest.hawaii.edu/oceanography/faculty/zeebe_files/Publications/ ZeebeEtAl-NGS16.pdf
50. Zhou, Y., et al. (2026). Global monthly ocean dissolved oxygen (1960–2023). Earth System Science Data, 18, 3757. https://essd.copernicus.org/articles/18/3757/2026/
51. Bozec, Y.-M., Adam, A. A. S., Arellano-Nava, B., et al. (2025). A rapidly closing window for coral persistence under global warming. Nature Communications, 16, 9704. https://doi.org/10.1038/s41467-025-65015-4
52. Breitburg, D., Levin, L. A., Oschlies, A., Gregoire, M., Chavez, F. P., Conley, D. J., et al. (2018). Declining oxygen in the global ocean and coastal waters. Science, 359(6371), eaam7240. https://doi.org/10.1126/science.aam7240
53. Eddy, T. D., Lam, V. W. Y., Reygondeau, G., Cisneros-Montemayor, A. M., Greer, K., Palomares, M. L. D., Bruno, J. F., Ota, Y., & Cheung, W. W. L. (2021). Global decline in capacity of coral reefs to provide ecosystem services. One Earth, 4(9), 1278-1285. https://doi.org/10.1016/j.oneear.2021.08.016
54. Ferrario, F., Beck, M. W., Storlazzi, C. D., Micheli, F., Shepard, C. C., & Airoldi, L. (2014). The effectiveness of coral reefs for coastal hazard risk reduction and adaptation. Nature Communications, 5, 3794. https://doi.org/10.1038/ncomms4794
55. Field, C. B., Behrenfeld, M. J., Randerson, J. T., & Falkowski, P. (1998). Primary production of the biosphere: Integrating terrestrial and oceanic components. Science, 281(5374), 237-240. https://doi.org/10.1126/science.281.5374.237
56. Fielding, C. R., Frank, T. D., McLoughlin, S., Vajda, V., Mays, C., Tevyaw, A. P., Winguth, A., Winguth, C., Nicoll, R. S., Bocking, M., & Crowley, J. L. (2019). Age and pattern of the southern high-latitude continental end-Permian extinction constrained by multiproxy analysis. Nature Communications, 10, 385. https://doi.org/10.1038/s41467-018-07934-z
57. Fisher, R., O'Leary, R. A., Low-Choy, S., Mengersen, K., Knowlton, N., Brainard, R. E., & Caley, M. J. (2015). Species richness on coral reefs and the pursuit of convergent global estimates. Current Biology, 25(4), 500-505. https://doi.org/10.1016/j.cub.2014.12.022
58. Global Coral Reef Monitoring Network. (2026). The most intense global coral bleaching event on record has likely concluded. https://gcrmn.net/2026/06/08/4gbe-ended/
59. Huey, R. B., & Ward, P. D. (2005). Hypoxia, global warming, and terrestrial Late Permian extinctions. Science, 308(5720), 398-401. https://doi.org/10.1126/science.1108019
60. International Coral Reef Initiative. (2025). 84% of the world's coral reefs impacted in the most intense global bleaching event on record. https://icriforum.org/4gbe-2025/
61. Kiessling, W., & Simpson, C. (2011). On the potential for ocean acidification to be a general cause of ancient reef crises. Global Change Biology, 17(1), 56-67. https://doi.org/10.1111/j.1365-2486.2010.02204.x
62. McLeod, E., Chmura, G. L., Bouillon, S., Salm, R., Bjork, M., Duarte, C. M., Lovelock, C. E., Schlesinger, W. H., & Silliman, B. R. (2011). A blueprint for blue carbon: Toward an improved understanding of the role of vegetated coastal habitats in sequestering CO2. Frontiers in Ecology and the Environment, 9(10), 552-560. https://doi.org/10.1890/110004
63. Mumby, P. J., Edwards, A. J., Arias-Gonzalez, J. E., Lindeman, K. C., Blackwell, P. G., Gall, A., et al. (2004). Mangroves enhance the biomass of coral reef fish communities in the Caribbean. Nature, 427, 533-536. https://doi.org/10.1038/nature02286

64. Nagelkerken, I., Dorenbosch, M., Verberk, W. C. E. P., Cocheret de la Moriniere, E., & van der Velde, G. (2000). Importance of shallow-water biotopes of a Caribbean bay for juvenile coral reef fishes. Marine Ecology Progress Series, 202, 175-192.
65. National Oceanic and Atmospheric Administration, National Ocean Service. (2024). How much oxygen comes from the ocean? https://oceanservice.noaa.gov/facts/ocean-oxygen.html
66. Partensky, F., Hess, W. R., & Vaulot, D. (1999). Prochlorococcus, a marine photosynthetic prokaryote of global significance. Microbiology and Molecular Biology Reviews, 63(1), 106-127. https://doi.org/10.1128/mmbr.63.1.106-127.1999
67. Payne, J. L., & Clapham, M. E. (2012). End-Permian mass extinction in the oceans: An ancient analog for the twenty-first century? Annual Review of Earth and Planetary Sciences, 40, 89-111. https://doi.org/10.1146/annurev-earth-042711-105329
68. Sun, Y., Joachimski, M. M., Wignall, P. B., Yan, C., Chen, Y., Jiang, H., Wang, L., & Lai, X. (2012). Lethally hot temperatures during the Early Triassic greenhouse. Science, 338(6105), 366-370. https://doi.org/10.1126/science.1224126
69. Zapalski, M. K., Bridge, T. C. L., Baird, A. H., Pandolfi, J. M., & McWilliam, M. J. (2022). Functional consequences of Palaeozoic reef collapse. Scientific Reports, 12, 1386. https://doi.org/10.1038/s41598-022-05154-6

PART II

70. Bach, L. T., et al. (2023). Toward a consensus framework to evaluate air-sea CO_2 equilibration for marine CO_2 removal. Frontiers in Climate, 5, 1206929. https://www.frontiersin.org/journals/climate/articles/10.3389/fclim.2023.1206929/full
71. California Air Resources Board. (2010, updated 2020). Landfill Methane Regulation. Title 17 California Code of Regulations, Sections 95460–95476. https://ww2.arb.ca.gov/our-work/programs/landfill-methane-regulation
72. Convention on Biological Diversity. (2022). Kunming-Montreal Global Biodiversity Framework, Target 3 (30x30). Decision 15/4, CBD COP15. https://www.cbd.int/doc/decisions/cop-15/cop-15-dec-04-en.pdf
73. Department of Energy. (2019). GeoVision: Harnessing the Heat Beneath Our Feet. U.S. Department of Energy. https://www.energy.gov/eere/geothermal/geovision
74. Department of Energy. (2012). Protocol for Addressing Induced Seismicity Associated with Enhanced Geothermal Systems. DOE/EE-0662. https://www1.eere.energy.gov/geothermal/pdfs/geothermal_seismicity_protocol_012012.pdf
75. European Union. (1999). Council Directive 1999/31/EC on the landfill of waste. Official Journal L 182, 16 July 1999. https://eur-lex.europa.eu/legal-content/EN/TXT/?uri=CELEX%3A31999L0031
76. Fakhraee, M., Li, Z., Planavsky, N. J., & Reinhard, C. T. (2025). Ocean alkalinity enhancement — challenges, opportunities, and pathways forward. Environmental Science & Technology. https://doi.org/10.1021/acs.est.4c11024
77. Fang, J., et al. (2026). Hyperscale data-cnter waste-heat coupling for direct air capture with carbon storage. arXiv:2605.13114. https://arxiv.org/abs/2605.13114
78. Fuss, S., et al. (2018). Negative emissions — Part 2: Costs, potentials and side effects. Environmental Research Letters, 13, 063002. https://iopscience.iop.org/article/10.1088/1748-9326/aabf9f
79. Grorud-Colvert, K., et al. (2021). The MPA Guide: A framework to achieve global goals for the ocean. Science, 373(6560), eabf0861. https://doi.org/10.1126/science.abf0861

80. International Energy Agency. (2022). Direct Air Capture: A key technology for net zero. IEA, Paris. https://www.iea.org/reports/direct-air-capture-2022
81. International Energy Agency. (2024). Global Methane Tracker 2024. IEA, Paris. https://www.iea.org/reports/global-methane-tracker-2024
82. International Energy Agency. (2024). World Energy Outlook 2024. IEA, Paris. https://www.iea.org/reports/world-energy-outlook-2024
83. International Energy Agency. (2019). Nuclear Power in a Clean Energy System. IEA, Paris. https://www.iea.org/reports/nuclear-power-in-a-clean-energy-system
84. Intergovernmental Panel on Climate Change. (2022). AR6 WG3, Chapter 3: Mitigation pathways compatible with long-term goals. https://www.ipcc.ch/report/ar6/wg3/chapter/chapter-3/
85. Intergovernmental Panel on Climate Change. (2022). AR6 WG3, Chapter 7: Agriculture, Forestry, and Other Land Uses (AFOLU). https://www.ipcc.ch/report/ar6/wg3/chapter/chapter-7/
86. Intergovernmental Panel on Climate Change. (2022). AR6 WG3, Chapter 12: Cross-sectoral perspectives (including CDR). https://www.ipcc.ch/report/ar6/wg3/chapter/chapter-12/
87. Intergovernmental Panel on Climate Change. (2022). AR6 WG3 Summary for Policymakers. https://www.ipcc.ch/report/ar6/wg3/downloads/report/IPCC_AR6_WGIII_SummaryForPolicymakers.pdf
88. Kim, S., et al. (2023). Meta-analysis of 3-nitrooxypropanol effects on enteric methane emissions in dairy and beef cattle. Frontiers in Veterinary Science, 10, 1204174. https://www.frontiersin.org/journals/veterinary-science/articles/10.3389/fvets.2023.1204174/full
89. Kim, H., et al. (2025). Long-term efficacy of ocean alkalinity enhancement for atmospheric CO_2 removal. Biogeosciences, 22. https://doi.org/10.5194/bg-2024-215
90. Klein, M. (2013). A Call to Arms: Mobilizing America for World War II. Bloomsbury Press. https://www.bloomsbury.com/us/call-to-arms-9781608194117/
91. Majer, E. L., et al. (2007). Induced seismicity associated with enhanced geothermal systems. Geothermics, 36(3), 185–222. https://doi.org/10.1016/j.geothermics.2007.03.003
92. McCormick, M. P., Thomason, L. W., & Trepte, C. R. (1995). Atmospheric effects of the Mt Pinatubo eruption. Nature, 373, 399–404. https://doi.org/10.1038/373399a0
93. Massachusetts Institute of Technology. (2018). The Future of Nuclear Energy in a Carbon-Constrained World. MIT Energy Initiative. https://energy.mit.edu/wp-content/uploads/2018/09/The-Future-of-Nuclear-Energy-in-a-Carbon-ConstrainedWorld.pdf
94. National Academies of Sciences, Engineering, and Medicine. (2019). Negative Emissions Technologies and Reliable Sequestration: A Research Agenda. National Academies Press. https://doi.org/10.17226/25259
95. National Academies of Sciences, Engineering, and Medicine. (2019). A Research Review of Interventions to Increase the Persistence and Resilience of Coral Reefs. National Academies Press. https://doi.org/10.17226/25279
96. National Academies of Sciences, Engineering, and Medicine. (2021). Reflecting Sunlight: Recommendations for Solar Geoengineering Research and Research Governance. National Academies Press. https://doi.org/10.17226/25762
97. National Academies of Sciences, Engineering, and Medicine. (2022). A Research Strategy for Ocean-Based Carbon Dioxide Removal and Sequestration. National Academies Press. https://doi.org/10.17226/26278

98. Nuclear Regulatory Commission. (2024). Regulatory Basis for Part 53 — Risk-Informed, Technology-Inclusive Framework for Advanced Reactors. https://www.nrc.gov/reactors/new-reactors/advanced/rulemaking/part-53.html
99. Parker, A., & Irvine, P. J. (2018). The risk of termination shock from solar geoengineering. Earth's Future, 6(3), 456–467. https://doi.org/10.1002/2017EF000735
100. Renforth, P., & Henderson, G. (2017). Assessing ocean alkalinity for carbon sequestration. Reviews of Geophysics, 55(3), 636–674. https://doi.org/10.1002/2016RG000533
101. Reynolds, J. L. (2019). Solar geoengineering to reduce climate change: A review of governance proposals. Proceedings of the Royal Society A, 475(2229). See also Reynolds, Yale Law Journal (2019). https://doi.org/10.1098/rspa.2019.0255
102. Ricke, K. L., & Caldeira, K. (2014). Maximum warming occurs about one decade after a carbon dioxide emission. Environmental Research Letters, 9, 124002. https://doi.org/10.1088/1748-9326/9/12/124002
103. Robock, A. (2000). Volcanic eruptions and climate. Reviews of Geophysics, 38(2), 191–219. https://doi.org/10.1029/1998RG000054
104. Roque, B. M., et al. (2021). Red seaweed (Asparagopsis taxiformis) supplementation reduces enteric methane by over 80 percent in beef steers. PLOS ONE, 16(3), e0247820. https://doi.org/10.1371/journal.pone.0247820
105. Smith, P., et al. (2016). Biophysical and economic limits to negative CO_2 emissions. Nature Climate Change, 6, 42–50. https://doi.org/10.1038/nclimate2870
106. Tester, J. W., et al. (2006). The Future of Geothermal Energy: Impact of Enhanced Geothermal Systems on the United States in the 21st Century. MIT/DOE. https://www1.eere.energy.gov/geothermal/pdfs/future_geo_energy.pdf
107. United Nations Environment Programme and Climate and Clean Air Coalition. (2021). Global Methane Assessment: Benefits and costs of mitigating methane emissions. https://www.unep.org/resources/report/global-methane-assessment-benefits-and-costs-mitigating-methane-emissions
108. United States Geological Survey. (2008). Assessment of Moderate- and High-Temperature Geothermal Resources of the United States. USGS Fact Sheet 2008-3082. https://pubs.usgs.gov/fs/2008/3082/
109. Van Oppen, M. J. H., et al. (2015). Building coral reef resilience through assisted evolution. Proceedings of the National Academy of Sciences, 112(8), 2307–2313. https://doi.org/10.1073/pnas.1422301112
110. Wilson, M. R. (2016). Destructive Creation: American Business and the Winning of World War II. University of Pennsylvania Press. https://www.pennpress.org/9780812224184/destructive-creation/

PART III

111. Armstrong McKay, D. I., Staal, A., Abrams, J. F., Winkelmann, R., Sakschewski, B., Loriani, S., Fetzer, I., Cornell, S. E., Rockström, J., & Lenton, T. M. (2022). Exceeding 1.5 °C global warming could trigger multiple climate tipping points. Science, 377(6611), eabn7950. https://doi.org/10.1126/science.abn7950
112. Climate Action Tracker. (2024). Warming projections global update: November 2024. Climate Analytics and NewClimate Institute.
113. Cordell, D., & White, S. (2011). Peak phosphorus: Clarifying the key issues of a vigorous debate about long-term phosphorus security. Sustainability, 3(10), 2027–2049. https://doi.org/10.3390/su3102027

114. Ditlevsen, P., & Ditlevsen, S. (2023). Warning of a forthcoming collapse of the Atlantic meridional overturning circulation.* Nature Communications, 14, 4254. https://www.nature.com/articles/s41467-023-39810-w
115. Food and Agriculture Organization of the United Nations. (2015). Status of the world's soil resources: Main report. FAO and ITPS. https://www.fao.org/documents/card/en/c/c6814873-efc3-41db-b7d3-2081a10ede50/
116. Food and Agriculture Organization of the United Nations. (2022). Global status of salt-affected soils: Main report. FAO.
117. Food and Agriculture Organization of the United Nations. (2024). The state of world fisheries and aquaculture 2024: Blue transformation in action. FAO. https://openknowledge.fao.org/handle/20.500.14283/cd0683en
118. Gatti, L. V., Basso, L. S., Miller, J. B., Gloor, M., Gatti Domingues, L., Cassol, H. L. G., Tejada, G., Aragão, L. E. O. C., Nobre, C., Peters, W., Marani, L., Arai, E., Sanches, A. H., Corrêa, S. M., Anderson, L., Von Randow, C., Correia, C. S. C., Crispim, S. P., & Neves, R. A. L. (2021). Amazonia as a carbon source linked to deforestation and climate change. Nature, 595, 388–393. https://doi.org/10.1038/s41586-021-03629-6
119. Intergovernmental Panel on Climate Change. (2021). Climate change 2021: The physical science basis. Contribution of Working Group I to the Sixth Assessment Report of the IPCC (Chapter 5: Global carbon and other biogeochemical cycles and feedbacks; Chapter 7: The Earth's energy budget, climate feedbacks and climate sensitivity).* Cambridge University Press. https://www.ipcc.ch/report/ar6/wg1/
120. Intergovernmental Panel on Climate Change. (2022). Climate change 2022: Impacts, adaptation and vulnerability. Contribution of Working Group II to the Sixth Assessment Report of the IPCC. Cambridge University Press. https://www.ipcc.ch/report/ar6/wg2/
121. Intergovernmental Panel on Climate Change. (2022). Climate change 2022: Mitigation of climate change. Contribution of Working Group III to the Sixth Assessment Report of the IPCC.* Cambridge University Press. https://www.ipcc.ch/report/ar6/wg3/
122. Intergovernmental Science-Policy Platform on Biodiversity and Ecosystem Services. (2016). The assessment report on pollinators, pollination and food production. Secretariat of the IPBES. https://www.ipbes.net/assessment-reports/pollinators
123. International Energy Agency. (2024). World Energy Outlook 2024.* IEA, Paris. https://www.iea.org/reports/world-energy-outlook-2024
124. Kaufhold, C., Willeit, M., Talento, S., & Ganopolski, A. (2025). Interactive permafrost strongly influences Earth system response to future orbital forcing. Communications Earth & Environment. https://www.pik-potsdam.de/en/news/latest-news/permafrost-decisive-for-the-climate-system
125. Kelley, C. P., Mohtadi, S., Cane, M. A., Seager, R., & Kushnir, Y. (2015). Climate change in the Fertile Crescent and implications of the recent Syrian drought. Proceedings of the National Academy of Sciences, 112(11), 3241–3246. https://doi.org/10.1073/pnas.1421533112
126. Lovejoy, T. E., & Nobre, C. (2018). Amazon tipping point. Science Advances, 4(2), eaat2340. https://doi.org/10.1126/sciadv.aat2340
127. Rahmstorf, S., Boers, N., Ditlevsen, P., Michel, E., & Waite, A. M. (2026, in review). The AMOC is weakening – time to take the evidence seriously.* EGUsphere preprint. https://egusphere.copernicus.org/preprints/2026/egusphere-2026-2110/
128. Rantanen, M., Karpechko, A. Y., Lipponen, A., Nordling, K., Hyvärinen, O., Ruosteenoja, K., Vihma, T., & Laaksonen, A. (2022). The Arctic has warmed nearly four times faster than

the globe since 1979. Communications Earth & Environment, 3, 168. https://doi.org/10.1038/s43247-022-00498-3

129. Ripple, W. J., Wolf, C., Gregg, J. W., Rockström, J., Mann, M. E., Oreskes, N., Lenton, T. M., Rahmstorf, S., Newsome, T. M., Xu, C., Svenning, J.-C., Pereira, C. C., Law, B. E., & Crowther, T. W. (2024). The 2024 state of the climate report: Perilous times on planet Earth.* BioScience. https://oeco.org.br/wp-content/uploads/2024/10/Ripple-et-al.-2024.pdf
130. Sánchez-Bayo, F., & Wyckhuys, K. A. G. (2019). Worldwide decline of the entomofauna: A review of its drivers. Biological Conservation, 232, 8–27. https://doi.org/10.1016/j.biocon.2019.01.020
131. Steffen, W., Rockström, J., Richardson, K., Lenton, T. M., Folke, C., Liverman, D., Summerhayes, C. P., Barnosky, A. D., Cornell, S. E., Crucifix, M., Donges, J. F., Fetzer, I., Lade, S. J., Scheffer, M., Winkelmann, R., & Schellnhuber, H. J. (2018). Trajectories of the Earth System in the Anthropocene. Proceedings of the National Academy of Sciences, 115(33), 8252–8259. https://doi.org/10.1073/pnas.1810141115
132. Swiss Re Institute. (2021). The economics of climate change: No action not an option. Swiss Re Management Ltd. https://www.swissre.com/institute/research/topics-and-risk-dialogues/climate-and-natural-catastrophe-risk/expertise-publication-economics-of-climate-change.html
133. United Nations Department of Economic and Social Affairs, Population Division. (2024). World Population Prospects 2024. United Nations. https://population.un.org/wpp/
134. U.S. Bureau of Reclamation. (2021). Colorado River Basin August 2021 24-Month Study projections and Lake Mead Tier 1 shortage declaration. https://www.usbr.gov/newsroom/#/news-release/3950
135. U.S. Geological Survey. (2024). Mineral commodity summaries 2024: Phosphate rock. USGS. https://pubs.usgs.gov/periodicals/mcs2024/mcs2024-phosphate.pdf
136. Van Westen, R. M., Kliphuis, M., & Dijkstra, H. A. (2024a). Physics-based early warning signal shows that AMOC is on tipping course.* Science Advances, 10(6). https://www.science.org/doi/10.1126/sciadv.adk1189
137. Van Westen, R. M., Jacques-Dumas, V., Boot, A. A., & Dijkstra, H. A. (2024b). Probability estimates of a 21st century AMOC collapse.* arXiv preprint. https://arxiv.org/html/2406.11738v1
138. World Bank. (2021). Groundswell Part 2: Acting on internal climate migration. World Bank, Washington, DC. https://openknowledge.worldbank.org/handle/10986/36248
139. World Economic Forum & 2030 Water Resources Group. (2023). Global water gap: Projected 40% shortfall by 2030. WEF. https://www.weforum.org/reports/
140. World Health Organization. (2014). Quantitative risk assessment of the effects of climate change on selected causes of death, 2030s and 2050s. WHO. https://www.who.int/publications/i/item/9789241507691
141. World Health Organization. (2021). Climate change and health: Fact sheet. WHO. https://www.who.int/news-room/fact-sheets/detail/climate-change-and-health
142. Wunderling, N., Winkelmann, R., Rockström, J., Loriani, S., Armstrong McKay, D. I., Ritchie, P. D. L., Sakschewski, B., & Donges, J. F. (2024). Climate tipping point interactions and cascades: A review.* Earth System Dynamics. https://hal.science/hal-04446670v1/file/esd2024Wunderling15.pdf
143. Xu, C., Kohler, T. A., Lenton, T. M., Svenning, J.-C., & Scheffer, M. (2020). Future of the human climate niche. Proceedings of the National Academy of Sciences, 117(21), 11350–11355. https://doi.org/10.1073/pnas.1910114117

144. Zeebe, R. E., Ridgwell, A., & Zachos, J. C. (2016). Anthropogenic carbon release rate unprecedented during the past 66 million years.* Nature Geoscience, 9, 325–329. https://www.soest.hawaii.edu/oceanography/faculty/zeebe_files/Publications/ZeebeEtAl-NGS16.pdf

Asterisked entries (*) also appear in the Parts I/II bibliography of the main paper.